CONTROLLING PROTEIN-SURFACE INTERACTIONS IN CHROMATOGRAPHY USING MIXED SELF-ASSEMBLED MONOLAYERS

By

Chrysanty Tedjo

Dissertation

Submitted to the Faculty of the

Graduate School of Vanderbilt University

in partial fulfillment of the requirements

for the degree of

DOCTOR OF PHILOSOPHY

in

Chemical Engineering

May, 2011

Nashville, Tennessee

Approved:

Professor Paul E. Laibinis

Professor David E. Cliffel

Professor Scott A. Guelcher

Professor G. Kane Jennings

Professor M. Douglas LeVan

To my parents, for their continuous support and endless love

ACKNOWLEDGEMENTS

I would first like to acknowledge my advisor Professor Paul Laibinis for his guidance during my research at Vanderbilt University. I am grateful for all the valuable lessons that I have learnt from him. His critical advice and analytical skills have helped me in solving many research problems.

I would like to thank the members of my thesis committee Professor Doug LeVan, Kane Jennings, Scott Guelcher, and David Cliffel, who have assisted me since the beginning of my research. Their critical advice from their own research background has provided me with different perspectives on how to approach my research. I would also like to thank Professor Bridget Rogers for her assistance with the x-ray photoelectron spectroscopy (XPS) in her laboratory.

The staff of the Department of Chemical and Biomolecular Engineering also deserves to be recognized for their contribution to my research. I would like to thank Mark Holmes for his assistance in setting the equipments in the laboratory and for various technical advice. I am grateful to know Mary Gilleran and am thankful for her assistance and enjoyable discussions about life in general. I would also like to thank Rae Uson for her very diligent work in helping me with administrative issues. I am grateful to know fellow graduate students and researchers in the Department of Chemical and Biomolecular Engineering. I would first like to thank Zhou Xu, my cohort in the Laibinis group for his assistance in using some of the equipments in our laboratory. I would like to thank Chris Faulkner, Brandon Booth, Steve Vilt, Juan Carlos Tuberquia from the Jennings group for their help in one way or another and valuable research discussions. I

would like to thank Ben Schmidt from the Rogers group for teaching me how to operate XPS and for his insightful knowledge about XPS. I wish to thank Katarzyna Zienkiewicz for her advice in operating HPLC. I would also like to thank the Young group for letting me to use their centrifuge, pH meter and hood.

It is also necessary that I acknowledge my family and friends for their support during my period at Vanderbilt University. I will be forever grateful to my parents who taught me that I can accomplish any goal with continual hard work and high expectations. I cherish my sisters for their never ending love and support. I am thankful for my wonderful roommate here in Nashville, who has been through this process with me for the last one and a half year. Finally, none of this would be possible without the continual support from my husband.

TABLE OF CONTENT

LIST OF TABLES

LIST OF FIGURES

Page

CHAPTER I

INTRODUCTION

With the advances in cellular and genetic engineering, therapeutic proteins are by far the largest class of biologics produced by the biopharmaceutical industry. It is predicted that their market will reach $70 billion per year by the end of 2010[1]. The upstream processing for these proteins usually involves genetic engineered mammalian cells or microbes that serve as tiny chemical reactors. The downstream processing of the generated proteins mainly involves several purification steps to remove processing reagents, proteins and DNA from host cells, and impurities (particularly those resembling the desired protein)[1]. For some of these purification steps, chromatographic methods play a significant role in concentrating the intended product and polishing it from other proteins and impurities.

High performance liquid chromatography (HPLC) has been a workhorse for the biopharmaceutical industry, where it is used to identify, characterize, and purify molecules with high resolution and efficiency[2-5]. A variety of different molecular traits can be used as the basis for separation in HPLC (Table 1). As a result, these various types of protein chromatography rely on different types of supports and mobile phases for their operation. Normal-phase chromatography utilizes a polar stationary phase such as a silica support and a mobile phase consisting of a mixture of water and an organic solvent. Here, the separation is based on the interactions of the polar functional groups of the analytes with the polar sites on the surface of the support[4]. In contrast to the normal-phase

chromatography, reversed-phase chromatography utilizes a non-polar stationary phase in conjunction with a polar, largely aqueous mobile phase. Retention in reversed-phase chromatography is based on the interactions between the non-polar support and hydrophobic patches on the surface of the protein[4]. Differences in hydrophobicity between proteins result in their separation. Hydrophobic interaction chromatography is related to reversed-phase chromatography wherein the separation is based on hydrophobic interactions between the support and the surface of the protein. Hydrophobic interaction chromatography utilizes aqueous salt solutions as mobile phase. In both chromatographic modes, proteins are retained on the stationary phases under conditions of high surface tension in the mobile phase and are eluted at different rates by a gradual decrease in the surface tension of the mobile phase[6].

In its operation, ion-exchange chromatography utilizes the interaction between the charged proteins in the mobile phase with oppositely charged functional groups present on a stationary support. During this operation, the elution of proteins is effected by either an increase in the ionic strength of the buffer, thus increasing the concentration of competing counter-ions, or through changes in the pH of the mobile phase, as a way to effect changes in the charge of the proteins or of the support[4]. In contrast with these other methods, size-exclusion chromatography utilizes a highly hydrophilic porous stationary phases as a way to minimize non-specific interactions between the proteins and the support. Here the separation is effected by the ability of the proteins to penetrate the pores of the supports such that the proteins can be separated based on their sizes. Smaller proteins are able to diffuse into the internal porous structures of the support, thus getting eluted later. Larger proteins are instead excluded from regions within the porous support,

thus getting eluted earlier[7]. Lastly, affinity chromatography has been developed as a specific approach for isolating particular proteins from a mixture by chromatography. In this method, a high resolution of a separation is achieved due to specific interactions between a protein and a ligand immobilized on the support in a column[7]. This method works extremely well for the protein of interest. However, its use for another target protein requires the use of a support with specific properties for this other species. The other methods listed in Table 1-1 offer the advantage of having broad utility for protein separation.

Although each type of chromatographic method is successful in its ability to effect separation, often times there is the additional challenge that the separation must produce the purified protein of interest in its active form. In some cases, additional processing may be able to reconvert purified proteins in their unfolded state back to their active forms[1]; however, this refolding is not possible for all proteins. For these proteins, methods that yield the purified proteins in their active folded form are highly preferred.

Table 1-1: Types of Protein Chromatography and the Basis for their Separation[6]

Type	Separation based on
Normal-phase chromatography	Hydrophobicity
Reversed-phase chromatography	Hydrophobicity
Hydrophobic interaction chromatography	Hydrophobicity and hydrophobicity patches
Ion-exchange chromatography	Surface charge
Size-exclusion chromatography	Molecular size and shape
Affinity chromatography	Molecular structure/specific binding

1.1. Chromatography of Proteins using Hydrophobic Interactions

As mentioned above, a protein is active when it is in its native conformation, also known as its folded state[8]. This folded state of a protein is usually held together by a collection of van der Waals interactions, hydrogen bonds, electrostatic interactions, and/or disulfides linkages. Most folded proteins contain an inner hydrophobic core and a less hydrophobic outer surface that shields the inner core from interacting with surrounding water molecules. It is generally accepted that minimizing the number of hydrophobic side-chains exposed to water is a primary driving force behind the folding process[9].

In systems where the surface of a material is exposed to an aqueous solution containing protein, hydrophobic interactions between protein molecules and a contacting surface can result in protein adsorption. This adsorption event generally proceeds with a decrease in the interfacial energy between water and the surface. In a chromatographic process, some level of protein adsorption onto the surface of a chromatographic support is usually required for separation to be achieved. Such adsorption events can sometimes disrupt the weak forces that hold the folded structure of a protein together. The protein may unfold during the adsorption and expose its inner hydrophobic core to the surface, resulting in denaturation of the protein and loss of its activity.

There are two main types of chromatography that rely on hydrophobic interactions for effective separation. Reversed-phase chromatography is one type and it separates proteins based on strong hydrophobic interactions between the proteins and a hydrophobic support. The most commonly used supports are particles made of materials such as a cross-linked hydrophobic polymer or of silica, with the latter modified with

hydrophobic coating[10]. Silica supports functionalized with alkyl chains of one or more lengths[10-16] are commonly used due to their ability to withstand high pressures in the chromatographic column. In general, reversed-phase chromatography provides a higher resolving ability than most other chromatographic methods and typically requires short times for operation[4]. One problem with this method is that its use of organic solvents as the mobile phase and a highly hydrophobic material as the support often causes proteins to denature during the separation process. Because of this effect, reversed-phase chromatography is primarily used in analytical applications for identifying or quantifying a specific protein of interest, where obtaining the pure protein in its active state is not required.

Another method of separation, hydrophobic interaction chromatography, utilizes less hydrophobic surfaces to effect the separation of proteins. This separation is typically performed using an aqueous stream as the mobile phase, and the interactions between the proteins and the surface of the stationary phase are modulated by changing the concentration of salt in the mobile phase. These changes cause the proteins to 'salt out' onto the support. The early stationary phases for hydrophobic interaction chromatography were usually made of hydrophilic materials that had been functionalized with short alkyl chains to provide surface hydrophobicity for interactions with the proteins. Examples include hydrophilic polymers coated-silica particles functionalized with short alkyl or benzyl units[3, 6, 17, 18], and polymeric supports based on agarose[3, 19-21], cellulose[3], and polymethacrylate[22, 23] that are modified to include alkyl or aromatic groups. Although the aqueous medium and the weakly hydrophobic supports provide a more favorable environment for retaining the folded state of the protein than do the conditions for

reversed-phase chromatography, protein denaturation can still occur[3]. To overcome this problem, a tendency has been to utilize highly hydrophilic chromatographic supports to minimize the irreversible adsorption of proteins onto these surfaces. There have been several efforts to produce such supports by coating the surface of a support with hydrophilic polymers such as poly(ethylene glycol)[24-28], poly(vinyl alcohol)[29, 30], and poly(propylene glycol)[31, 32]. The use of these highly hydrophilic supports for separation usually results in lesser abilities to resolve different proteins as compared to reversed-phase chromatography, as the levels of protein-surface interactions are limited.

Column manufacturers offer a variety of stationary supports with different based materials and surface functional groups with varying surface densities[2, 3]. In general, the hydrophobicity of the support and the strength of protein-support interactions increase with the increase in the length of the alkyl chain[3, 33]. An increase in the density of the alkyl chain on the support leads to an increase in the binding capacity of the support, due to the higher likelihood of forming multipoint attachment. This, in some cases, can cause protein denaturation during elution through a chromatographic column[19]. Kato et al.[34] have reported that hydrophobic proteins can by separated by hydrophobic interaction chromatography when the hydrophobicities of the supports are properly adjusted respectively for each protein.

Several researchers have suggested methods of selecting the appropriate support for the chromatography of a target protein. Shaltiel[21] introduced a commercial kit that contains a homologous series of small columns of sepharose-based supports modified with alkyl groups of various alkyl chain lengths (e.g. C1 to C10). The usage of the kit was to determine the lowest member of the homologous series capable of retaining the

desired protein at low salt concentration (10-100 mM). Hjerten et al. [19] also employed a similar approach to Shaltiel's using a homologous alkyl agarose series with charged and uncharged surfaces. Jennissen[33] introduced the concept of critical hydrophobicity for selecting chromatographic supports. In order to achieve separation, a protein has to adsorb on the support and the coating of the support has to be chosen such that adsorption is achieved without protein denaturation. The procedure of selecting the appropriate support includes the selection of suitable alkyl chain length and the chain surface density. Finally the salt concentration in the mobile phase has to be optimized for a complete adsorption of a specified amount of protein on the critical hydrophobicity support (at the previously chosen alkyl chain length and chain surface density)[33].

All the above works clearly indicate that the level of hydrophobicity of a chromatographic support plays an important role in protein separation and specifically on protein retention in a column. The ability to systematically relate the level of hydrophobicity of a support to protein retention in the column would be very useful in the column selection and in predicting the retention time of a target protein.

1.2. Self-Assembled Monolayers (SAMs)

SAMs provide a reliable means for tailoring surfaces at the molecular scale[35-37]. These systems allow the ability to control the surface properties of a material. Figure 1-1 schematically illustrates their self-assembly process. In the figure, the formation of the SAM is driven by a specific interaction between the surface and the head group of molecules used to form the SAM. Lateral interactions between adjacent molecules aid in the assembly to produce densely packed, oriented monomolecular films. The tail group of

the assembling molecules is presented on the surface of the SAM and its selection provides a means for controlling the surface properties of the films. Some applications of SAMs includes their use in constructing biosensors[38-41], anti-stiction coatings for MEMS devices[42], linkers for attaching various biomolecules to surfaces[43-45], and as barrier coatings[46].

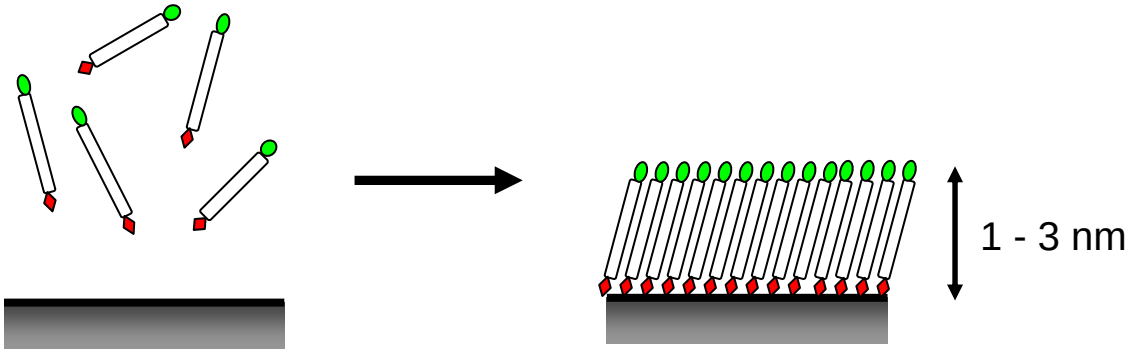

Figure 1-1: Formation of self-assembled monolayer.

The most explored self-assembled monolayer system is the assembly of organothiols onto gold surfaces. This system is formed based on strong specific interactions between the sulfur head group of the molecules and the gold surface. The thiol-gold system is noteworthy in that gold interacts poorly with many chemical functionalities thereby allowing many functional groups (e.g., halogens, hydroxyls, carboxylic acids, amides, etc.) to be included within the self-assembling molecules. In addition, the films are easy to prepare and exhibit good stability at room temperature However, these films have been reported to decompose at elevated temperatures[47] and to extended exposures to air[48, 49]. Another commonly studied system is the self-assembly of organotrialkoxysilanes and organotrichlorosilanes onto metal oxide surfaces, with SiO_2

being the most investigated substrate. In this system, a covalent bond is formed upon reaction between the silane head group (e.g. $-SiCl_3$, $-Si(OCH_2CH_3)_3$) and surface hydroxyl groups (e.g. Si-OH). Further, crosslinking between silane molecules through lateral Si-O-Si bonds between head groups also occurs in this system. The resulting covalent linkages between the SAMs and the surface and the crosslinks between the molecules yield silane-based SAMs that are more stable than their thiol-on-gold counterpart[50]. However, the self-assembly of silanes onto oxide surfaces poses more challenges in comparison to that of thiolates on metallic surfaces. Silanes are hydrolytically unstable and prone to unwanted polymerization in a solution or when stored for a prolonged period of time. The type of solvent used for self-assembly and the water content in the solvent greatly affect the quality of the formed films[41, 51].

The ability of a SAM to expose a wide range of functionalities on its surface has allowed researchers to probe protein-surface interactions in a controlled manner[52]. This has resulted in new approaches for generating protein resistant surfaces. The traditional approach for modifying surfaces to render them protein resistant has been to attach long chain ethylene glycol compounds (e.g. PEG) as a way to fully cover the surface and limit protein-surface interactions. The fouling resistance of PEG coated surfaces is due to “steric repulsion”. Here an entropic effect is caused by the unfavorable change in free energy associated with the dehydration and confinement of PEG polymer chains when a protein approaches the PEG surface[53, 54]. In a series of seminal papers, Whitesides and coworkers found that surfaces formed from SAMs of alkanethiol terminating in short ethylene glycol chains (only 3 to 6 repeat units in length) exhibited 'inertness' toward protein adsorption[55-58]. In these films, the oligo(ethylene glycol) (OEG) chain provides a

fouling resistance to the SAM due to the highly hydrophilic nature of EG chains and their ready adsorption of water to form a hydrogel-like barrier that repels proteins and cells from the surface. A molecular simulation study of OEG thiolate SAMs by Zheng et al.[59, 60] suggested that a large number of tightly bound water molecules around the OEG chains and the high flexibility of the OEG chains are the key factors that determine the non-fouling properties of a surface.

The protein resistant properties of methoxy-terminated tri(ethylene glycol) (EG_3OMe) thiolate SAMs were found to be dependent on the conformation of the OEG chains[61]. Figure 1-2 shows a cartoon of EG_3OMe thiolates assembled on gold and silver surfaces. On gold, these SAMs have a helical or amorphous conformation and exhibit protein resistance. On silver, these SAMs adopt a planar all-trans conformation and show no protein repellent properties. The packing density of the SAMs on silver is higher as compared to that on gold due to the smaller cross section per molecule available. Simulation studies by Wang et al.[62] concluded that the SAM surface of helical OEG provides a template for water nucleation, whereas water is not stable on a surface of planar OEG strands. This result provides an explanation for the repellent properties of the EG_3OMe thiolate SAMs on gold substrates. The influence of packing density of a SAM on protein repellent properties has also been reported by several researchers. Herrwerth et al.[63] investigated various OEG terminated thiolate SAMs and found a transition from non-adsorbing to adsorbing surface when the packing density of the OEG SAM was above 3.85 molecule/nm^2. This packing density translates to ~80% of densely packed thiolate SAM on gold (i.e. 4.67 molecule/nm^2)[61]. Studies by Jiang et al.[59, 64, 65] on pure and mixed hydroxyl-terminated OEG thiolate SAMs showed that protein resistance was

achieved when the coverage of OEG molecules on the surface was between 50 to 80% of the maximum coverage. This result is in agreement with the work by Vanderah et al.[66]. In their work, surfaces coated with $HS(CH_2)_3O(CH_2CH_2O)_5CH_3$ SAMs exhibited protein resistant properties when the densities of the SAMs were about 60 to 80%.

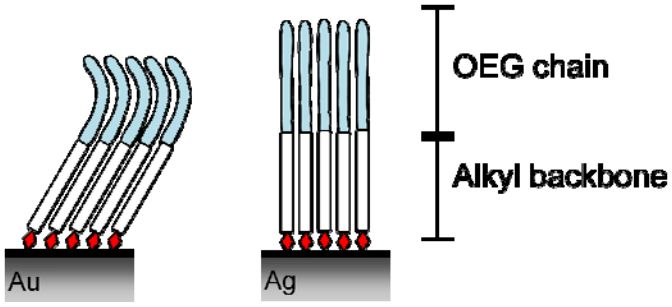

Figure 1-2: Molecular configurations of EG_3OMe thiolates on gold and silver substrates. EG_3OMe thiolate SAM on gold substrate adopts a helical configuration (left cartoon), while on silver substrate it adopts a planar all-trans configuration (right cartoon).

As the surface energy of a substrate depends on the chemical constituency of its surface, pure SAMs can be used to define the surface energy of a substrate by selection of their tail groups. Another way of modulating the surface energy of a substrate is by utilizing mixed SAMs of two or more components. Figure 1-3 shows a two-component mixed SAM displaying mixed functionalities on its surface. Several two-component mixed SAMs comprised of alkanethiols and hydrophilic organothiols displaying terminal moieties such as -COOH[67], -OH[67-69], $(OCH_2CH_2)_nOR$[55, 56, 58, 70, 71] where n = 3-6 and R = H or CH_3, have been investigated for their protein adsorption and/or cell attachment behaviors. In general, the level of protein adsorption decreased on surfaces containing high proportion of hydrophilic moieties, i.e. highly hydrophilic surfaces[55, 56, 58, 70, 71]. Mixed SAMs comprised of alkyl- and OEG-terminated thiolates (i.e. $(OCH_2CH_2)_nOR$)

exhibited resistance to protein adsorption when a critical density of OEG-terminated thiolate in the mixed SAM was reached[56, 58, 72]. Capadona et al.[70] reported that fibronectin adsorption on gold substrates can be controlled by modification of the substrates with mixed methyl and tri(ethylene glycol) terminated thiolate SAMs. This result was attributed to the reversible nature of the fibronectin adsorption to tri(ethylene glycol)-terminated SAMs, whereas fibronectin irreversibly adsorbs to methyl-terminated SAMs[72].

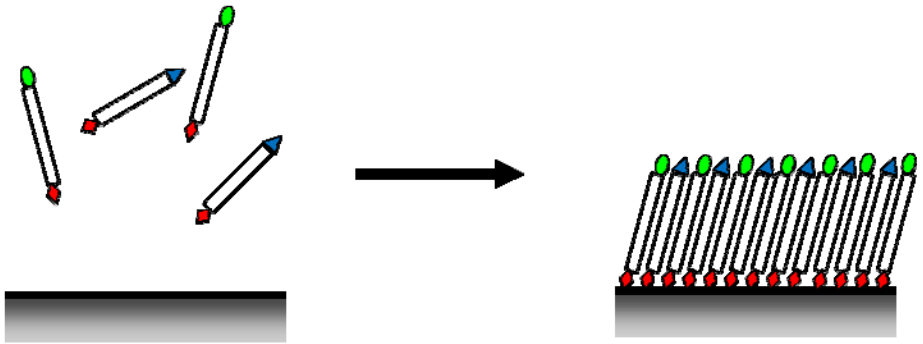

Figure 1-3: Two-component mixed SAM formed from molecules of different terminal groups.

In many ways, SAMs of oligo(ethylene glycol)-terminated alkanethiols, $HS(CH_2)_n(OCH_2CH_2)_mOH$, remain the 'gold standard' in terms of approaches to form biologically inert surfaces. In contrast to the well studied OEG-thiolate SAMs, there is much less data on SAMs formed from the corresponding OEG-silanes[47, 73-76].Lee and Laibinis[47] introduced SAMs of $Cl_3Si(CH_2)_{11}(OCH_2CH_2)_nOCH_3$ (n=2-4) as protein resistant coatings on SiO_2 surfaces. The presence of the $-OCH_3$ group on the EG tail is required for compatibility with the $SiCl_3$ head group and gives similar non-fouling abilities to that of the -OH terminus EG tail. The use of the trichlorosilane compound

yields robust anchoring to the surface and films that are able to maintain their anti-fouling properties when exposed to proteinaceous solutions[47]. Yanker and Maurer[75] used SAMs of $Cl_3Si(CH_2)_{11}(OCH_2CH_2)_3OCH_3$ to pattern SiO_2 substrates to selectively direct protein adsorption and cell growth. Hoffmann and Tovar[74] investigated mixed SAMs of $ClSi(CH_3)_2(CH_2)_{11}(OCH_2CH_2)_3OCH_3$ and $ClSi(CH_3)_2(CH_2)_{11}CH_3$ for controlling non-specific protein adsorption on oxide surfaces. Lee and Laibinis reported stability studies of OEG trichlorosilane films in comparison to the OEG thiolate films by exposing them to conditions where thiolate films decomposed[47]. For example, about 30% of OEG thiolate film desorbed within 5 min in boiling water and within 1 min in decahydronaphthalene at 90^oC and lost their abilities to resist non-specific adsorption of proteins, while OEG trichlorosilane films were stable for at least 1 h under these conditions. It is expected that well formed OEG trichlorosilane films on substrates are relatively stable due to their covalent linkages to the substrates. However, less stable OEG films have been reported by Dekeyser et al.[76] for pure SAMs of $(CH_3O)_3Si(CH_2)_3(OCH_2CH_2)_nOCH_3$ and $Cl_3Si(CH_2)_3(OCH_2CH_2)_nOCH_3$ (n=6-9) deposited onto SiO_2/Si substrates. The films were degraded upon 24 h incubation in phosphate buffer saline (PBS) due to surface hydrolysis. In contrast, I have observed that OEG trichlorosilane films were stable upon incubation in PBS for more than a week in our laboratory. Thus, OEG trichlorosilane is a suitable coating material for application in protein chromatography.

1.3. Motivation

This thesis aims to provide a generic chromatographic approach for separating proteins efficiently with high retention of their biological activity. For this purpose, I used supports that were surface functionalized to modulate protein-support interactions in a controlled manner and examine the performance of these systems for improving chromatographic processes. Porous silica particles were chosen as the support material as they can withstand the high pressures used in typical operations and their surfaces can be readily modified using silane reagents. Here, a silane reagent with a tri(ethylene glycol) tail group ($Cl_3Si(CH_2)_{11}(OCH_2CH_2)_3OCH_3$ (referred hereafter as EG_3OMe)) was used to form self-assembled monolayers on the silica surface. The goal was to create hydrophilic surfaces that interact minimally with proteins. Mixed self-assembled monolayers of EG_3OMe and $Cl_3Si(CH_2)_7CH_3$ (C8) were used to create surfaces with varying surface energies. The presence of hydrophobic tail groups among the hydrophilic OEG tail groups within a SAM will change the wetting properties of the surface and its level of interaction with a protein. Figure 1-4 illustrates an expected result for the proposed studies in that as the wettability of a surface decreases, a greater level of protein-surface interaction will result due to an increase in the interfacial energy between the surface and water. As the surface becomes more hydrophobic, its greater interfacial energy with water will lead to enhanced levels of protein adsorption that may be irreversible on the surface. The adsorption event may result in the disruption of the protein's native conformation and cause irreversible loss in its activity.

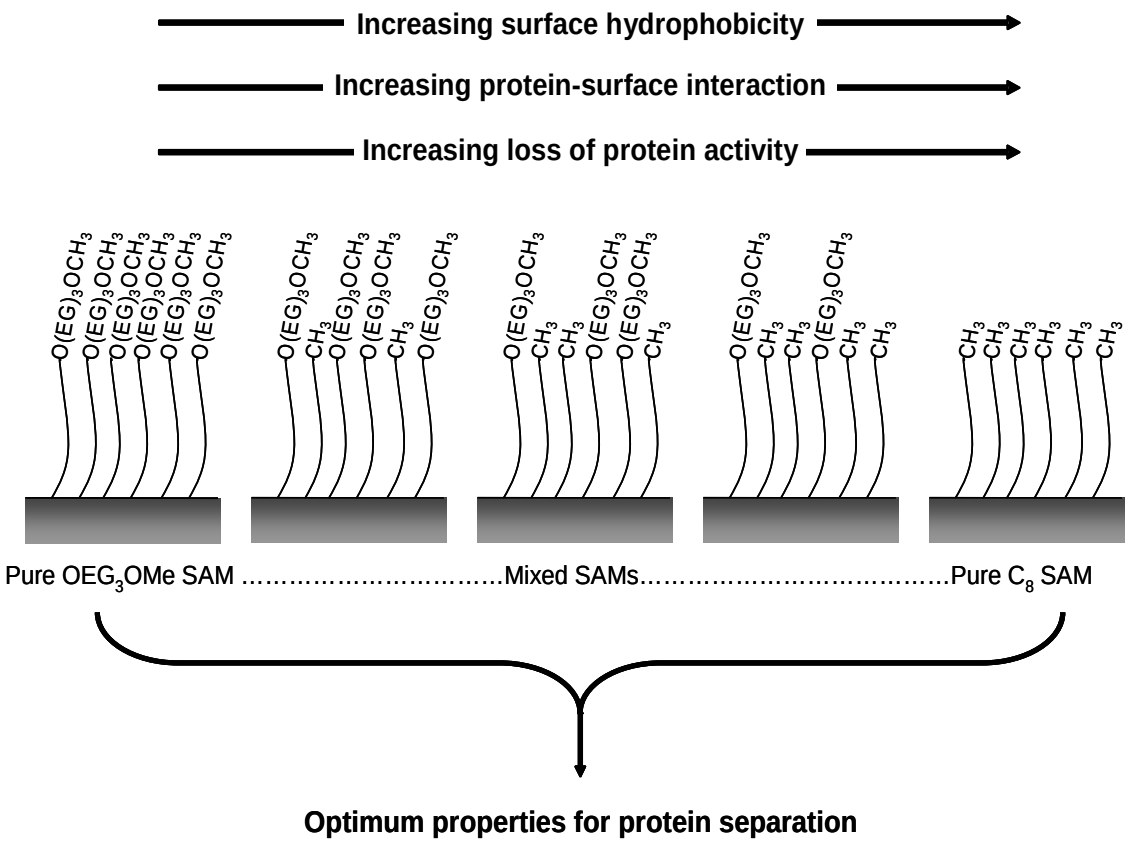

Figure 1-4: Use of mixed SAMs to control properties on a surface.

1.4. Thesis Overview

A key point for the success of this research is an ability to create well-controlled surface coatings on silica particles using mixed SAMs for the purpose of modulating protein separation in a chromatographic column. Chapter 2 of this thesis serves as the foundation for the rest of this thesis and it describes the establishment of self-assembly conditions for forming good quality mixed SAMs of various surface energies on flat substrates (i.e. SiO_2/Si). The advantage of working with flat substrates is that their surfaces can be conveniently characterized for determining film thicknesses, wettabilities, and surface chemical compositions using various surface characterization techniques.

Modulation of protein-surface interaction is demonstrated by mixed SAMs of varying surface energies.

The third chapter of this thesis describes the self-assembly of mixed SAMs on porous silica particles. The presence of surface coatings on these particles and their surface chemistries are characterized using the appropriate techniques. X-ray photoelectron spectroscopy (XPS) provides surface chemical composition of the functionalized porous silica. A microscale method based on flotation is developed for measuring the surface energies of mixed SAMs-coated silica particles. The properties of SAMs deposited on silica particles are compared to the same SAMs deposited on flat substrates, the results show that SAMs deposited on both supports have similar surface chemical properties.

Chapter 4 describes the set up of the chromatographic system for protein separation and the preparation of chromatographic columns that are packed with mixed SAMs-coated silica particles. The void time of a typical chromatographic column used in this research is determined and the column efficiency is analyzed in comparison to commercial columns.

In Chapter 5, the influence of surface hydrophobicity of mixed SAMs-coated supports on protein retention in chromatography is investigated using several model proteins. Isocratic protein retention data are obtained from chromatographic experiments. For comparison, the wettabilities of the supports' surfaces are determined by measuring the contact angle of a liquid on the corresponding mixed SAMs-coated SiO_2/Si. The energies involved in protein adsorption both on SiO_2/Si and silica particles are described by considering a reversible process of protein adsorption with minimal change in protein

conformation during the adsorption process. The results show that protein retention and separation in a chromatographic column is controllable by selecting the appropriate level of column hydrophobicity in addition to the effect of salt in the mobile phase on protein retention. The approach here could allow one to systematically select the appropriate column for protein separation and reduce the 'trial and error' process during the column selection.

Further analysis of the data from the protein retention experiments is presented in Chapter 6. Here, the effect of surface hydrophobicity of the column is related to the protein mass recovery from the chromatographic experiments. Finally, the last chapter of this thesis provides a summary of the key findings of my research and provides a brief discussion of future work that could stem from these results.

1.5. References

1. Ritter, S. K., *Chemical and Engineering News* **2008,** *86,* 63.

2. Gooding, K. M.; Regnier, F. E., *HPLC of Biological Macromolecules*. 2002; Vol. 87, p 162-168.

3. Queiroz, J. A.; Tomaz, C. T.; Cabral, J. M. S., Hydrophobic interaction chromatography of proteins. *Journal of Biotechnology* **2001,** *87* (2), 143-159.

4. Neue, U. D., *HPLC Columns Theory, Technology, and Practice*. Wiley-VCH, Inc.: New York, 1997.

5. Lienqueo, M. E.; Asenjo, J. A., Use of expert systems for the synthesis of downstream protein processes. *Computers and Chemical Engineering* **2000,** *24*, 2339-2350.

6. Jungbauer, A., Chromatographic media for bioseparation. *Journal of Chromatography A* **2005,** *1065* (1), 3-12.

7. Meyer, V. R., *Practical High-Performance Liquid Chromatography*. 4th ed.; John Wiley & Sons: Chichester, 2004.

8. Alberts, B.; Johnson, A.; Julian, L.; Raff, M.; Roberts, K.; Walter, P., *Molecular Biology of the Cell*. 4th ed.; Garland Science: New York, 2002.

9. Pace, C. N.; Shirley, B. A.; McNutt, M.; Gajiwala, K., Forces contributing to the conformational stability of proteins. *Federation of American Societies for Experimental Biology* **1996,** *10* (1), 75-83.

10. Buchmeiser, M. R., New synthetic ways for the preparation of high-performance liquid chromatography supports. *Journal of Chromatography A* **2001,** *918*, 233-266.

11. Sander, L. C.; Glinka, C. J.; Wise, S. A., Determination of bonded phase thickness in liquid chromatography by small angle neutron scattering. *Analytical Chemistry* **1990,** *62* (10), 1099-1101.

12. Sander, L. C.; Wise, S. A., Synthesis and characterization of polymeric C18 stationary phases for liquid chromatography. *Analytical Chemistry* **1984,** *56* (3), 504-510.

13. Sander, L. C.; Wise, S. A., Influence of Stationary Phase Chemistry on Shape Recognition in Liquid Chromatography. *Analytical Chemistry* **1995,** *67* (18), 3284-3292.

14. Srinivasan, G.; Meyer, C.; Welsch, N.; Albert, K.; Muller, K., Influence of synthetic routes on the conformational order and mobility of C18 and C30 stationary phases *Journal of Chromatography A* **2006,** *1113* (1-2), 45-54.

15. Wirth, M. J.; Fairbank, R. W. P.; Fatunmbi, H. O., Mixed self-assembled monolayers in chemical separations. *Science* **1997,** *275*, 44-47.

16. Wirth, M. J.; Fatunmbi, H. O., Horizontal polymerization of mixed trifunctional silanes on silica. 2. Application to chromatographic silica gel. *Analytical Chemistry* **1993,** *65* (6), 822-826.

17. Gooding, D. L.; Schmuck, M. N.; Gooding, K. M., Analysis of Proteins with new, mildly hydrophobic high-performance liquid chromatography packing materials. *Journal of Chromatography A* **1984,** *296*, 107-114.

18. Gooding, D. L.; Schmuck, M. N.; Nowlan, M. P.; Gooding, K. M., Optimization of preparative hydrophobic interaction chromatographic purification methods. *Journal of Chromatography A* **1986,** *359*, 331-337.

19. Hjertén, S.; Rosengren, J.; Pahlman, S., Hydrophobic interaction chromatography: The synthesis and the use of some alkyl and aryl derivatives of agarose. *Journal of Chromatography A* **1974,** *101* (2), 281-288.

20. Jennissen, H. P.; Demiroglou, A., Base-atom recognition in protein adsorption to alkyl agaroses. *Journal of Chromatography A* **1992,** *597* (1-2), 93-100.

21. Shaltiel, S., Hydrophobic chromatography. *Methods in Enzymology* **1974,** *34*, 126-140.

22. Kato, Y.; Kitamura, T.; Hashimoto, T., New support for hydrophobic interaction chromatography of proteins. *Journal of Chromatography A* **1984,** *292* (2), 418-426.

23. Kato, Y.; Kitamura, T.; Hashimoto, T., New resin-based hydrophilic support for high-performance hydrophobic interaction chromatography. *Journal of Chromatography A* **1986,** *360*, 260-165.

24. Chang, J.-p.; El Rassi, Z.; Horva´th, C., Silica-bound polyethyleneglycol as stationary phase for separation of proteins by high-performance liquid chromatography. *Journal of Chromatography A* **1985,** *319*, 396-399.

25. Chang, J.; An, J., Polyethylene glyco-bonded phases for protein separation by high-performance hydrophobic interaction chromatography. *Chromatographia* **1988,** *25* (4), 350-355.

26. Hatch, R. G., Chromatography of Proteins on a Silica-Based Support with Polyethylene Glycol Ligands. *Journal of Chromatographic Science* **1990,** *28* (4), 210-214.

27. Janzen, R.; Unger, K. K.; Giesche, H.; Kinkel, J. N.; Hearn, M. T. W., Evaluation of advanced silica packings for the separation of biopolymers by high-perforamnce liquid chromatography : V. Performance of non-porous monodisperse 1.5-um bonded silicas in the separation of proteins by hydrophobic-interaction chromatography. *Journal of Chromatography A* **1987,** *397*, 91-97.

28. Miller, N. T.; Feibush, B.; Karger, B. L., Wide-pore silica-based ether-bonded phases for separation of proteins by high-performance hydrophobic-interaction and size exclusion chromatography. *Journal of Chromatography A* **1985,** *316*, 519-536.

29. Hubert, P.; Mathis, R.; Dellacherie, E., Polymer ligands for mild hydrophobic interaction chromatography --principles, achievements and future trends. *Journal of Chromatography A* **1991,** *539* (2), 297-306.

30. Ling, T. G. I.; Mattiasson, B., Poly(ethylene glycol)- and poly(vinyl alcohol)-substituted carbohydrate gels for "mild" hydrophobic chromatography. *Journal of Chromatography A* **1983,** *254*, 83-89.

31. Dias-Cabral, A. C.; Pinto, N. G.; Queiroz, J. A., Studies on hydrophobic interaction adsorption of bovine serum albumin on polypropylene glycol–sepharose under overloaded conditions. *Separation Science and Technology* **2002,** *37* (7), 1505 - 1520.

32. Diogo, M. M.; Silva, S.; Cabral, J. M. S.; Queiroz, J. A., Hydrophobic interaction chromatography of Chromobacterium viscosum lipase on polypropylene glycol immobilised on Sepharose. *Journal of Chromatography A* **1999,** *849* (2), 413-419.

33. Jennissen, H. P., Hydrophobic interaction chromatography: the critical hydrophobicity approach. *International Journal of Biochromatography* **2000,** *5* (2), 131-163.

34. Kato, Y.; Nakamura, K.; Kitamura, T.; Moriyama, H.; Hasegawa, M.; Sasaki, H., Separation of proteins by hydrophobic interaction chromatography at low salt concentration. *Journal of Chromatography A* **2002,** *971* (1-2), 143-149.

35. Ulman, A., *An introduction to Ultrathin organic films*. Academic Press: Boston, 1991.

36. Ulman, A., Formation and structure of self-assembleld monolayers. *Chemical Reviews* **1996,** *96*, 1533-1554.

37. Love, J. C.; Estroff, L. A.; Kriebel, J. K.; Nuzzo, R. G.; Whitesides, G. M., Self-assembled monolayers of thiolates on metals as a form of nanotechnology. *Chemical Reviews* **2005,** *105*, 1103-1169.

38. Parikh, A. N.; Allara, D. L.; Azouz, I. B.; Rondelez, F., An Intrinsic Relationship between Molecular Structure in Self-Assembled n-Alkylsiloxane Monolayers and Deposition Temperature. *The Journal of Physical Chemistry* **1994,** *98* (31), 7577-7590.

39. Le Grange, J. D.; Markham, J. L.; Kurkjian, C. R., Effects of surface hydration on the deposition of silane monolayers on silica. *Langmuir* **1993,** *9* (7), 1749-1753.

40. Wasserman, S. R.; Whitesides, G. M.; Tidswell, I. M.; Ocko, B. M.; Pershan, P. S.; Axe, J. D., The structure of self-assembled monolayers of alkylsiloxanes on silicon: a comparison of results from ellipsometry and low-angle x-ray reflectivity. *Journal of the American Chemical Society* **1989,** *111* (15), 5852-5861.

41. Silberzan, P.; Leger, L.; Ausserre, D.; Benattar, J. J., Silanation of silica surfaces. A new method of constructing pure or mixed monolayers. *Langmuir* **1991,** *7* (8), 1647-1651.

42. Ladd, J.; Boozer, C.; Yu, Q.; Chen, S.; Homola, J.; Jiang, S., DNA-Directed Protein Immobilization on Mixed Self-Assembled Monolayers via a Streptavidin Bridge. *Langmuir* **2004,** *20* (19), 8090-8095.

43. Nelson, B. P.; Grimsrud, T. E.; Liles, M. R.; Goodman, R. M.; Corn, R. M., Surface Plasmon Resonance Imaging Measurements of DNA and RNA Hybridization Adsorption onto DNA Microarrays. *Analytical Chemistry* **2000,** *73* (1), 1-7.

44. Hodneland, C. D.; Lee, Y.-S.; Min, D.-H.; Mrksich, M., Selective immobilization of proteins to self-assembled monolayers presenting active site-directed capture ligands. *Proceedings of the National Academy of Sciences of the United States of America* **2002,** *99* (8), 5048-5052.

45. Heise, A.; Menzel, H.; Yim, H.; Foster, M. D.; Wieringa, R. H.; Schouten, A. J.; Erb, V.; Stamm, M., Grafting of Polypeptides on Solid Substrates by Initiation of N-Carboxyanhydride Polymerization by Amino-Terminated Self-Assembled Monolayers. *Langmuir* **1997,** *13* (4), 723-728.

46. Meagher, R. J.; Seong, J.; Laibinis, P. E.; Barron, A. E., A very thin coating for capillary zone electrophoresis of proteins based on a tri(ethylene glycol)-terminated alkyltrichlorosilane. *Electrophoresis* **2004,** *25* (3), 405-414.

47. Lee, S.-W.; Laibinis, P. E., Protein resistant coatings for glass and metal oxide surfaces derived from oligo(ethylene glycol)-terminated alkyltrichlorosilanes. *Biomaterials* **1998,** *19* (18), 1669-1675.

48. Schoenfisch, M. H.; Pemberton, J. E., Air Stability of Alkanethiol Self-Assembled Monolayers on Silver and Gold Surfaces. *Journal of the American Chemical Society* **1998,** *120* (18), 4502-4513.

49. Mani, G.; Johnson, D. M.; Marton, D.; Dougherty, V. L.; Feldman, M. D.; Patel, D.; Ayon, A. A.; Agrawal, C. M., Stability of Self-Assembled Monolayers on Titanium and Gold. *Langmuir* **2008,** *24* (13), 6774-6784.

50. Onclin, S.; Ravoo, B. J.; Reinhoudt, D. N., Engineering Silicon Oxide Surfaces Using Self-Assembled Monolayers. *Angewandte Chemie International Edition* **2005,** *44* (39), 6282-6304.

51. McGovern, M. E.; Kallury, K. M. R.; Thompson, M., Role of Solvent on the Silanization of Glass with Octadecyltrichlorosilane. *Langmuir* **1994,** *10* (10), 3607-3614.

52. Mrksich, M.; Whitesides, G. M., Using Self-Assembled Monolayers to Understand the Interactions of Man-Made Surfaces with Proteins and Cells. *Annual Review of Biophysics and Biomolecular Structure* **1996,** *25*, 55-78.

53. Jeon, S. I.; Andrade, J. D., Protein--surface interactions in the presence of polyethylene oxide: II. Effect of protein size. *Journal of Colloid and Interface Science* **1991,** *142* (1), 159-166.

54. Jeon, S. I.; Lee, J. H.; Andrade, J. D.; De Gennes, P. G., Protein--surface interactions in the presence of polyethylene oxide: I. Simplified theory. *Journal of Colloid and Interface Science* **1991,** *142* (1), 149-158.

55. Ostuni, E.; Grzybowski, B. A.; Mrksich, M.; Roberts, C. S.; Whitesides, G. M., Adsorption of proteins to hydrophobic sites on mixed self-assembled monolayers *Langmuir* **2003,** *19* (5), 1861-1872.

56. Pale-Grosdemange, C.; Simon, E. S.; Prime, K. L.; Whitesides, G. M., Formation of self-assembled monolayers by chemisorption of derivatives of oligo(ethylene glycol) of structure $HS(CH_2)_{11}(OCH_2CH_2)_mOH$ on gold. *Journal of the American Chemical Society* **1991,** *113* (1), 12-20.

57. Prime, K. L.; Whitesides, G. M., Self-assembled organic monolayers: model systems for studying adsorption of proteins at surfaces. *Science* **1991,** *252*, 1164-1167.

58. Prime, K. L.; Whitesides, G. M., Adsorption of proteins onto surfaces containing end-attached oligo(ethylene oxide): a model system using self-assembled monolayers. *Journal of the American Chemical Society* **1993,** *115* (23), 10714-10721.

59. Zheng, J.; Li, L.; Chen, S.; Jiang, S., Molecular Simulation Study of Water Interactions with Oligo (Ethylene Glycol)-Terminated Alkanethiol Self-Assembled Monolayers. *Langmuir* **2004,** *20* (20), 8931-8938.

60. Zheng, J.; Li, L.; Tsao, H.-K.; Sheng, Y.-J.; Chen, S.; Jiang, S., Strong repulsive forces between protein and oligo (ethylene glycol) self-assembled monolayers: a molecular simulation study. *Biophysical Journal* **2005,** *89*, 158-166.

61. Harder, P.; Grunze, M.; Dahint, R.; Whitesides, G. M.; Laibinis, P. E., Molecular conformation in oligo(ethylene glycol)-terminated self-assembled monolayers on gold and silver surfaces determines their ability to resist protein adsorption. *Journal of Physical Chemistry B* **1998,** *102* (2), 426-436.

62. Wang, R. L. C.; Kreuzer, H. J., Molecular conformation and solvation of oligo(ethylene glycol)-terminated self-assembled monolayers and their resistance to protein adsorption. *Journal of Physical Chemistry B* **1997,** *101*, 9767-9773.

63. Herrwerth, S.; Eck, W.; Reinhardt, S.; Grunze, M., Factors that Determine the Protein Resistance of Oligoether Self-Assembled Monolayers: Internal Hydrophilicity, Terminal Hydrophilicity, and Lateral Packing Density. *Journal of the American Chemical Society* **2003,** *125* (31), 9359-9366.

64. Li, L.; Chen, S.; Jiang, S., Protein interactions with oligo(ethylene glycol) (OEG) self-assembled monolayers: OEG stability, surface packing density and protein adsorption. *Journal of Biomaterials Science Polymer Edition* **2007,** *18*, 1415-1427.

65. Li, L.; Chen, S.; Zheng, J.; Ratner, B. D.; Jiang, S., Protein Adsorption on Oligo(ethylene glycol)-Terminated Alkanethiolate Self-Assembled Monolayers: The Molecular Basis for Nonfouling Behavior. *The Journal of Physical Chemistry B* **2005,** *109* (7), 2934-2941.

66. Vanderah, D. J.; La, H.; Naff, J.; Silin, V.; Rubinson, K. A., Control of Protein Adsorption: Molecular Level Structural and Spatial Variables. *Journal of the American Chemical Society* **2004,** *126* (42), 13639-13641.

67. Arima, Y.; Iwata, H., Effect of wettability and surface functional groups on protein adsorption and cell adhesion using well-defined mixed self-assembled monolayers. *Biomaterials* **2007,** *28* (20), 3074-3082.

68. Barrias, C. C.; Martins, M. C. L.; Almeida-Porada, G.; Barbosa, M. A.; Granja, P. L., The correlation between the adsorption of adhesive proteins and cell behaviour on hydroxyl-methyl mixed self-assembled monolayers. *Biomaterials* **2009,** *30* (3), 307-316.

69. Rodrigues, S. N.; Gonçalves, I. C.; Martins, M. C. L.; Barbosa, M. A.; Ratner, B. D., Fibrinogen adsorption, platelet adhesion and activation on mixed hydroxyl-/methyl-terminated self-assembled monolayers. *Biomaterials* **2006,** *27* (31), 5357-5367.

70. Capadona, J. R.; Collard, D. M.; Garcia, A. J., Fibronectin Adsorption and Cell Adhesion to Mixed Monolayers of Tri(ethylene glycol)- and Methyl-Terminated Alkanethiols. *Langmuir* **2003,** *19* (5), 1847-1852.

71. Hayashi, T.; Makiuchi, N.; Hara, M., Self-assembled monolayers with chemical gradients: fabrication and protein adsorption experiments. *Japanese Journal of Applied Physics* **2009,** *48*, 0955031-0955035.

72. Raynor, J. E.; Capadona, J. R.; Collard, D. M.; Petrie, T. A.; Garcia, A. J., Polymer brushes and self-assembled monolayers: Versatile platforms to control cell adhesion to biomaterials. *Biointerphases* **2009,** *4* (2), FA3-FA16.

73. Chan, Y.-H. M.; Schweiss, R.; Werner, C.; Grunze, M., Electrokinetic Characterization of Oligo- and Poly(ethylene glycol)-Terminated Self-Assembled Monolayers on Gold and Glass Surfaces. *Langmuir* **2003,** *19* (18), 7380-7385.

74. Hoffmann, C.; Tovar, G. E. M., Mixed self-assembled monolayers (SAMs) consisting of methoxy-tri(ethylene glycol)-terminated and alkyl-terminated dimethylchlorosilanes control the non-specific adsorption of proteins at oxidic surfaces. *Journal of Colloid and Interface Science* **2006,** *295* (2), 427-435.

75. Yanker, D. M.; Maurer, J. A., Direct printing of trichlorosilanes on glass for selective protein adsorption and cell growth. *Molecular BioSystems* **2008,** *4* (6), 502-504.

76. Dekeyser, C. M.; Buron, C. C.; Mc Evoy, K.; Dupont-Gillain, C. C.; Marchand-Brynaert, J.; Jonas, A. M.; Rouxhet, P. G., Oligo(ethylene glycol) monolayers by silanization of silicon wafers: Real nature and stability. *Journal of Colloid and Interface Science* **2008,** *324* (1-2), 118-126.

CHAPTER II

SELF-ASSEMBLY OF TRI(ETHYLENE GLYCOL)-TERMINATED SILANES IN PURE AND MIXED MONOLAYERS ON SiO_2/Si SUBSTRATES

2.1. Introduction

Self-assembled monolayers (SAMs) provide a reliable means for tailoring surfaces at the molecular scale. The ability of a SAM to expose a wide range of functionalities on its surface has allowed researchers to probe protein-surface interactions in a controlled manner[1]. This has resulted in new approaches for generating protein resistant surfaces. The traditional approach for modifying surfaces to render them protein resistant has been to attach long chain ethylene glycol compounds as a way to fully cover the surface and limit protein-surface interactions. In a series of seminal papers, Whitesides and coworkers found that surfaces formed from SAMs of alkanethiol terminating in short ethylene glycol chains (only 3 to 6 repeat units in length) exhibited 'inertness' toward protein adsorption[2-5]. In the films, oligo (ethylene glycol) (OEG) chain provides a fouling resistance to the SAM due to the highly hydrophilic nature of EG chains and their ready adsorption of water to form a hydrogel-like barrier that repels proteins and cells from the surface. In many ways, SAMs of oligo(ethylene glycol)-terminated alkanethiols, $HS(CH_2)_n(OCH_2CH_2)_mOH$, remain the 'gold standard' in terms of approaches to form biologically inert surfaces. Lee and Laibinis[6] introduced SAMs of $Cl_3Si(CH_2)_{11}(OCH_2CH_2)_nOCH_3$ (n=2-4) to produce a protein resistant coating on SiO_2 substrates. The presence of the $-OCH_3$ group on the EG tail is required for compatibility with the $SiCl_3$ head group and gives similar non-fouling abilities to that of the -OH

terminus EG tail. The use of the trichlorosilane compound yields robust anchoring to the surface and films that are able to maintain their protein resistant properties. OEG-terminated SAMs have been widely used for fabricating biosensors as a means to reduce the non-specific interaction of the probed protein with the surface[7].

As the surface energy of a substrate depends on the chemical constituency of its surface, SAMs can be used to modulate the surface energy of a substrate by selection of their tail groups. Further, the adsorption of a protein onto a surface in an aqueous environment is influenced by the surface energy of the substrate. Typically, surfaces with low energies such as octadecyltrichlorosilane (C18)-coated surface has strong interactions with proteins which lead to protein adsorption. On the other hand, the driving force for protein adsorption onto surfaces with high energies, like the above mentioned poly or oligo(ethylene glycol)-coated surfaces, is much less as compared to the low energy surfaces, which often results in reduced protein adsorption. For most biomedical applications, it is preferable to create surfaces of high protein repellency, i.e. high energy surfaces. For other application such as protein chromatography, the intermediate levels of surface energy are likely useful in providing moderate protein-surface interactions such that one could achieve efficient separation while preserving the bioactivity of the separated proteins[8].

Mixed SAMs of two or more components provide a way to create surfaces of different energies in a well-controlled manner. Several mixed SAMs of hydrophilic and hydrophobic moieties (eg. $HS(CH_2)_{11}(OCH_2CH_2)_3OCH_3/HS(CH_2)_nCH_3$ (n=1-2)[5, 9], $HS(CH_2)_{10}COOH/HS(CH_2)_{11}CH_3$[10],$ClSi(CH_3)_2(CH_2)_{11}(OCH_2CH_2)_3OCH_3/ClSi(CH_3)_2(C$

$H_2)_{11}CH_3$[11], $HS(CH_2)_{11}OH/HS(CH_2)_{15}CH_3$[12, 13]) have been investigated for their protein adsorption and/or cell attachment behaviors.

In this work, I used mixed SAMs of $Cl_3Si(CH_2)_{11}(OCH_2CH_2)_3OCH_3$ (EG_3OMe) and $Cl_3Si(CH_2)_7CH_3$ (C8) to create coatings of varying surface energies on SiO_2/Si substrates. The pure SAMs of the individual silanes have opposite properties. Pure EG_3OMe SAM exhibits surface hydrophilicity while pure C8 SAM exhibits surface hydrophobicity. The eight-alkyl chain length was chosen instead of longer alkyl-chain lengths to ensure homogeneous assembly of C8 molecules in between the eleven-alkyl backbone of EG_3OMe molecules in the mixed SAMs. Mixed SAMs with an enrichment of one component were obtained using a specified self-assembly condition. These mixed SAMs were characterized for their thicknesses, wettabilities, and surface compositions using various surface characterization techniques. Static protein adsorption experiments were performed to investigate the influence of surface energy on the level of protein-substrate interaction.

2.2. Materials and Methods

2.2.1. Materials

Solvents and most reagents were obtained from Sigma and used as received. Octadecyltrichlorosilane (C18) was purchased from Fisher, while octyltrichlorosilane (C8) was from Gelest. Test grade Silicon wafers (SiO_2/Si <100>, boron-doped, 675 μm thickness) were purchased from Montco Silicon Technologies Inc. Albumin (bovine serum), fibrinogen (fraction 1, type I-S, bovine plasma), catalase (bovine liver), and

lysozyme (chicken egg white) were from Sigma. Phosphate buffer saline (PBS) was obtained from MP Biomedicals.

2.2.2. Synthesis of EG_3OMe

Scheme 2-1 shows the two-step synthesis of EG_3OMe. First, 8.7 mmol NaH was dissolved in 30 mL of anhydrous dimethylformamide (DMF). 26 mmol of tri(ethylene)glycol monomethyl ether ($H(OCH_2CH_2)_3OCH_3$) was then added to the DMF solution and the mixture was stirred for 30 min. Finally, 8.6 mmol of 11-bromo-1-undecene ($CH_2=CH(CH_2)_9Br$) was added and the mixture was stirred under N_2 atmosphere at room temperature. After 7 h of reaction, the mixture was extracted four times with hexane, and the collected extracts were concentrated using a rotary evaporator. The extracts were separated by flash chromatography on silica gel with gradient elution of hexane/ethyl acetate mixtures. The yield of the purified product (1) was ~80%. ^{1}H-NMR (400 MHz, $CDCl_3$): δ 1.2-1.5 (m, 12 H), 1.56 (p, 2 H), 2.05 (q, 2H), 3.38 (s, 3 H), 3.45 (t, 2 H), 3.5-3.75 (m, 12 H), 4.95 (q, 2 H), 5.8 (m, 1 H).

The second step of the synthesis is the following. 0.12 mmol of $H_2PtCl_6.6H_2O$ was first dissolved in 1 mL of anhydrous tetrahydrofuran (THF). This THF solution was then added to a mixture of 5.8 mmol of **(1)** and 17.4 mmol of $HSiCl_3$ in a N_2 glove box. The resulting mixture was stirred for ~2 h. The completion of the silylation reaction was identified when the yellowish milky solution mixture turned into a clear solution. The final product **(2)** in a yield of ~88% was obtained after the removal of unreacted $HSiCl_3$ in Kugelrohr (operated at 180^{o}C). ^{1}H-NMR (400 MHz, $CDCl_3$): δ 1.2-1.5 (m, 16 H), 1.56 (m, 4 H), 3.38 (s, 3 H), 3.45 (t, 2 H), 3.5-3.75 (m, 12 H).

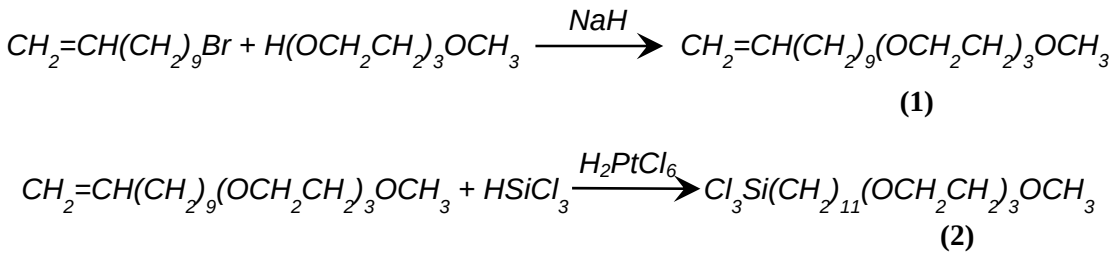

Scheme 2-1: Synthesis of EG_3OMe

2.2.3. Formation of Self-Assembled Monolayers (SAMs) on SiO_2/Si

SiO_2/Si substrates (1 x 3 cm^2) were cleaned by immersion in freshly prepared piranha solution (conc. H_2SO_4/H_2O_2 (7/3 v/v) for 1 h at room temperature) or freshly prepared RCA solution ($NH_4OH/H_2O_2/H_2O$ (5/2/2 v/v/v) solution for 20 min at 80^oC). The substrates were then washed with copious amounts of deionized water, and blown dried with N_2 before use.

SAMs were typically formed from 2 mM solution of pure silane (or mixed silanes) in toluene at 25 ^oC or 60 ^oC. After 4-24 h of reaction, the substrates were removed from the silane solution, washed with toluene, followed by ethanol, and blown dried with N_2. The ellipsometric thicknesses of the films on the SiO_2 substrates were usually measured immediately, followed by water contact angle measurements.

2.2.4. Characterizations of SAM

Water Contact Angle Measurements

The advancing and receding contact angles on the surfaces were measured with a goniometer (Ramé-Hart Inc, NJ) equipped with an automatic pipeting system that

delivered ~3 μL of water drops on each measurement. At least three measurements were done on each sample surface.

Ellipsometric Measurements

The thicknesses of the films on the SiO_2/Si surfaces were measured with a Stokes Ellipsometer LSE (Gaertner Scientific Corporation, IL). The light source was 6328 Å HeNe Laser with 70^o incidence angle. The range of error from the equipment was ± 1 Å. The refractive index of the film was assumed to be 1.45[14]. For each sample surface, the film thickness was measured at three different locations.

X-Ray Photoelectron Spectroscopy (XPS) Measurements

The chemical compositions of the films on SiO_2/Si surfaces were analyzed by XPS (Phi 5000 VersaProbe, Ulvac-Phi Inc.) using a monochromatic Al Kα x-ray source (1486.6 eV) and a concentric hemispherical analyzer. The take-off angle (angle between the surface parallel and the axis of the electron analyzer) was 45^o. C(1s), Si(2p), and N(1s) spectra were averaged over 20, 10, and 45 scans, respectively. The step width for all elemental scans was set at 0.1 eV. The pass energy for C(1s) and Si(2p) scans was 23.5 eV, while that for N(1s) was 58.7 eV. The XPS spectra were fitted using CasaXPS software (version 2.3.14) with 30% Gaussian/Lorentzian peaks and a Shirley background.

2.2.5. Protein Adsorption Experiments

Various proteins were dissolved in 1 M of PBS with a protein concentration of 0.25 mg/mL. SAM-functionalized SiO_2/Si substrates were incubated in a protein solution

for 16-24 h at 25 ^{o}C. After incubation, the substrates were washed several times with PBS and deionized water. Further, the substrates were blown dried with N_2 before their ellipsometric thicknesses were measured. The levels of protein adsorption were also measured using XPS by quantifying the level of N(1s) signal on the surface.

2.3. Results and Discussion

2.3.1. Self-Assembled Monolayers of EG_3OMe and Octadecyltrichlorosilanes (C18)

Various parameters can affect the self-assembly of trichlorosilane molecules from solution to form well-defined monolayer films on a surface: water content in the solvent, the type of solvent, the temperature of self-assembly, etc. The presence of water in the solution and at the surface of the substrates is critical as water participates in coupling silanol groups to link the silane molecules to hydroxyl groups on the substrate's surface[15-18]. Trace water is needed, but excess amounts of water promote unwanted polymerization of the silane in solution and lead to the formation of poor quality monolayers or multilayers. The selection of solvent also affects self-assembly. McGovern et al.[19] found that aromatic solvents such as toluene and benzene can extract significant amounts of water from the substrate causing polymerization of silane to occur in solution prior to deposition on a surface. For self-assembly, the solvent needs to provide a driving force that can direct the silane to the reacting surface. Further, several researchers[17, 18, 20, 21] have observed the effect of temperature on the formation of SAMs. For example, SAMs of C18 exhibit a critical temperature of ~28 ^{o}C above which lower quality monolayers are formed[17, 18].

In this work, I used SAMs of C18 as a benchmark in establishing the conditions for forming pure and mixed SAMs of EG_3OMe on SiO_2/Si substrates. The SAM of C18 is a well-studied example of a densely packed monolayer and its surface properties have been well characterized by many researchers. I used 2 mM of C18 in toluene to form the SAMs on SiO_2/Si substrates using 24 h of reaction time at room temperature. The resulting films had a thickness of 26 ± 1 Å with advancing and receding water contact angles of 112 ± 1° and 107 ± 2°, respectively. The thickness of the C18 SAMs compares well to the theoretical thickness of an extended C18 chain oriented normal to a surface[15]. The surface properties of the C18 SAMs here are in agreement with various published results[15, 19, 22].

To obtain the best conditions for the self-assembly of EG_3OMe, I performed a series of experiments using two different solutions for surface cleaning (i.e. piranha and RCA solutions) and various temperatures for the self-assembly. Toluene was used as the solvent for the self-assembly of EG_3OMe. Toluene from a freshly opened bottle was found to work best for forming good EG_3OMe films. Figure 2-1 shows the water contact angles, film thicknesses, and protein (BSA) adsorption behavior of EG_3OMe films formed at four different conditions. In this figure, EG_3OMe films formed on SiO_2/Si surfaces cleaned with piranha solution, regardless the self-assembly temperature, generally had thicknesses of less than 16.5 Å and advancing water contact angles of 61° or greater. These films adsorbed ~5-11 Å of protein. Similar film properties were obtained for EG_3OMe SAMs formed on RCA cleaned SiO_2/Si substrates in the silane solution at 25 °C. However, when the self-assembly temperature was raised to 60 °C, I obtained films of EG_3OMe SAM that were thicker and more hydrophilic than those

formed under the other conditions. These films also showed excellent protein repellant properties (i.e. adsorbed <1 Å of protein). It is worth noting that the thickest obtained EG_3OMe film was 18 ± 1 Å. This value was less than that predicted for an extended chain of the molecule oriented normal to the surface suggesting that these films were not as densely packed as films formed from the self-assembly of hydrocarbon trichlorosilanes, such as C18[15]. However, similar film thicknesses have been obtained previously by Pale et al.[3] and Zhu et al.[16] for EG_3OH and EG_3OMe-terminated alkanethiols on gold surfaces, respectively. Another interesting phenomenon shown in Figure 2-1 is that a difference in only a few degrees in the water contact angle can lead to a moderate change in protein adsorption. This is exemplified by the lack of protein adsorption on EG_3OMe films having water contact angle of 60^o or less, while some level of protein adsorption was observed on films having water contact angles of greater than ~60^o.

The protein repellant abilities of the EG_3OMe films were examined against four proteins having different molecular weights. As a comparison, protein adsorption experiments were also done on hydrophobic surfaces formed from the self-assembly of C18. The levels of protein adsorption onto the C18 and EG_3OMe SAMs are illustrated in Figure 2-2. In all cases, the C18 SAMs adsorbed roughly a monolayer of protein[6], with the thickness of the adsorbed protein increasing with the size of the protein. The presence of the ethylene glycol chains in the SAM reduced the level protein adsorption by ~90% or more for the investigated proteins.

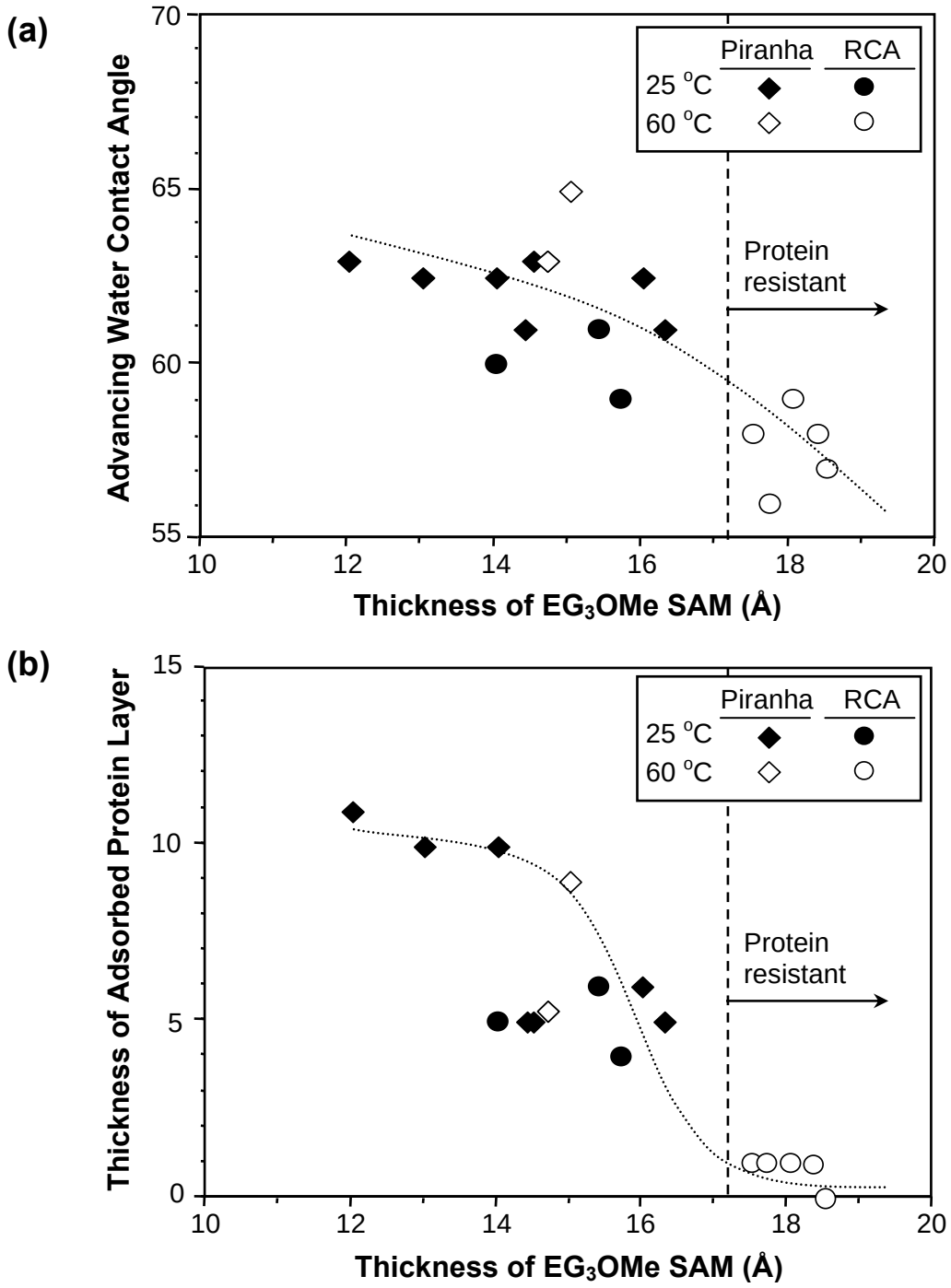

Figure 2-1: Properties of EG_3OMe SAMs formed from various self-assembly conditions: (a) advancing water contact angles, and (b) ellipsometric thickness of adsorbed protein layer. Protein adsorption was performed in solutions containing 0.25 mg/mL of bovine serum albumin in PBS for the period of 16-24 h. Lines are provided as guides to the eye.

I also examined the level of protein adsorption using XPS by quantifying the N(1s) signals from the protein-treated samples. Table 2-1 shows the integrated areas under the N(1s) envelopes for BSA and fibrinogen-treated samples. All values in this table had been subtracted with the values of N(1s) signals from the untreated substrates. The results in Table 2-1 agree well with the ellipsometric measurements shown in Figure 2-2 and indicate that the levels of protein adsorption on EG_3OMe surfaces treated with BSA and fibrinogen were less than 5% of that on the C18 surfaces.

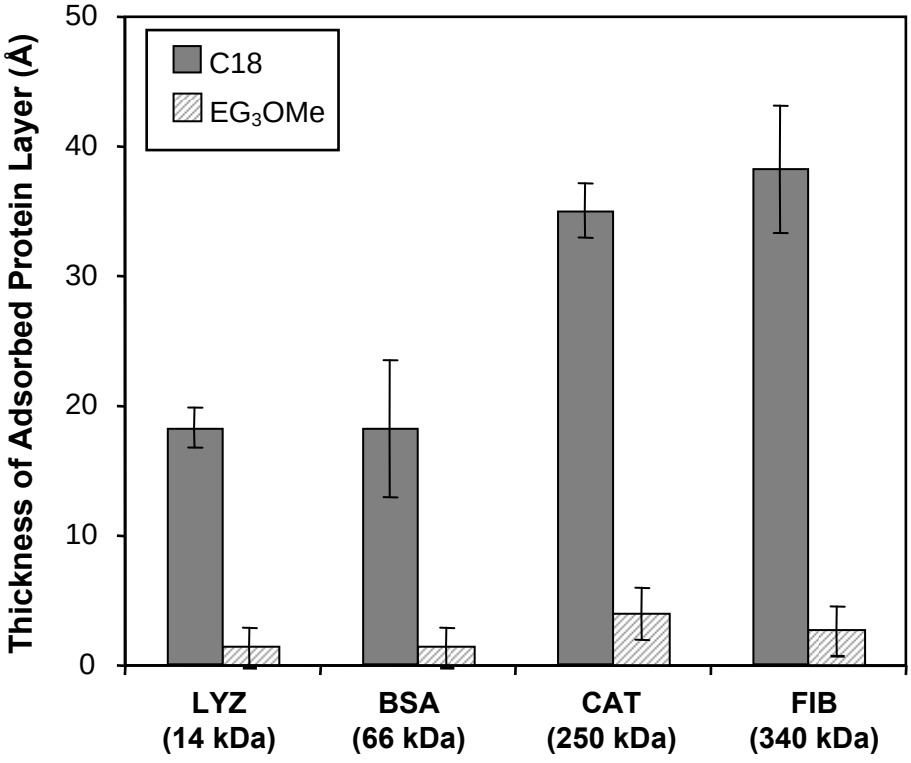

Figure 2-2: Differences in the adsorption of lysozyme (LYZ), bovine serum albumin (BSA), catalase (CAT), and fibrinogen (FIB) onto pure EG_3OMe and C18 SAMs as detected by ellipsometry. C18 SAMs were formed from 2 mM solution of silane in toluene for 24 h at room temperature.

Table 2-1: N(1s) Signals from Protein-Treated Samples

	BSA	Fibrinogen
EG_3OMe SAM	15 ± 35	40 ± 30
C18 SAM	4310 ± 115	9790 ± 120

Influence of Trace Water in Toluene on the Properties of SAMs

At the inception of this research, it was observed that the 'wetness' of the toluene affected the properties of EG_3OMe films. A series of experiments were performed to systematically examine the above observation by forming EG_3OMe films from solutions containing anhydrous toluene that had been spiked with various amounts of trace water. Figure 2-3 shows the effect of trace water in toluene on the properties of EG_3OMe films. In Figure 2-3(a), the average thickness for all freshly formed films was ~ 17 ± 1 Å. After wiping these films with a wet Kimwipe paper, changes in the film thickness were observed. The data in Figure 2-3(a) show that for films formed from toluene with an added water concentration of less than 0.1 mM, the thicknesses of the films were unchanged after wiping. On the other hand, the thicknesses of the wiped films decreased when the films were formed from toluene containing more than 0.1 M of added water concentration. Thus, too much water in toluene promotes unwanted polymerization of the EG_3OMe silane in the solution as compared to surface polymerization as indicated by the result in Figure 2-3(a). Figure 2-3(b) shows the advancing and receding water contact angles on the wiped EG_3OMe films. The water contact angles on these films increased along with the decrease in the film thicknesses. This result is in agreement with the previous result in Figure 2-1 that thin EG_3OMe films have less wettable surfaces. The behavior of BSA adsorption on EG_3OMe films in Figure 2-3(a) is also in accord with the previous result that the films with water contact angle of 60^o or less have protein repellent

properties, while those with water contact angle of just few degrees higher than 60^{o} exhibit some levels of protein adsorption.

It is worth noting in Figure 2-3(a) that the film formed from anhydrous toluene, despite being the thickest film as compared to other films, exhibited some degree of protein adsorption. This also means that a film with a high packing density does not completely repel protein. Similar behavior has been observed before by Jiang et al.[22, 23] for densely packed $HS(CH_2)_{11}(OCH_2CH_2)_nOH$ (n=2-4) films on gold in that these films adsorbed 6-9 % of a protein layer. Slightly less dense films exhibit protein resistance properties. Interestingly, the effect of water on the formation of OEG films from thiol- and silane-based molecules exhibit an opposite trend. In this research, trace water in toluene results in reduced density of the silane-based films, while in Jiang's work[22, 23] the inclusion of 5% of water in ethanoic solution increases the density of the thiol-based films. The common result is that films with less dense packing exhibit the best protein resistance properties.

The results in Figure 2-3 suggest that the presence of trace amount of water (in this case for the concentration of added water of less than 0.1 mM) is essential for forming good quality EG_3OMe films. Aside from this study, regular toluene from a freshly opened bottle was used for most of the experiments in my research as it produced good quality films. It can be expected the toluene contained a suitable amount of trace water.

The influence of trace water in toluene on the properties of C18 films is shown in Figure 2-4. The film thicknesses for C18 films formed from toluene with differing water content were unchanged after wiping (data of original thicknesses not shown). In Figure

2-4(a), the films formed from anhydrous toluene were thinner than a fully grown monolayer (i.e. film thickness of 26 ± 1 Å) which suggests incomplete monolayer formation after 24 h of reaction. The presence of trace water in the toluene promotes the formation of good quality C18 films (i.e. film thickness of 26 ± 1 Å with advancing and receding water contact angles of 112 ± 1^{o} and 107 ± 2^{o}, respectively), regardless of the amount. Figure 2-5 shows the growth rates of C18 films in toluene solution containing various amounts of added trace water. A complete monolayer was not obtained when the C18 silanes were assembled in anhydrous toluene, even after 48 h of reaction. The addition of up to 0.55 mM of trace water in the toluene resulted in the formation of complete C18 monolayers within 24 h of reaction. The presence of 5.5 mM of added water in the toluene expedited the formation of C18 monolayers since complete monolayers were obtained in 2-5 h of reaction. These results suggest that the role of trace water in toluene appears to enhance the self-assembly of C18 silanes onto the substrates.

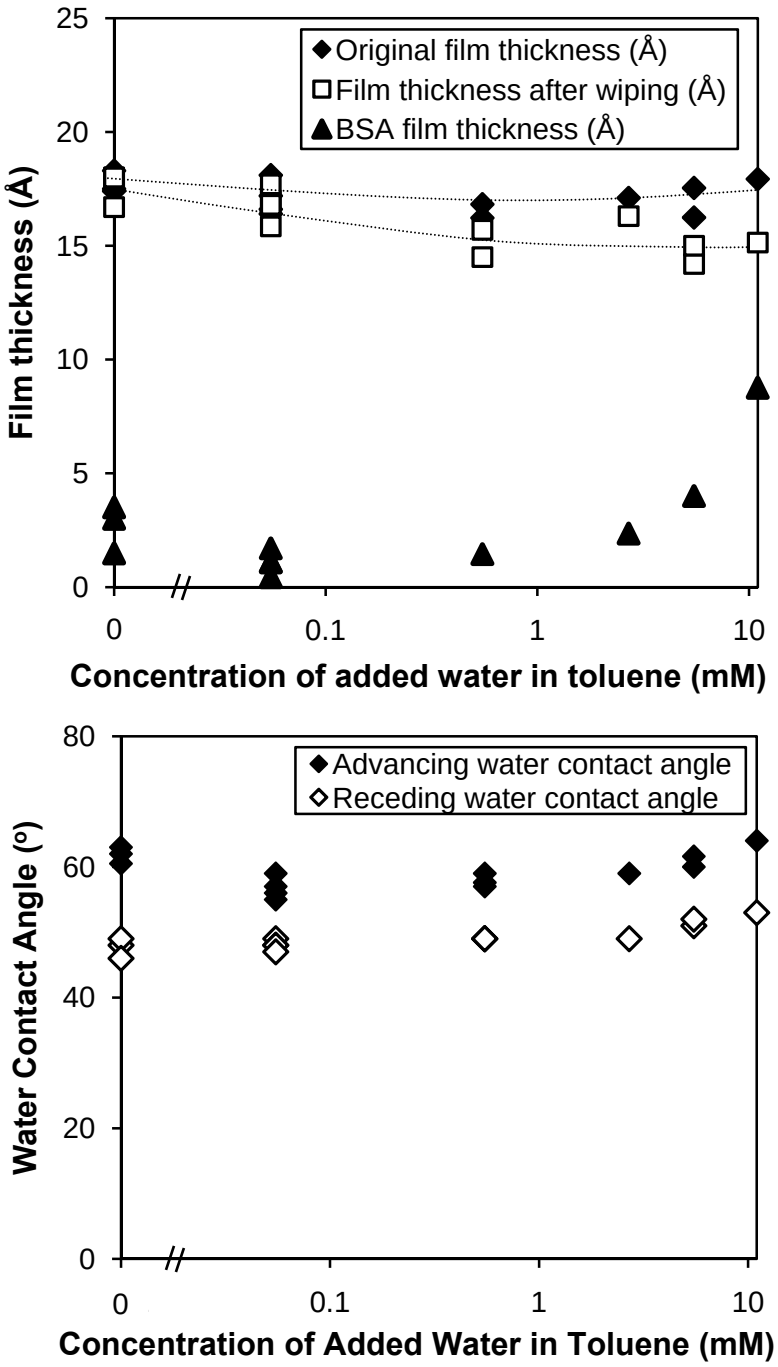

Figure 2-3: Effect of trace water in toluene on (a) the thickness of EG_3OMe films and film repellency towards BSA adsorption, (b) wettability of EG_3OMe films after wiping. Experiments were performed by dissolving various amounts of trace water in anhydrous toluene. The solutions were left to equilibrate for overnight before they were used for the self-assembly experiments. The concentration of EG_3OMe silane in the solution was 2 mM. Period of self-assembly was 4 h. Lines are provided as guides to the eye.

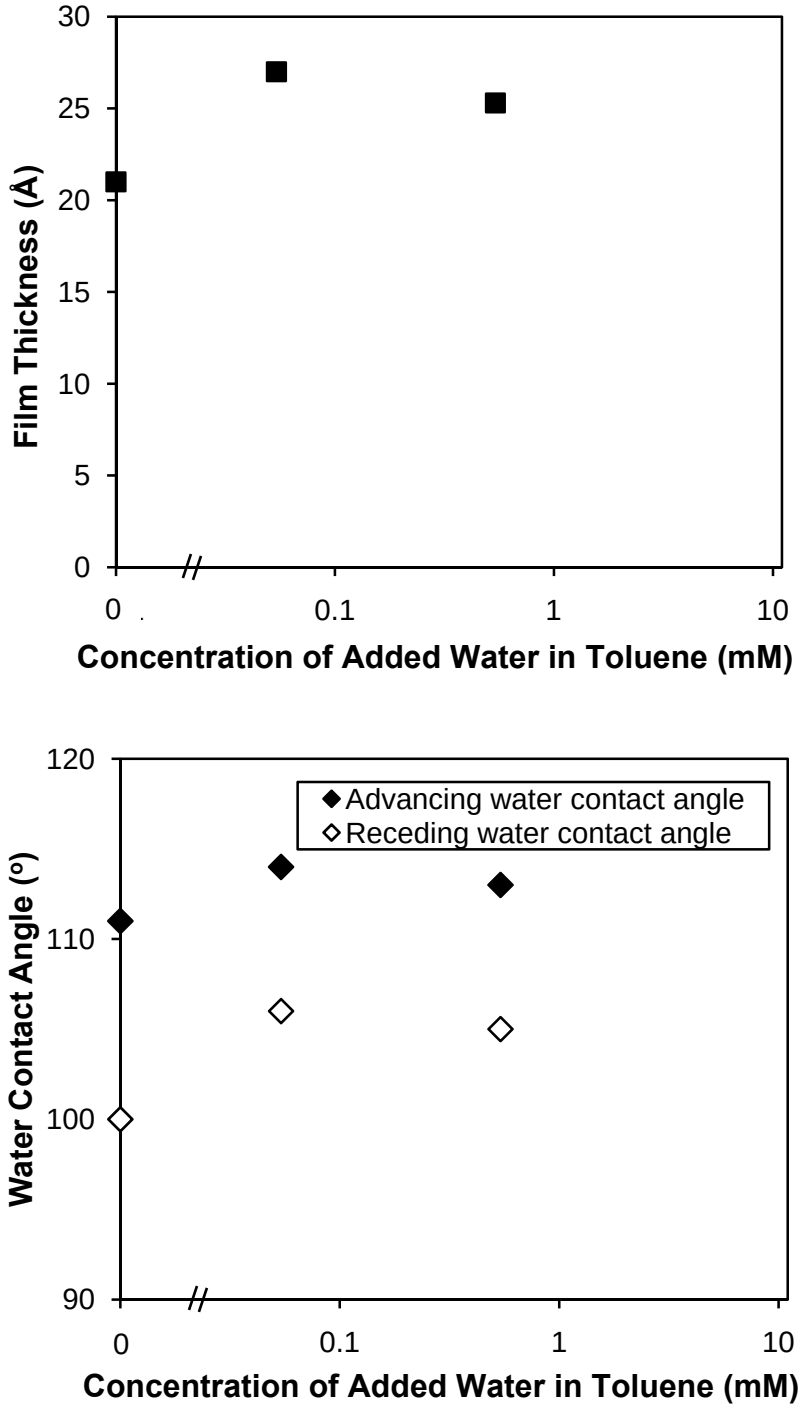

Figure 2-4: Effect of trace water in toluene on (a) the thickness and (b) wettability of C18 films after wiping. Experiments were performed by dissolving various amounts of trace water in anhydrous toluene. The solutions were left to equilibrate for overnight before they were used for the self-assembly experiments. The concentration of C18 silane in the solution was 2 mM. The period of self-assembly was 24 h.

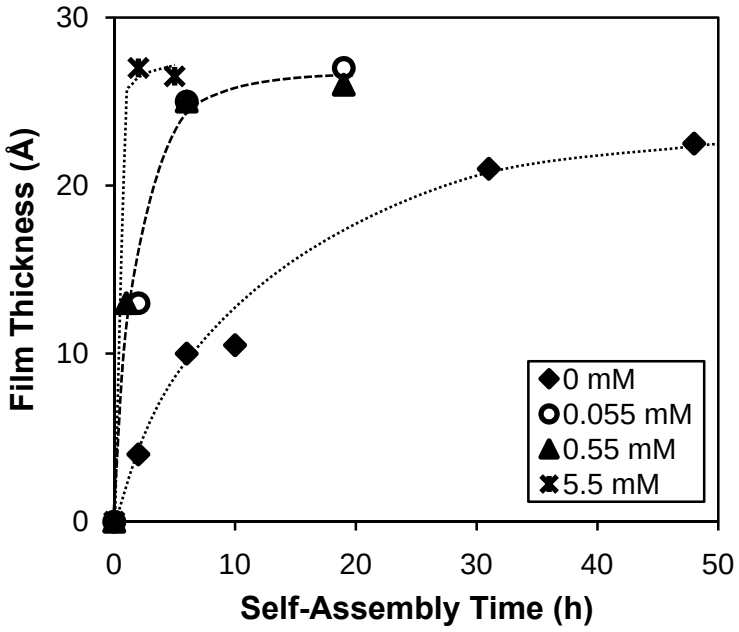

Figure 2-5: The influence of added trace water in toluene on the growth rates of C18 SAMs. Self-assembly was carried out at room temperature. Lines are added as guides to the eye.

2.3.2. Mixed Self-Assembled Monolayers of EG_3OMe and C8

Surface Characterization of Mixed SAMs

The established self-assembly conditions from the previous section were used to form mixed SAMs of EG_3OMe and C8. These films were formed on RCA cleaned SiO_2/Si substrates from 2 mM of toluene solutions for 4 h at 60 ^oC. Figure 2-6 shows the advancing and receding water contact angles on mixed SAMs at various compositions. The water contact angles decrease with increases in the concentration of EG_3OMe in the forming solutions. This result is as expected as more hydrophilic OEG groups are more available to shield the underlying alkyl groups on the surface from interacting with water. Hoffmann and Tovar[11] reported a linear decrease in water contact angles on their mixed SAMs of EG-terminated dimethylsilane and dodecyldimethylsilane with increasing mol

fraction of EG silane in the silanization solution. The differences with these results is probably due to the self-assembly temperature used in this work that favored the deposition of EG_3OMe on the surfaces as compared to that of C8. Several researchers[17, 18, 20, 21] have observed the effect of temperature on the formation of SAMs. I have found that forming C8 SAM at 60 ^oC resulted in films that were less dense as compared to those formed at room temperature. This is indicated by the lowered values of water contact angle and ellipsometric thickness as compared to those of densely packed C8 SAM[15].

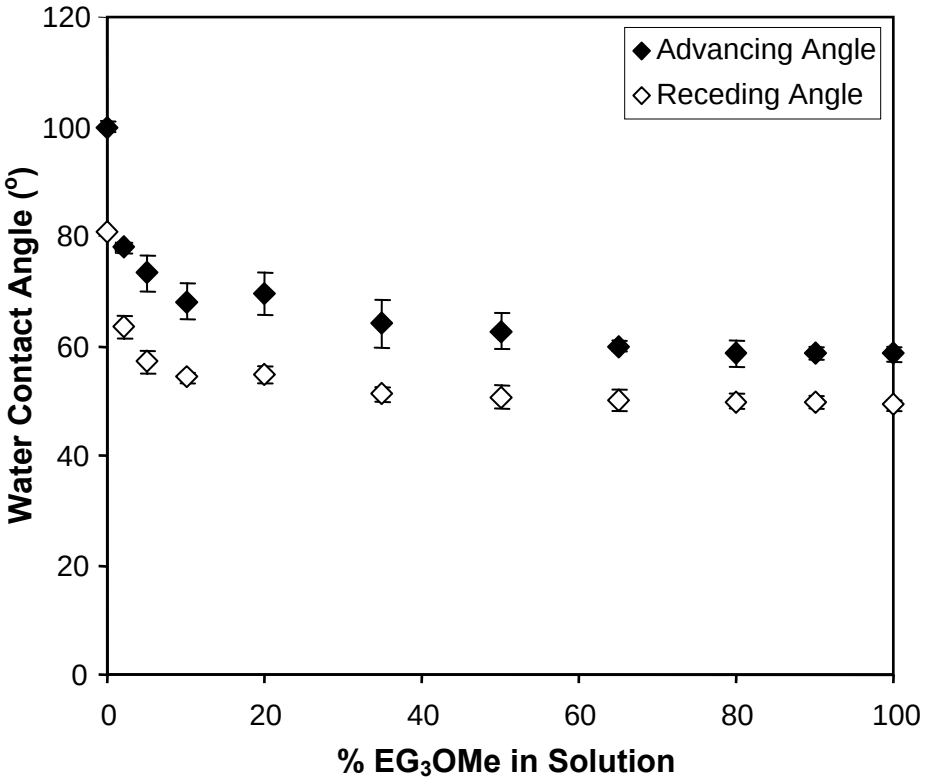

Figure 2-6: Water contact angles on mixed SAMs at various compositions of EG_3OMe and C8 in the forming solutions.

Figure 2-7(a) shows the result of ellipsometric measurements on surfaces coated with mixed SAMs. At the low concentrations of EG_3OMe in the solutions, the measured

film thicknesses were thicker than both the thicknesses of the pure C8 and pure EG_3OMe SAMs. This unexpected result may be due to the C8 molecules being able to pack well among the EG_3OMe molecules thus providing a denser packed underlying alkyl regions in the mixed SAM than for the pure EG_3OMe SAM. At the lower amounts of C8, the film thicknesses approached a thickness of ~18 Å for the pure EG_3OMe SAM. In Figure 2-7(b), the intensity ratios of C(1s)/Si(2p) obtained from XPS on mixed SAMs formed at various silane compositions agree well with the ellipsometric measurements. Mixed SAMs formed from solutions of low concentration of C8 exhibited higher attenuation of Si(2p) signals as compared to those formed from other solution compositions, indicating a greater amount of material on the SiO_2/Si surface.

Figure 2-8 shows XPS spectra of the C(1s) regions of mixed SAMs at selected mixture compositions. In Figure 2-8(a), the alkyl carbons in pure C8 SAM are indicated by the photoelectron intensity from a carbon atom next to another carbon atom with a peak intensity at the binding energy of 284.6 eV (labeled as C-C). There are two identifiable peak intensities in the C(1s) spectrum of the EG_3OMe SAM in Figure 2-8(c). The C-C intensity is contributed by the underlying alkyl carbons in the EG_3OMe SAM, while carbons in the OEG segments in the EG_3OMe SAM are indicated by the photoelectron intensity for carbon atoms at a higher binding energy. These carbons are next to an oxygen atom (labeled as C-O). Thus, the amount of EG_3OMe incorporated in a mixed SAM could be tracked from its C-O photoelectron intensity in the C(1s) spectral region. Figure 2-9 shows the C-O intensity from a series of mixed SAMs normalized to that for a pure EG_3OMe SAM, with respect to the percentage of EG_3OMe in the forming solution. This figure demonstrates that the amount of EG_3OMe on the mixed SAM

surface increases when the percentage of EG_3OMe is increased in the forming solutions. The relationship in Figure 2-9 is not linear due to the preferential incorporation of EG_3OMe in the mixed SAMs. This is as expected due to the use of self-assembly condition that favors the formation of EG_3OMe SAMs. The enrichment in the EG_3OMe on the surface relative to its composition in solution is possibly caused by the higher solubility of C8 at 60 ^oC in toluene that would decrease its partitioning to the surface.

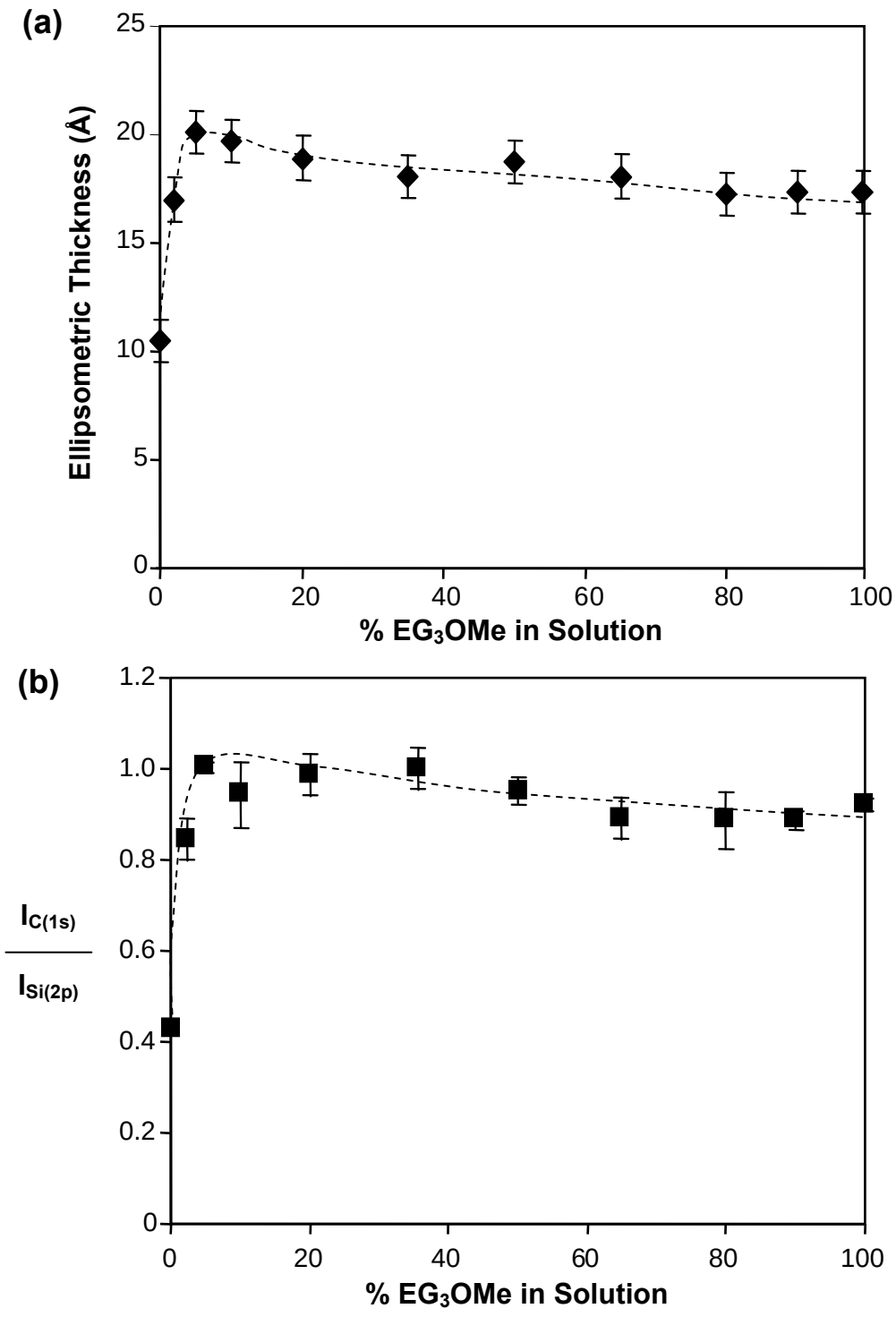

Figure 2-7: (a) Ellipsometric thickness of and (b) XPS intensity ratio of C(1s) and Si(2p) on mixed SAMs formed at various solution compositions. Lines are provided as guides to the eye.

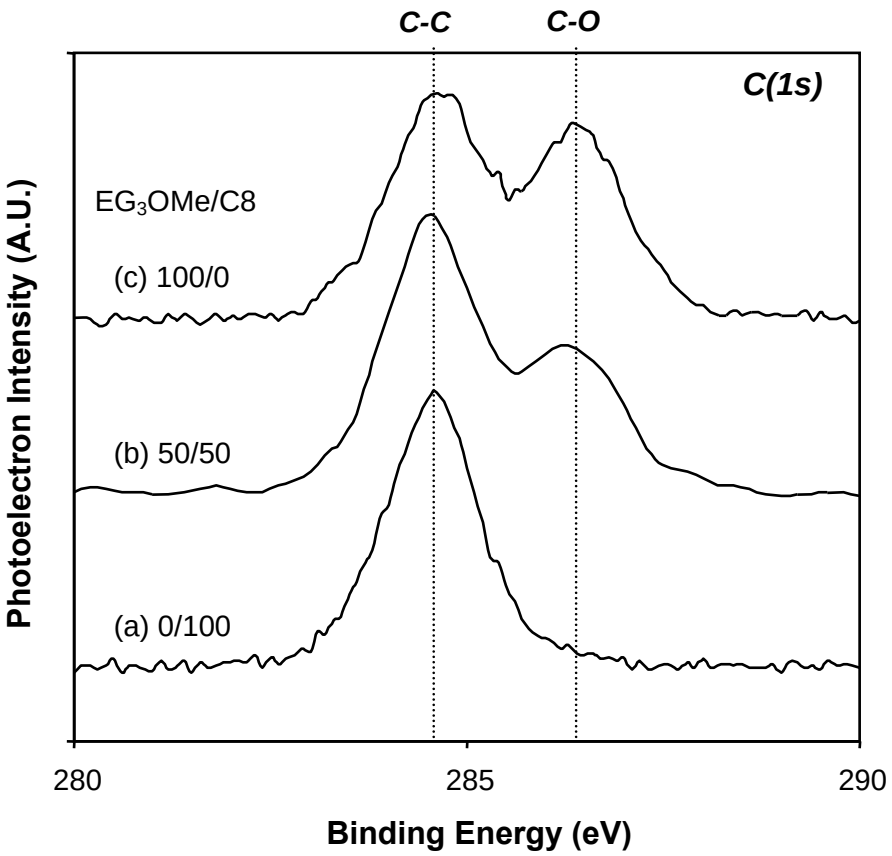

Figure 2-8: XPS spectra of the C(1s) region for (a) pure C8 SAM, (b) mixed SAM formed from a mixture of 50% EG_3OMe and 50% C8 in the solution, and (c) pure EG_3OMe SAM. Each spectrum was adjusted to have the C-C peak intensity at 284.6 eV.

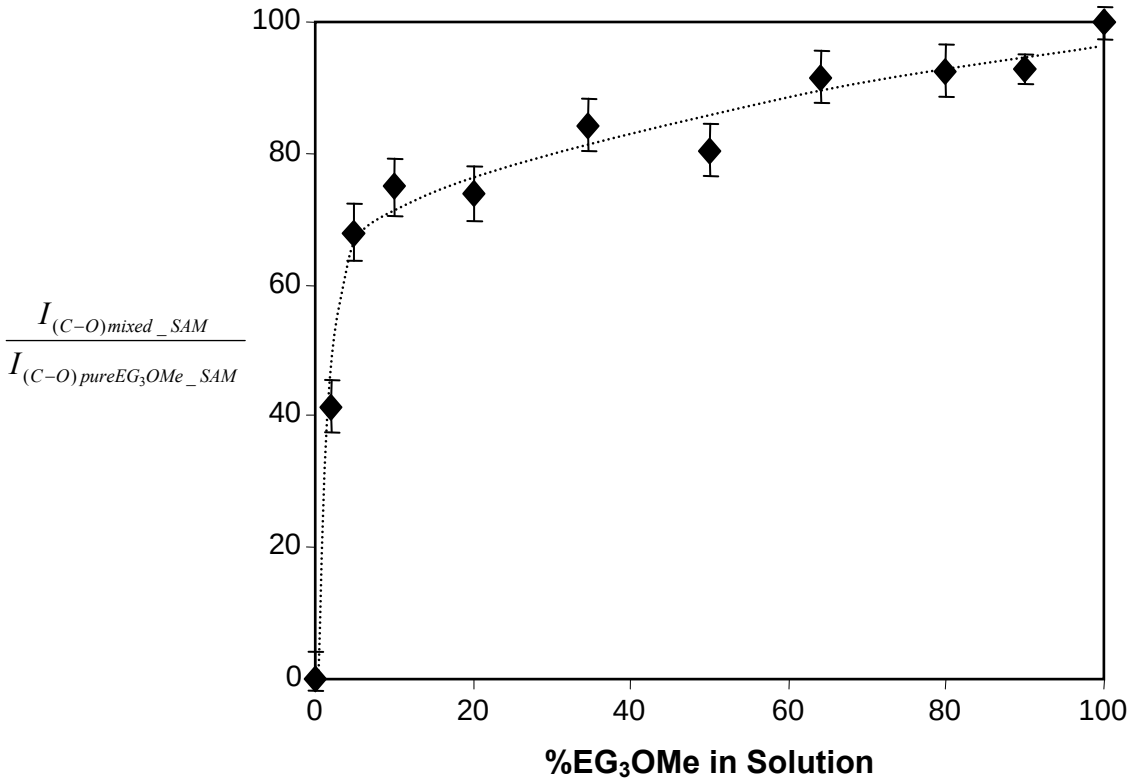

Figure 2-9: Relationship between the normalized XPS C-O intensity on the mixed SAM (with respect to that of the pure EG_3OMe SAM) and the percentage of EG_3OMe in the forming solution. Line is provided as a guide to the eye.

Determination of Surface Composition of Mixed SAMs

The total surface chain density (Γ_{total}) of a mixed SAM, as represented in Figure 2-10, can be described by the following equation,

$$\Gamma_{total} = \Gamma_{pureEG_3OMe} \times \%EG_3OMe + \Gamma_{pureC8} \times \%C8 \ (\mu mol/m^2) \qquad (2\text{-}1)$$

where Γ_{pureEG_3OMe} and Γ_{pureC8} are the surface chain density of pure EG_3OMe and C8 SAMs, respectively. $\%EG_3OMe$ is the normalized amount of EG_3OMe in a mixed SAM with respect to the amount of EG_3OMe in the pure EG_3OMe SAM. Likewise, $\%C8$ is the normalized amount of C8 in a mixed SAM with respect to the amount of C8 in the pure

C8 SAM. The values of Γ_{pureEG_3OMe} and Γ_{pureC8} can be estimated from the XPS intensities of Si(2p) on pure EG_3OMe and C8 SAMs by comparing them with that from a reference SAM with a known surface chain density using eq. 2-2[24]

$$\frac{I}{I_0} = \exp\left(-\frac{d}{\lambda \sin\theta}\right) \tag{2-2}$$

where I is the attenuated intensity of photoelectrons from a modified substrate, I_0 is the intensity of photoelectrons from a bare substrate, d is film thickness on a substrate, λ is an attenuation length, and θ is the angle between the surface parallel and the axis of the electron analyzer in the XPS system.

For this purpose, I chose C18 SAM as the reference SAM since it is widely studied and known to form densely packed monolayer with a surface chain density of 7.9 μmol/m^2 [15]. The intensity ratio of Si(2p) from C18 and other alkyltrichlorosilane SAMs can be described as

$$\frac{I_{C18}}{I_{Cn}} = \exp\left(-\frac{d_{C18} - d_{Cn}}{\lambda \sin\theta}\right) \tag{2-3}$$

where d_{Cn} is the thickness of alkyltrichlorosilane SAM with n numbers of carbon. The value of λ can be estimated using the following expression[24],

$$\lambda(\text{Å}) = 9.0 + 0.022\ KE(\text{eV}) \tag{2-4}$$

where KE is the kinetic energy of the electrons. A set of values of d_{Cn} can be estimated using an expression derived by Wasserman et al.[15],

$$d_{Cn} = 1.26n + 4.78 \tag{2-5}$$

where n is the number of carbon in the alkyltrichlorosilane molecule. A set of data of I_{C18}/I_{Cn} vs. d_{Cn} can then be generated using the calculated values of d_{Cn} and eq. 2-3. By comparing the value of I_{C18}/I_{EG3OMe} with that of I_{C18}/I_{Cn}, I found that the attenuation of the

Si(2p) substrate by the EG_3OMe SAM was similar to the attenuation by a C14 SAM on the SiO_2/Si substrate. This implies that the EG_3OMe SAM had a surface chain density of ~5 μmol/m^2 or ~64% of a densely packed SAM. For comparison, Herrwerth et al.[25] reported a surface chain density of ~6 μmol/m^2 for EG_3OMe terminated thiolate SAM suggesting that the EG units pack less well than their alkyl counterparts. It is worth noting that the surface density of the EG_3OMe SAM falls in the region of minimal protein adsorption levels (i.e. ~60% to ~80% of surface coverage) that have been reported using thiol SAMs on gold[23, 26]. Using a similar method, the surface chain density of a pure C8 SAM was ~5.9 μmol/m^2. This value is lower than that for a densely packed alkylsilane SAM (i.e. ~7.9 μmol/m^2)[15] which agrees with the ellipsometry and water contact angle results for C8 SAM in the previous section.

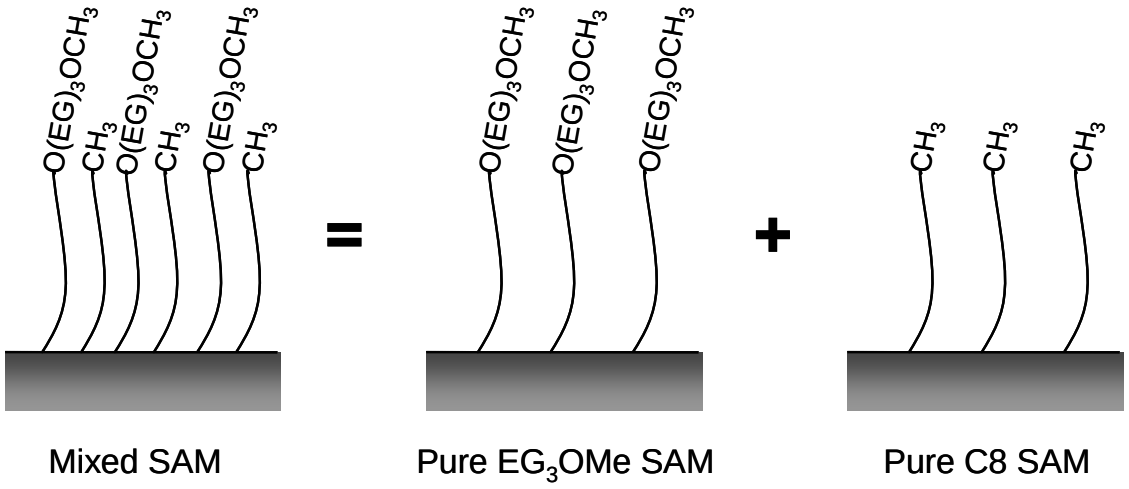

Figure 2-10: Schematic representation of a mixed SAM that is formed from two different pure SAMs.

Ellipsometry allows the determination of film thicknesses by measuring the change in polarization state of light reflected from the surface of a substrate. The

effective ellipsometric thickness of a mixed SAM results from the thicknesses of EG_3OMe and C8 SAMs with respect to their surface densities (Figure 2-10), or as described by the following equation

$$d_{eff} = d_{pureEG_3OMe} \times \%EG_3OMe + d_{pureC8} \times \%C8 \quad (2\text{-}6)$$

where d_{eff}, $d_{pureEG3OMe}$, d_{pureC8} are the effective ellipsometric thickness of a mixed SAM, a pure EG_3OMe SAM, and a pure C8 SAM, respectively. $\%EG_3OMe$ and $\%C8$ are as defined previously. Specifically, $\%EG_3OMe$ is equal to the normalized C-O XPS intensity from a particular mixed SAM as quantified in Figure 2-9. $\%C8$ in a mixed SAM is then determined from eq. 2-6 as the values of other variables are available from the ellipsometric and XPS results.

Figure 2-11 shows the densities of mixed SAMs as estimated using eq. 2-1. As expected, the amount of C8 in the mixed SAM decreased, while that of EG_3OMe increased, at the increasing concentration of EG_3OMe in the solution. At low concentrations of EG_3OMe in the solutions, the total densities of chains in the mixed SAMs were higher than those of the pure SAMs. Presumably, this is because the low density of C8 on the surface allows the insertions of EG_3OMe molecules between them, resulting in a denser packing of the underlying alkyl regions within the mixed SAMs. At high concentrations of EG_3OMe in the solutions, the total surface chain densities were similar to that of the pure EG_3OMe SAM. The combination of the low amount of C8 in the solution and the selection of self-assembly conditions that favor the deposition of EG_3OMe over C8, results in a low insertion of C8 among the EG_3OMe molecules.

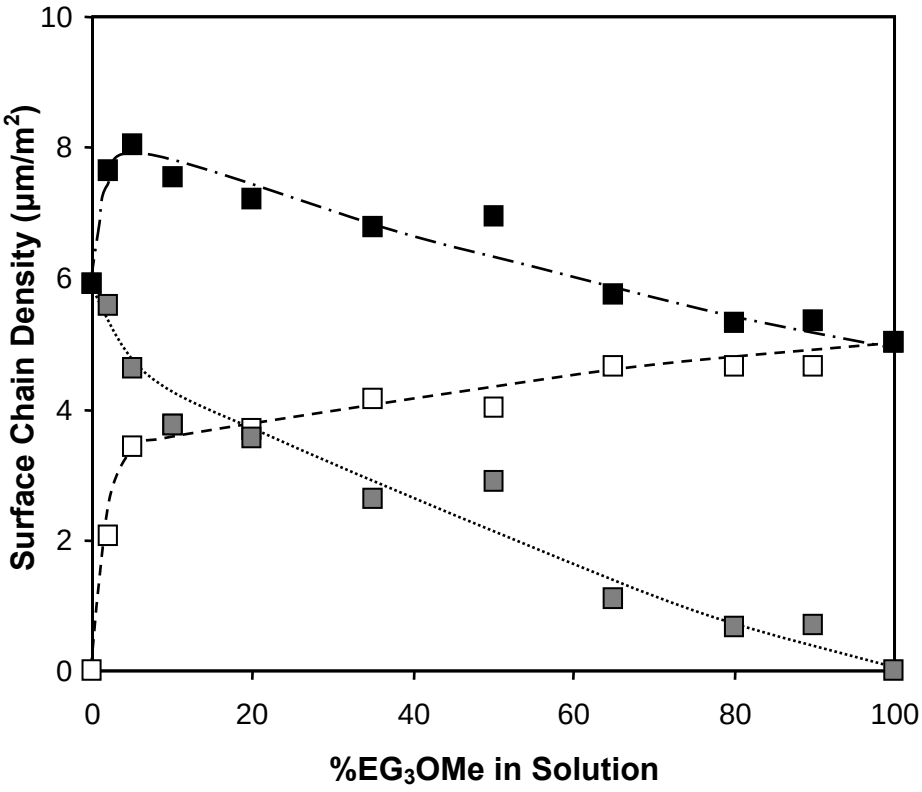

Figure 2-11: Relationship between the surface and the solution compositions of the mixed monolayers of EG_3OMe and C8 silanes. (■) Total chain density, (□) density of EG_3OMe, and (▩) density of C8 in the mixed SAM. Lines are provided as guides to the eye.

Protein Adsorption on Mixed SAMs

Figure 2-12 shows that the levels of BSA and fibrinogen adsorption on the mixed SAMs decreased when the surfaces became more hydrophilic. In addition, this figure also shows that mixed SAMs having similar values of advancing water contact angle exhibited similar levels of protein adsorption. An interesting phenomenon observable from this figure is that a decrease in the level of protein adsorption on the mixed SAMs is not directly proportional to the decrease in the water contact angle measurements. Most of the changes in adsorbed protein amounts occur in the region where the surfaces are

highly hydrophilic. For example, a decrease in the water contact angle from 110° to 70° resulted in a decrease in protein adsorption by ~45%. However, an additional 10° drop in the value of water contact angle (see data at 20% and 50% EG_3OMe in solution) resulted in a further decrease in protein adsorption by ~60%. Further, a subtle change in the wettability of the mixed SAMs by only a few degrees (from ~61° to ~58°) resulted in a significant reduction in protein adsorption (roughly 50-100% of reduction). The result here shows that the surface properties of the mixed SAMs can be readily modulated by changing the ratio of the concentration of EG_3OMe and C8 silanes in the solutions used to prepare the mixed SAMs. More importantly, the ability to modulate surface energies of mixed SAMs provides a way to control the level of protein-surface interactions.

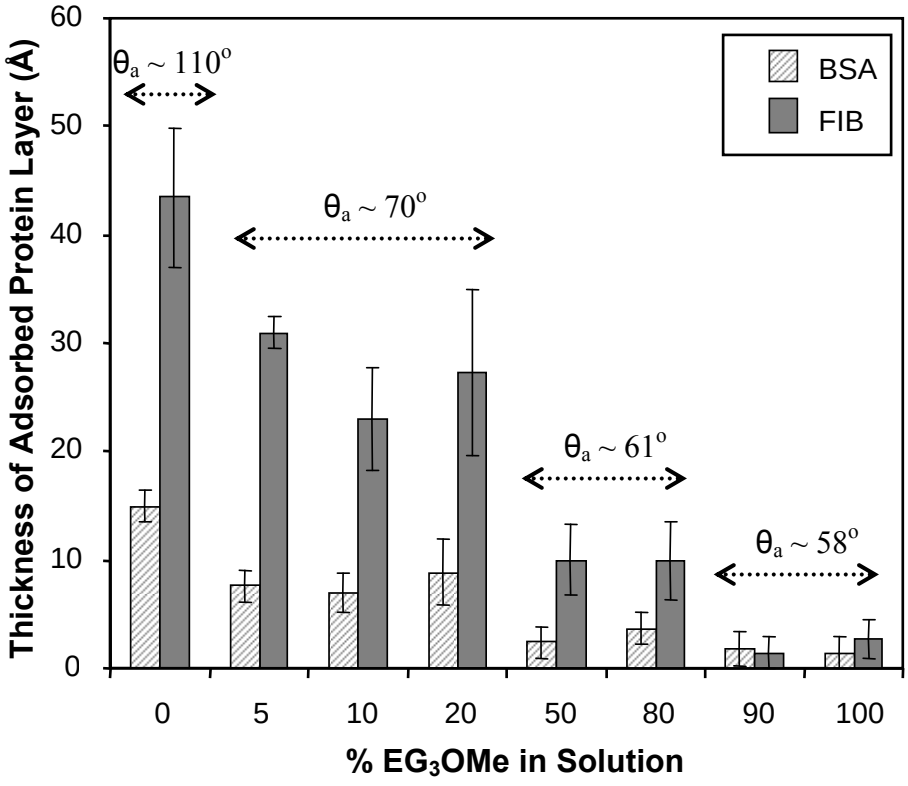

Figure 2-12: Bovine serum albumin (BSA) and fibrinogen (FIB) adsorption on mixed SAMs. Note: θ_a is an advancing water contact angle.

2.4. Conclusions

The self-assembly conditions for forming good quality EG_3OMe films on SiO_2/Si substrates are established and the conditions are: (1) use RCA cleaned substrates, (2) a self-assembly temperature of 60 ^oC, (3) and toluene-based solutions containing a trace amount of water. The presence of trace amount of water in the toluene is essential for forming good quality EG_3OMe and C18 films. Poor quality EG_3OMe films are obtained if the films are formed from toluene solution containing concentrations of added water of more than 0.1 mM. Good quality EG_3OMe films exhibit protein repellent properties as tested against proteins of various molecular weights. For C18 films, the role of water in the toluene is mainly to expedite the self-assembly of C18 silanes on the surface. The results show that the quality of the formed C18 films is not affected by the various concentrations of trace water used in this study.

Surfaces of different energies are successfully created using mixed SAMs of EG_3OMe and C8 silanes. The densities of the mixed SAMs are estimated using the data obtained from ellipsometric and XPS measurements. The results show that the densities of mixed SAMs are higher than those of the pure SAMs. This observation is interpreted as due to the ability of C8 silanes to incorporate in between EG_3OMe silanes thus forming a denser underlying alkyl region in the mixed SAMs. Static protein adsorption experiments show that the level of protein adsorption on a substrate can be modulated by varying the surface energy of the substrate using mixed SAMs of EG_3OMe and C8. A significant finding in this work is that in the regions of highly hydrophilic surfaces (e.g. high proportion of EG_3OMe in the mixed SAMs), a slight change in the wetting properties results in a significant change in their protein repellent properties.

2.5. References

1. Mrksich, M.; Whitesides, G. M., Using Self-Assembled Monolayers to Understand the Interactions of Man-Made Surfaces with Proteins and Cells. *Annual Review of Biophysics and Biomolecular Structure* **1996,** *25*, 55-78.

2. Ostuni, E.; Grzybowski, B. A.; Mrksich, M.; Roberts, C. S.; Whitesides, G. M., Adsorption of proteins to hydrophobic sites on mixed self-assembled monolayers *Langmuir* **2003,** *19* (5), 1861-1872.

3. Pale-Grosdemange, C.; Simon, E. S.; Prime, K. L.; Whitesides, G. M., Formation of self-assembled monolayers by chemisorption of derivatives of oligo(ethylene glycol) of structure $HS(CH_2)_{11}(OCH_2CH_2)_mOH$ on gold. *Journal of the American Chemical Society* **1991,** *113* (1), 12-20.

4. Prime, K. L.; Whitesides, G. M., Self-assembled organic monolayers: model systems for studying adsorption of proteins at surfaces. *Science* **1991,** *252*, 1164-1167.

5. Prime, K. L.; Whitesides, G. M., Adsorption of proteins onto surfaces containing end-attached oligo(ethylene oxide): a model system using self-assembled monolayers. *Journal of the American Chemical Society* **1993,** *115* (23), 10714-10721.

6. Lee, S.-W.; Laibinis, P. E., Protein resistant coatings for glass and metal oxide surfaces derived from oligo(ethylene glycol)-terminated alkyltrichlorosilanes. *Biomaterials* **1998,** *19* (18), 1669-1675.

7. Roberts, C.; Chen, C. S.; Mrksich, M.; Martichonok, V.; Ingber, D. E.; Whitesides, G. M., Using mixed self-assembled monolayers presenting RGD and $(EG)_3OH$ groups to characterize long-term attachment of bovine capillary endothelial cells to surfaces. *Journal of the American Chemical Society* **1998,** *120* (26), 6548-6555.

8. Wu, S.-L.; Karger, B. L., Hydrophobic interaction chromatography of proteins. *Methods in Enzymology* **1996,** *270*, 27-47.

9. Capadona, J. R.; Collard, D. M.; Garcia, A. J., Fibronectin Adsorption and Cell Adhesion to Mixed Monolayers of Tri(ethylene glycol)- and Methyl-Terminated Alkanethiols. *Langmuir* **2003,** *19* (5), 1847-1852.

10. Arima, Y.; Iwata, H., Effect of wettability and surface functional groups on protein adsorption and cell adhesion using well-defined mixed self-assembled monolayers. *Biomaterials* **2007,** *28* (20), 3074-3082.

11. Hoffmann, C.; Tovar, G. E. M., Mixed self-assembled monolayers (SAMs) consisting of methoxy-tri(ethylene glycol)-terminated and alkyl-terminated dimethylchlorosilanes control the non-specific adsorption of proteins at oxidic surfaces. *Journal of Colloid and Interface Science* **2006,** *295* (2), 427-435.

12. Rodrigues, S. N.; Gonçalves, I. C.; Martins, M. C. L.; Barbosa, M. A.; Ratner, B. D., Fibrinogen adsorption, platelet adhesion and activation on mixed hydroxyl-/methyl-terminated self-assembled monolayers. *Biomaterials* **2006,** *27* (31), 5357-5367.

13. Barrias, C. C.; Martins, M. C. L.; Almeida-Porada, G.; Barbosa, M. A.; Granja, P. L., The correlation between the adsorption of adhesive proteins and cell behaviour on hydroxyl-methyl mixed self-assembled monolayers. *Biomaterials* **2009,** *30* (3), 307-316.

14. Allara, D. L.; Nuzzo, R. G., Spontaneously organized molecular assemblies. 2. Quantitative infrared spectroscopic determination of equilibrium structures of solution-adsorbed n-alkanoic acids on an oxidized aluminum surface. *Langmuir* **1985,** *1* (1), 52-66.

15. Wasserman, S. R.; Whitesides, G. M.; Tidswell, I. M.; Ocko, B. M.; Pershan, P. S.; Axe, J. D., The structure of self-assembled monolayers of alkylsiloxanes on silicon: a comparison of results from ellipsometry and low-angle x-ray reflectivity. *Journal of the American Chemical Society* **1989,** *111* (15), 5852-5861.

16. Zhu, B.; Eurell, T.; Gunawan, R.; Leckband, D., Chain-length dependence of the protein and cell resistance of oligo(ethylene glycol)-terminated self-assembled monolayers on gold. *Journal of Biomedical Materials Research* **2001,** *56* (3), 406-416.

17. Silberzan, P.; Leger, L.; Ausserre, D.; Benattar, J. J., Silanation of silica surfaces. A new method of constructing pure or mixed monolayers. *Langmuir* **1991,** *7* (8), 1647-1651.

18. Parikh, A. N.; Allara, D. L.; Azouz, I. B.; Rondelez, F., An Intrinsic Relationship between Molecular Structure in Self-Assembled n-Alkylsiloxane Monolayers and Deposition Temperature. *The Journal of Physical Chemistry* **1994,** *98* (31), 7577-7590.

19. McGovern, M. E.; Kallury, K. M. R.; Thompson, M., Role of Solvent on the Silanization of Glass with Octadecyltrichlorosilane. *Langmuir* **1994,** *10* (10), 3607-3614.

20. Carraro, C.; Yauw, O. W.; Sung, M. M.; Maboudian, R., Observation of Three Growth Mechanisms in Self-Assembled Monolayers. *The Journal of Physical Chemistry B* **1998,** *102* (23), 4441-4445.

21. Glaser, A.; Foisner, J.; Hoffmann, H.; Friedbacher, G., Investigation of the Role of the Interplay between Water and Temperature on the Growth of Alkylsiloxane Submonolayers on Silicon. *Langmuir* **2004,** *20* (13), 5599-5604.

22. Li, L.; Chen, S.; Jiang, S., Protein interactions with oligo(ethylene glycol) (OEG) self-assembled monolayers: OEG stability, surface packing density and protein adsorption. *Journal of Biomaterials Science Polymer Edition* **2007,** *18*, 1415-1427.

23. Li, L.; Chen, S.; Zheng, J.; Ratner, B. D.; Jiang, S., Protein Adsorption on Oligo(ethylene glycol)-Terminated Alkanethiolate Self-Assembled Monolayers: The Molecular Basis for Nonfouling Behavior. *The Journal of Physical Chemistry B* **2005,** *109* (7), 2934-2941.

24. Laibinis, P. E.; Bain, C. D.; Whitesides, G. M., Attenuation of photoelectrons in monolayers of n-alkanethiols adsorbed on copper, silver, and gold. *The Journal of Physical Chemistry* **1991,** *95* (18), 7017-7021.

25. Herrwerth, S.; Eck, W.; Reinhardt, S.; Grunze, M., Factors that Determine the Protein Resistance of Oligoether Self-Assembled Monolayers: Internal Hydrophilicity, Terminal Hydrophilicity, and Lateral Packing Density. *Journal of the American Chemical Society* **2003,** *125* (31), 9359-9366.

26. Vanderah, D. J.; La, H.; Naff, J.; Silin, V.; Rubinson, K. A., Control of Protein Adsorption: Molecular Level Structural and Spatial Variables. *Journal of the American Chemical Society* **2004,** *126* (42), 13639-13641.

CHAPTER III

MIXED SELF-ASSEMBLED MONOLAYERS OF TRI(ETHYLENE) GLYCOL TERMINATED SILANE AND OCTYLTRICHLOROSILANE ON POROUS SILICA PARTICLES

3.1. Introduction

Silica particles are widely used as supports for various types of chromatography or separation applications[1]. For high performance liquid chromatography (HPLC), porous silica particles are often the preferred material (as compared to polymeric-based particles) due to their ability to withstand high column pressure[1]. The surface of silica particles can be modified to display certain functionalities for specific applications[2]. One of the ways of modifying silica surface is by forming self-assembled monolayers (SAMs) of silane molecules on the silica surface. SAM provides a convenient and simple way to tailor surfaces of chromatographic supports with a wide range of functionalities at high precision[3, 4].

This chapter describes the functionalization of silica particles with mixed SAMs of $Cl_3Si(CH_2)_{11}(OCH_2CH_2)_3OCH_3$ (EG_3OMe) and $Cl_3Si(CH_2)_7CH_3$ (C8). The EG_3OMe SAM is hydrophilic and exhibits a high surface energy, while the C8 SAM is hydrophobic and displays a low surface energy. Mixtures of these two SAMs can generate intermediate surface energies on the silica particles. In the previous chapter, SAMs on flat substrates were characterized using ellipsometry, contact angle measurements and x-ray photoelectron spectroscopy (XPS) for their film thicknesses, surface wettabilities and surface chemical compositions, respectively. Most of these

methods are not suitable for characterizing particulate materials. Thus, other characterization methods were applied to characterize the SAMs-coated silica particles in this study. Here, the presence of SAMs on the silica particles was verified using thermogravimetric analysis (TGA) and XPS. XPS also provided an estimate on the chemical composition of the SAMs. Critical surface tensions of the SAM-coated particles were determined using a developed microscale flotation method. The critical surface tensions measured using the developed method were compared with the values obtained from contact angle measurements on the flat substrates coated with the SAMs as a way to verify similarities in their properties.

3.1.1. Flotation as a Method to Determine Critical Surface Tensions of Particles

The surface energy of a solid can be characterized by its critical surface tension (γ_c), where its value defines the conditions required for achieving complete spreading by a liquid across its surface. The concept of a critical surface tension for spreading was introduced and developed by Zisman[5] using contact angle measurements on flat substrates. By varying the surface tension of the liquid used in the wetting measurements, a critical surface tension for the solid is determined as the highest value for a liquid surface tension that results in the complete wetting of the surface (i.e., $\cos\theta = 1$ or $\theta = 0°$). Critical surface tensions have been used in a variety of ways. They allow comparisons of surface energies to be made across different solids and for different surface treatments. They have been used to interpret differences that supports have in their properties of adhesion and adsorption as well as to specify necessary conditions for a liquid surface tension so that complete wetting could be achieved on a particular solid.

For particles, the critical surface tension defines the condition necessary for a liquid to fully wet its entire surface and remove any contacts between the particle surface and air. As such, critical surface tensions have been used to determine the conditions under which particles in a suspension can be made to prefer contact with air and thus be collected at an air/liquid interface. Various separation processes rely on the ability to concentrate dispersed species at this interface. For example, aeration is used in water purification as a way to remove unwanted suspended materials, while in other operations, aeration can assist in the recovery of dispersed materials of interest (for example, minerals) from a slurry[6]. Differences in the critical surface tension of the different particles can be used for separating those that collect at the air/liquid interface from those that prefer to remain in the liquid[7].

The primary method for determining the critical surface tension for a particle surface has been flotation[8], whereby particles suspended in a less dense liquid of a defined surface tension are aerated to cause their extraction to the air/liquid interface. When the particles prefer to be fully wetted by the liquid, they remain in suspension during the aeration. Variations in the liquid surface tension and their effects on the wettability of the particles are reflected by changes in the preference for the particles to remain in suspension rather than to collect at the air/liquid interface. The distribution between these two states is determined by measurement of the weight fraction of material that can be recovered by flotation[8, 9]. From these measurements, the critical surface tension is determined as the highest liquid surface tension that results in the particles showing a complete preference to remain in suspension. Related film flotation experiments have also been reported[10] where the dried sample was sprinkled as

monolayer on a liquid/air interface and the fraction that remained there collected and its weight fraction measured. Contact angle measurements have also been used, where particle samples are compressed into pellets and their surface interrogated through wetting measurements[11]. Issues of surface roughness and damage to the particles during formation of the pellets (particularly for those with surface coatings) can complicate the use of this approach[12]. As a result, flotation-based approaches (with or without aeration) have largely been used.

Flotation methods have commonly been applied to industrial samples such as mineral slurries[8, 9, 13], coal powders[10, 14], particulate fibers[15], polymeric beads[16], and coated particles[16-18] for determining critical surface tensions. Typically, modest quantities of the particulate sample (~0.5 to 2 g)[9] are required for each examined surface tension, thus limiting the use of this method of characterization to samples that are available in such quantities. The reliance on a weight-based method for determining the sample weight fraction that floats (or remains in the liquid) has set a requirement for multigram-level quantities to achieve reliable measurements.

In many research studies involving the synthesis of microparticles, sample quantities can be small and insufficient to allow determination of a critical surface tension using traditional flotation approaches that rely on mass-based analyses. For such samples, measurements of their critical surface tension could provide confirmation of a surface functionalization process. Here, I developed a microscale flotation method that only requires small amounts of particulate samples (~2 mg) per floatability measurement. In this method, I applied optical measurements for quantifying the fractional amounts of

the particles that remained in solution or that were collected at the air/liquid interface as the surface tension of the liquid was varied.

3.2. Materials and Methods

3.2.1. Materials

All chemicals were obtained from Fisher and used as received unless otherwise specified. Viva Silica particles from Restek (Bellefonte, PA) were used for all of the work in this chapter unless noted. Viva Silica particles are porous, spherical in shape and have an average diameter of 5 μm. These particles have a surface area of ~116.6 m^2/g and an average pore diameter of 240 Å. Porasil particles obtained from Waters Corp (Milford, MA) were also used. These particles are porous, irregular in shape, and have an average particle size of 17.5 μm. The Porasil particles have a surface area of ~320 m^2/g and an average pore diameter of 125 Å. Test grade silicon wafers (SiO_2/Si <100>, boron-doped, 675 μm thickness) and n-octyltrichlorosilanes were obtained from Montco Silicon Technologies Inc. and Gelest, respectively. $Cl_3Si(CH_2)_{11}(OCH_2CH_2)_3OCH_3$ (EG_3OMe) was synthesized as described previously in Chapter 2[19].

3.2.2. Self-Assembled Alkylsiloxane Monolayers

Viva Silica particles were functionalized by suspending 100 mg of particles in a 10 mL of toluene solution containing 1.5 μmoles of alkyltrichlorosilane in a round bottom glass flask. The suspension was magnetically stirred for 4 h at 60 ^oC. After cooling to room temperature, the mixture was centrifuged to remove unreacted silane. The collected particles underwent a series of washing cycles involving alternating steps

of resuspension in a fresh solvent and centrifugation (3x with toluene, 3x with ethanol). The particles were finally resuspended in ethanol, and the suspension was filtered. The derivatized particles were collected after the removal of trace solvent under a reduced pressure. The above self-assembly procedure was also applied to Porasil particles, the only difference was that 3 μmoles of alkytrichlorosilane was added to the particles-in-toluene suspension.

For the purpose of comparison, monolayers of alkyltrichlorosilanes were also deposited on pre-cleaned SiO_2/Si substrates. The cleaning and self-assembly procedures were detailed the previous chapter.

3.2.3. Characterizations of SAMs

Thermogravimetric Analysis (TGA)

Thermogravimetric analysis using an Instrument Specialist Inc. Model TGA-1000 was used to provide an estimate of the carbon content of the silica particles as a result of the surface functionalization with the SAMs. Typically, ~5 mg of silica particles were used for an analysis, and samples were heated in air at a rate of 20 ^{o}C/min from 25 to 800 ^{o}C. Mass losses due to the coatings and to dehydration were determined by comparison to the data obtained in complementary TGA experiments on unfunctionalized silica particles.

Elemental Analysis

Combustion analyses performed by Atlantic Microlab Inc., GA were used to obtain weight fraction measurements for carbon on the native and functionalized silica particles.

X-ray Photoelectron Spectroscopy (XPS) Analysis

XPS spectra were obtained using a Phi 5000 VersaProbe spectrometer equipped with a monochromatic Al Kα x-ray source (1486.6 eV) and a concentric hemispherical analyzer. Spectra were obtained at a take-off angle of 45^{o}. Surface charge compensation was achieved using a neutralizer system comprised of an electron beam and Ar^{+} ion beam during the analysis of insulating samples such as the silica particles. C(1s) and Si(2p) spectra were acquired at the averages of 20 and 10 scans, respectively, using a step width of 0.1 eV and a pass energy of 23.5 eV. Spectral quantitation was performed using 30% Gaussian/Lorentzian peak shapes and a Shirley background.

Microscale Floatability Measurements of SAM-Coated Silica Particles

Light absorbance measurements at 350 nm using a Spectronic 20+ Series UV/visible spectrophotometer (Spectronic Instruments, Inc.) were used for determining the quantity of particles suspended in a liquid sample of known volume. A calibration curve was generated that established a linear relationship between absorbance at 350 nm and particle content using samples with particle concentrations of 0 to 0.67 mg/mL. This relationship was used for quantifying changes in the particle content in samples as a result of some fraction collecting at an air/liquid interface.

Microscale flotation experiments were conducted in Pyrex glass test tubes (12 mm x 100 mm) that each contained ~2 mg of particles and 6 mL of a binary liquid mixture with a composition selected to define its surface tension. Mixtures of absolute ethanol and deionized water were used to access surface tensions ranging from 22 to 72 mN/m. For each condition, the contents in the test tube were agitated using a Vortex

Genie 2™ (Fisher Scientific) with a speed setting at 2.5 for 15 s. This process resulted in a fraction of the particles localizing to the air/liquid interface. In a traditional flotation experiment, the particles at the air/liquid interface would be collected, dried, and measured gravimetrically. Instead, the fraction of particles that did not collect at the air/liquid interface was quantified due to the ease of making spectroscopic measurements on liquid samples. In one approach, the concentration of particles in the liquid phase was measured directly from light absorbance measurements made on the suspension. These measurements were performed immediately after vortex mixing to minimize changes in local concentration due to particle settling. In a second approach, the particle suspension was allowed to settle, particles at the air/liquid interface as well as the clarified supernatant liquid were removed from the sampling tube using a vacuum aspirator, and the remaining (settled) particles were analyzed. These particles were dried under vacuum and then dispersed in 3.0 mL of absolute ethanol to produce a suspension whose particle concentration was determined from light absorbance measurements.

Contact Angle Measurements of SAM-Coated SiO_2/Si Substrates

Advancing and receding contact angles of liquids on SAM-coated SiO_2/Si substrates were measured using a contact angle goniometer (Ramé-Hart Inc, Mountain Lakes, NJ). Liquid droplets (~3 μL) were dispensed and retracted on the surfaces using an automatic pipeting system at ~1 μL/s. The employed liquids were binary mixture of absolute ethanol and deionized water that were varied as in composition as a way to vary their surface tensions. Contact angle measurements were made on both sides of an

applied drop using an image processing software, and the reported values are averages from at least three independent wetting measurements.

3.3. Results and Discussion

Scanning electron micrographs of pristine Viva Silica particles were collected using a Raith eLINE electron beam lithography tool in image mode using an accelerating voltage of 10.0 kV and a working distance of 10 mm. These particles were coated with few nm of gold layer before the imaging process. Figure 3-1 shows that the silica particles have an average diameter of 5 μm with a relatively narrow size distribution. It is observable in this figure that the sphericity of the particles was quite uniform.

3.3.1. Self-Assembled Alkylsiloxane Monolayers on Silica Particles

The organic coating on silica particles is commonly characterized by elemental analysis as a way to determine its carbon content[3, 4, 20]. In this work, I relied on thermogravimetric analysis (TGA) for measuring the carbon content on the surface of silica particles as this instrument in readily accessible in campus. The use of TGA for such purpose has been reported by some research groups[17, 21]. Notably, Cestari et al.[21] demonstrated that TGA produced comparable result to the classical elemental analysis for elemental contents of silica particles modified with alkoxysilane reagents.

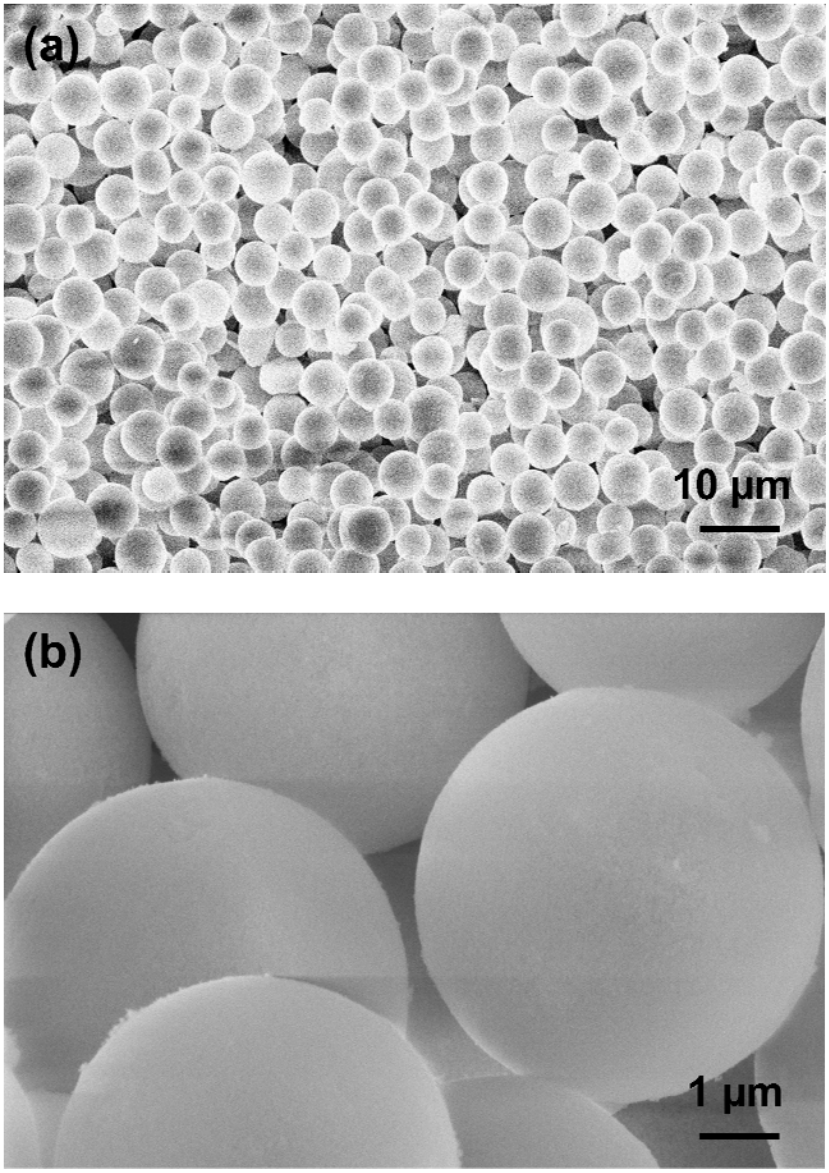

Figure 3-1: Scanning electron micrographs of pristine Viva Silica particles at the magnification of (a) 1000x and (b) 10,000x, respectively.

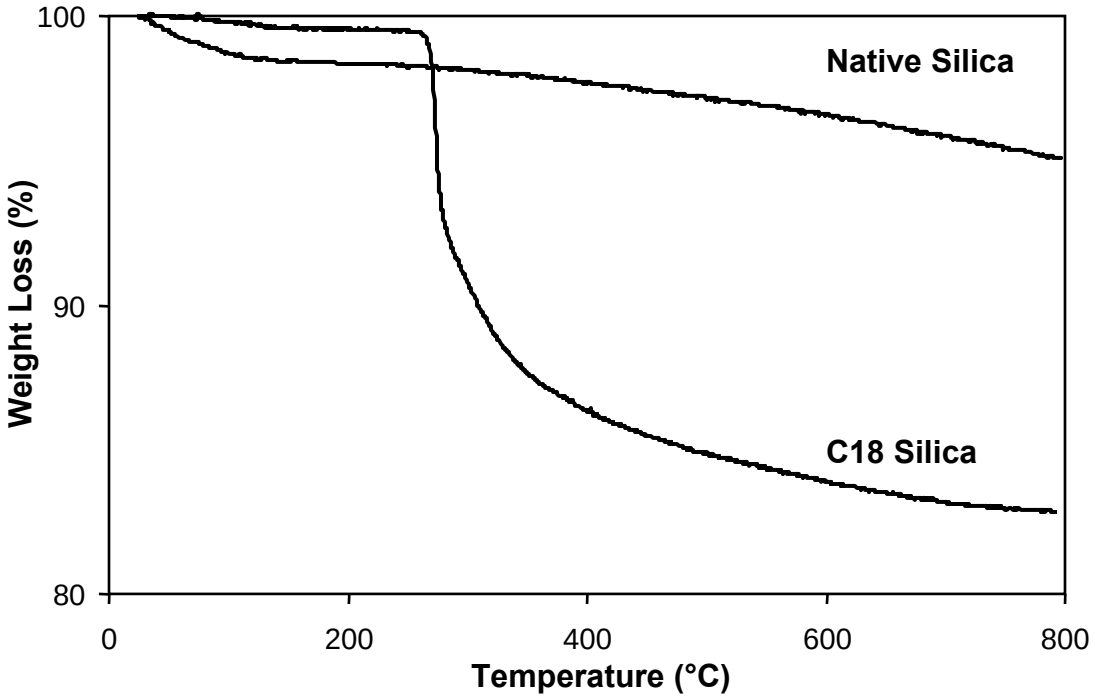

Figure 3-2: TGA behavior of pristine silica and C18 SAM-coated silica particles. C18 SAM was formed from 15 mM of C18 silane in toluene.

Figure 3-2 shows the typical TGA curves for pristine silica and C18 SAM-coated silica formed from 15 mM of silane in toluene. There are two observable weight loss regions on the TGA curve for pristine silica. The weight loss below 200 ^{o}C is attributed to the removal of adsorbed water. Above 200 ^{o}C, the remaining weight loss is due to dehydroxylation of silanols on the silica surface[22-24]. Assuming one molecule of water is removed during dehydroxylation of two silanols, the density of silanols on the pristine silica was estimated to be ~8 μmol/m^2. This value is in good agreement with values reported in the literature[25, 26].

For C18 silica, there are again two weight loss regions, as shown in Figure 3-2. Similar to the pristine silica, there is a loss of adsorbed water in the region below 200 ^{o}C. The amount of water loss is less than that on the pristine silica as C18 coating on C18

silica is hydrophobic in nature. From Figure 3-2, C18 SAM started to decompose at a temperature of about 240 ^{o}C. Similar decomposition temperature has been reported C18 deposited on silica beads[23] and mesoporous silica (SBA-15)[27, 28]. In addition to the C18 SAM decomposition, the weight loss in the region above 240 ^{o}C is also attributed to dehydroxylation on silanols that were not reacted with silane[23]. The difference in the weight loss between the coated silica and the pristine silica at the temperatures above 200 ^{o}C was used for estimating the amount of carbon on SAM-coated silica particles. Using the TGA curves in Figure 3-2 as an illustration, I estimated the amount of weight loss solely due to C18 SAM decomposition by subtracting the C18 Silica curve with the adjusted pristine silica curve (at temperature > 200 ^{o}C) such that the resultant curve at the very high temperatures leveled off. The adjusted pristine silica curve was obtained by multiplying the original pristine silica curve by 40 ± 10%.

Figure 3-3 depicts the amount of carbon loaded on the surface of silica particles after the self-assembly of C18 in toluene at various solution concentrations. It shows that the calculated values of percent carbon from TGA agreed well with those obtained from elemental analysis. For C18 concentrations below ~10 mM, Figure 3-3 shows that the percent carbon on the particles increases linearly with increases in the silane concentration in the solution. This change indicates that the concentrations of silane in these solutions were not adequate to form a complete monolayer. For the concentrations of C18 above ~10 mM, the percentage of carbon on the surface of particles levels off to about 13.5%. Based on the result in Figure 3-3, I determined 15 mM as the optimum silane concentration to form pure and mixed SAMs of silanes.

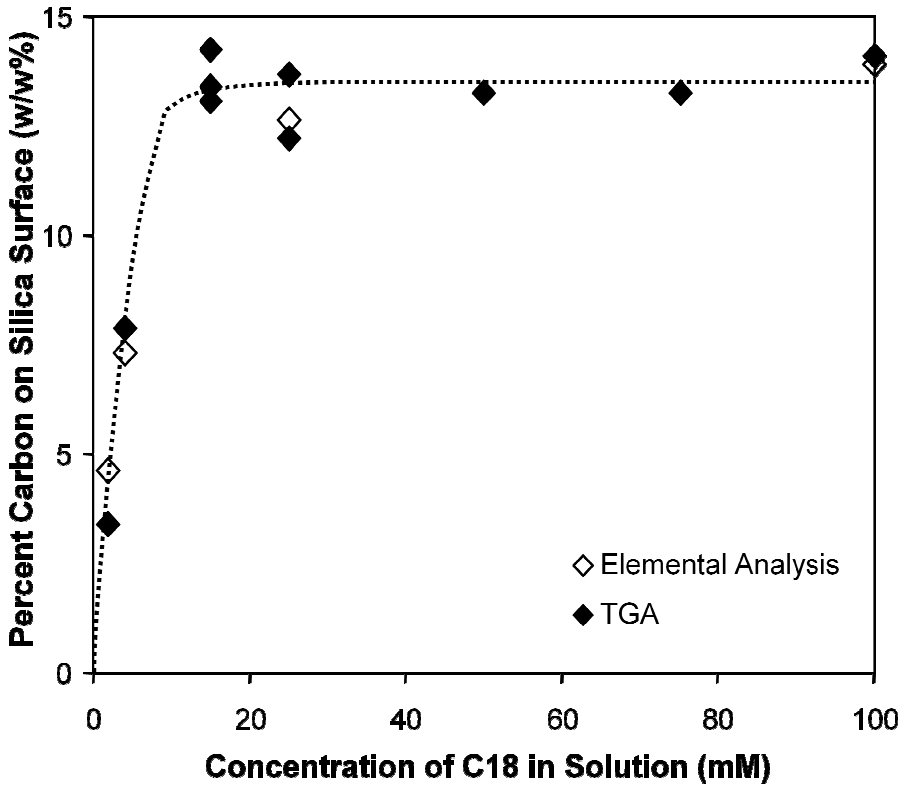

Figure 3-3: Weight percentage of carbon on silica particles functionalized with C18 at various silane concentrations as determined by TGA and elemental analysis. Self-assembly of C18 was performed at 25 °C for 24 h. The concentration of particles in the silane solution was 10 mg/mL. Each data point represents a single measurement. The line is provided as a guide to the eye.

The coverage of a SAM on the surface of particles can be estimated from the following equation,[2, 28, 37]

$$Surface\ coverage\ (\mu mol/m^2) = \frac{10^6 \cdot \%C}{S(1200 \cdot n_c - \%C \cdot Mw)} \qquad (3\text{-}1)$$

where *%C* is the weight percentage of carbon on the surface of functionalized silica particles, n_c is the number of carbons in the bonded silane molecule, *Mw* is the molecular weight of the bonded silane. For the C18 silane, *Mw* is the molecular weight of $(\text{-O}_3)\text{Si}(\text{CH}_2)_{17}\text{CH}_3$) or 329 g/mol. *S* is the surface area of the particles (116.6 m^2/g).

Table 3-1 summarizes the carbon loading (*%C*) and estimated surface coverages of SAMs on silica particles. The value of 13.5% of carbon loading for C18-coated particles corresponds to a calculated surface coverage of 6.7 μmol/m^2 using eq. 3-1. This density is in agreement with the published results from other researchers who obtained values of 4-7 μmol/m^2 for C18 SAMs deposited on various silica particles[3, 30-32]. For comparison, a densely packed C18 SAM on a flat substrate typically has a density of 7.6-7.9 μmol/m^2 [33, 34]. The lower values for the surface density of C18 on the porous supports as compared to those on the flat substrates may be a result of the concave shape of the inner surfaces within the porous supports and the possible inaccessibility of inner regions toward functionalization.

Table 3-1: Amount of Silane on SAM-Coated Silica Particles

Type of Silane	%C	Surface Coverage (μmol/m^2)
C18[a]	13.5 ± 0.6	6.7 ± 0.4
C8[b]	4.9 ± 0.2	4.9 ± 0.2
EG_3OMe[b]	8.4 ± 0.5	3.9 ± 0.3

[a] Self-assembly of C18 was performed at 25 °C for 24 h.

[b]Self-assembly of C8 or EG_3OMe was performed at 60 °C for 4 h.

The self-assembly of EG_3OMe was performed at 60 °C for 4 h, instead of at 25 °C for 24 h, because our previous result[35] showed that it was the optimum condition for forming EG_3OMe SAM on SiO_2/Si substrates. In Table 3-1, the surface coverage of EG_3OMe on particle surface was lower than that of C18 due to the configuration of the tri(ethylene glycol) chain that takes more molecular space than an alkyl chain (e.g. C18) that can assume an all trans configuration upon assembly onto a surface[34]. The surface coverage of EG_3OMe on particles in this work is comparable to that in the work of Miller

et al.[36]. They obtained the surface coverage of 4.5 μmol/m^2 for wide-pore silica particles coated with $(CH_2CH_2O)_3Si(CH_2)_3O(CH_2CH_2O)_3CH_3$. The surface coverage was calculated by assuming an average reaction of two ethoxy groups per silane molecule[36]. As listed in Table 3-1, the surface coverage of C8 on the particles is also lower than that of C18. This result is as expected since at high temperature n-alkyltrichlorosilane such as C8 silane assembled into a monolayer that is less dense than that assembled at room temperature[19, 37-39].

3.3.2. XPS Characterizations

Mixed SAMs of EG_3OMe and C8 were formed on silica particles from toluene solutions containing various mol% of EG_3OMe and C8. The total concentration of the silanes in the toluene was 15 mM. Figure 3-4(a) shows XPS spectra of the C(1s) regions of SAMs formed on the surface of silica particles. The alkyl carbons in the pure C8 SAM (the spectrum on the first row in Figure 3-4(a)) are indicated by the photoelectron intensity from a carbon atom next to another carbon atom. This intensity is fitted with a curve labeled C-C. The C(1s) spectrum of the EG_3OMe SAM (the last row in Figure 3-4(a)) has two identifiable peak intensities that can be fitted with two intensity curves. The underlying alkyl carbons in the EG_3OMe molecule are captured by the C-C curve, while the OEG segments of EG_3OMe SAM are indicated by an intensity curve of carbon atom next to an oxygen atom (labeled as C-O).

I also formed mixed SAMs on SiO_2/Si substrates using the same self-assembly conditions as those for the silica particles and obtained their C(1s) XPS spectra (Figure 3-4(b)). Similar spectral shapes can be observed for each solution mixture by comparing

both sets of spectra on particles and SiO_2/Si in Figure 3-4. However, it is noticeable in Figure 3-4 that the peaks on the C(1s) spectra obtained for SAMs on SiO_2/Si are generally sharper than those for SAMs on the silica particles. The broader peak widths in the C(1s) spectra of SAM-coated silica particles are probably due to the effect of surface charging on the insulating nature of silica particles, although a charge neutralizer was applied to these samples during the XPS analysis.

As the amount of EG_3OMe in the forming solution was increased, the area under the C-O curve increased relative to that under the C-C curve (Figure 3-4). Thus, the amount of EG_3OMe incorporated in a mixed SAM can be tracked from the C-O intensity. Using CasaXPS software to curve-fit the C(1s) spectra, the percentages of the area under the C-O curve with respect to the total area under the C(1s) envelope for each SAM on the silica particles and SiO_2/Si were calculated and are listed in Table 3-2. For both surfaces, the %[C-O] was larger when the SAMs were formed in solutions that had higher fraction of EG_3OMe. The values of %[C-O] on the silica particles and SiO_2/Si for a particular solution concentration were similar. This suggests that using the same self-assembly conditions and the same solution composition of silanes, similar surface compositions were obtained on both surfaces.

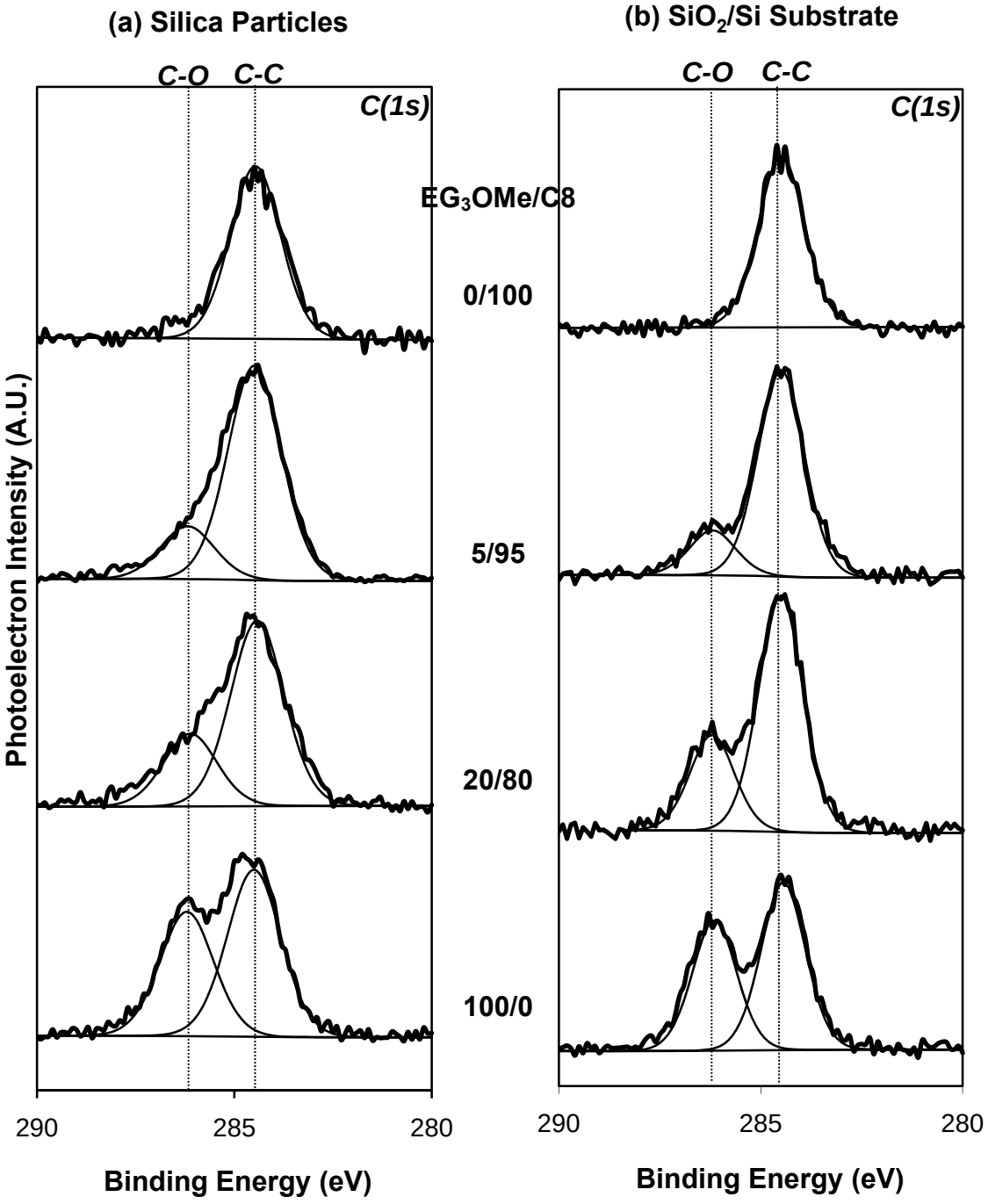

Figure 3-4: XPS spectra of the C(1s) region for (a) SAMs formed on silica particles and (b) SAMs formed on SiO_2/Si substrates from solutions containing 100 mol% C8, 5/95 mol% EG_3OMe/C8, 20/80 mol% EG_3OMe/C8, and 100 mol% EG_3OMe. Each spectrum was adjusted to have the peak of the C-C curve at 284.6 eV.

Table 3-2: %[C-O] or [C-O]/([C-O]+[C-C]) of Mixed SAMs on the Surface of Silica Particles and SiO_2/Si Substrates

Solution Composition	%[C-O] on Particles	%[C-O] on SiO_2/Si
100 mol% C8	0	0
5/95 mol% EG_3OMe/C8	20	18
20/80 mol% EG_3OMe/C8	29	29
100 mol% EG_3OMe	43	43

3.3.3. Floatability Measurements of Mixed SAM-Coated Silica Particles

Figure 3-5 shows a schematic diagram of the procedure for the developed microscale flotation method. As described in the experimental section, during the flotation process, a collection of particles was agitated in a liquid which resulted in a fraction of the particles localizing to the air/liquid interface. The fraction of particles that did not collect at the air/liquid interface was quantified using a UV/VIS spectrophotometer. As shown in Figure 3-5, there are two possible approaches for measuring the concentration of particles in the liquid after the flotation process: (A) measurement right after the mixing of particles in the liquid, and (B) measurement after the particles have settled in the liquid. Approach B requires more experimental work than Approach A since the particles collected at the air/liquid interface have to be removed and the settled particles have to be resuspended in a liquid (in this case 100% ethanol) before the spectroscopic measurement. Spectroscopic measurements of suspensions containing EG_3OMe-coated particles were performed with both approaches. Using Approach A, the spectroscopic measurements resulted in measured amounts of the suspended particles that were sometimes higher than the initial amount of the particles added into the liquid before the flotation process. Due to the unreliable measurements

using Approach A, all the data presented in this chapter were acquired using Approach B (Figure 3-5).

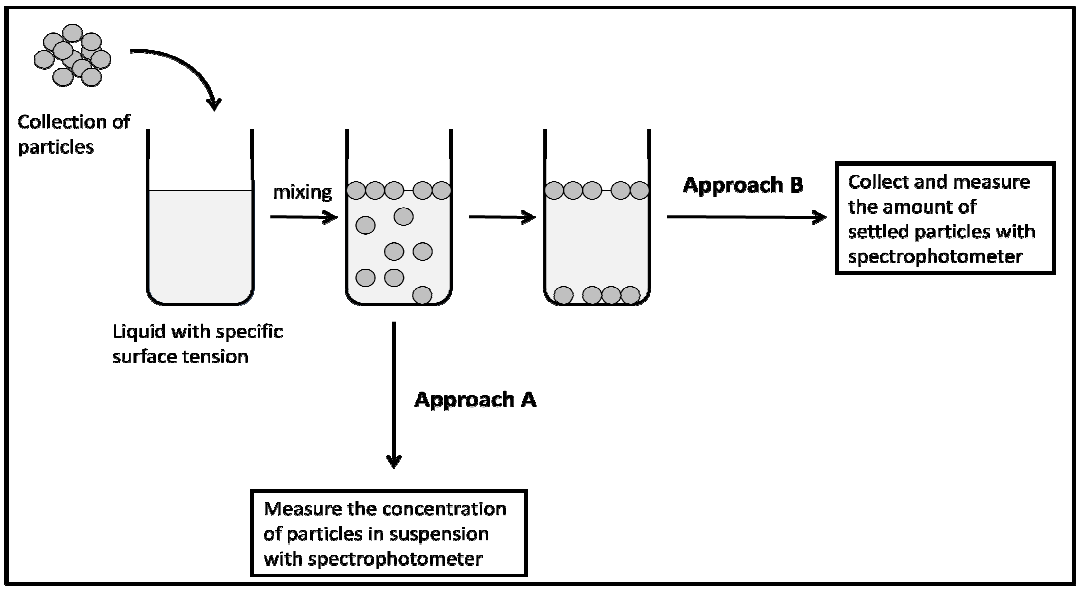

Figure 3-5: Schematic diagram of a microscale flotation method with two possible approaches for measuring the amount of particles left in the liquid after a flotation process.

Figure 3-6 shows the floatability data of silica particles functionalized with mixed SAMs. All curves show similar characteristics: all particles sink below a certain liquid surface tension and float above a certain liquid surface tension. In between the two regions, there is a transition region where the percentage of floating particles increases with the surface tension of liquid. The highest and the lowest liquid surface tensions at which all particle sink and float are termed Total Sinking Surface Tension (*TSS*) and Total Floating Surface Tension (*TFS*), respectively. The values of *TSS* and *TFS* for the SAM-coated silica particles in Figure 3-6 are listed in Table 3-3. The trend of the floatability curve shifts to the right with the increasing content of EG_3OMe on the surface of the silica particles as shown in Figure 3-6. This is as expected as the ethylene glycol

termini in the EG_3OMe SAMs increased the overall surface energy of the mixed SAM-coated silica particles. Thus, particles with a higher EG_3OMe content will sink in a liquid of higher surface tension, as demonstrated in Figure 3-6.

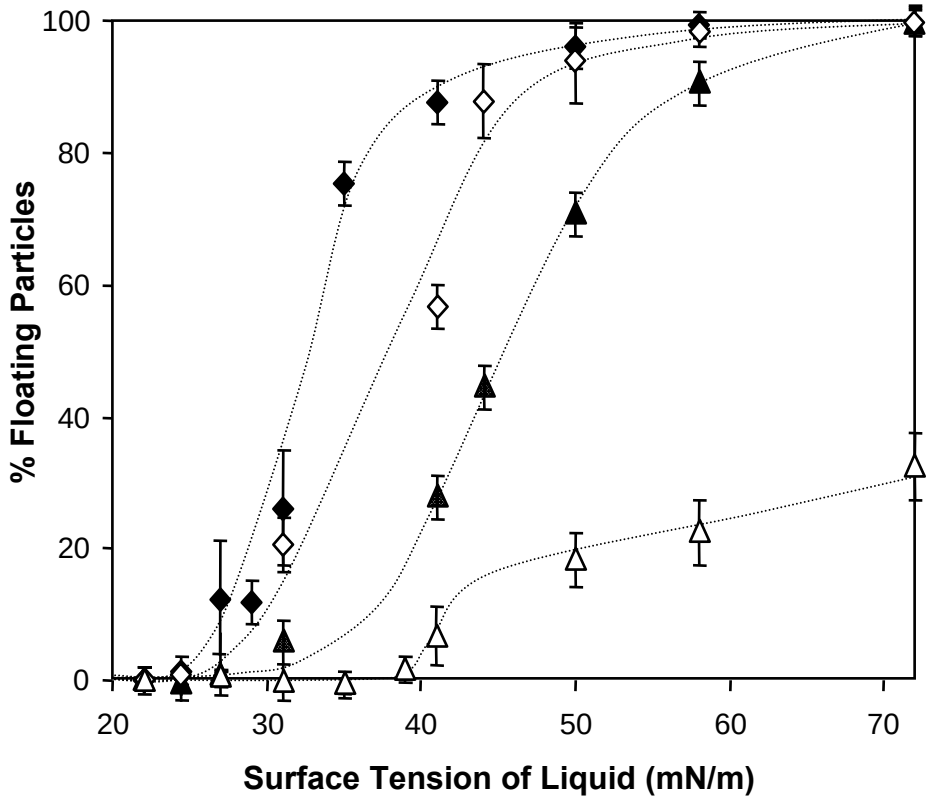

Figure 3-6: Floatability of silica particles functionalized with (♦) 100 mol% C8, (◊) 5/95 mol% EG_3OMe/C8, (▲) 20/80 mol% EG_3OMe/C8, and (Δ) 100 mol% EG_3OMe in toluene. The surface compositions on these particles are related with the silane compositions in the forming solutions (Table 3-2). The lines are added as guides to the eye.

Table 3-3: *TSS* and *TFS* Data for Mixed SAM-coated Particles

Solution Composition (mol%)	*TSS* (mN/m)	*TFS* (mN/m)
100 mol% C8	23.5	50
5/95 mol% EG_3OMe/C8	26	58
20/80 mol% EG_3OMe/C8	27	72
100 mol% EG_3OMe	35	>72

3.3.4. Determination of Critical Surface Tension from Floatability Data

Ideally, the values of *TSS* and *TFS* should be the same, which equals to the critical surface tension of the surface. The presence of a transition region between *TSS* and *TFS* on the same particle surface is likely due to variability in coating uniformity and contact angle hysteresis[16]. These are possibly associated with the curvatures on the porous silica particles. The critical surface tension of each mixed SAM-coated particles should lie between its *TSS* and *TFS*[15]. Yarar and Kaoma[8] estimated critical surface tensions of particulate solids by extrapolating the flotation curves like that in Figure 3-6 to *% Floating Particles* = 0. Table 3-4 show the critical surface tensions for the mixed SAM-coated particles estimated using Yarar and Kaoma's method. These estimated values are in the transition regions for each type of coating and are closer to the TSS values, rather than *TFS* values (compare with the data in Table 3-3). Marmur et al.[16] demonstrated that the *TSS* of coatings on polymeric beads closely resembled the reported critical surface tensions of these coatings on flat substrates.

Table 3-4: Critical Surface Tension (γ_c) Data from Flotation

Solution Composition	γ_c, *flotation* (mN/m)
100 mol% C8	26 ± 2
5/95 mol% EG_3OMe/C8	28 ± 2
20/80 mol% EG_3OMe/C8	35 ± 1
100 mol% EG_3OMe	38 ± 1

3.3.5. Determination of Critical Surface Tension from Zisman Plot

It is expected that the critical surface tension of a SAM deposited on any substrate would be similar if the formed SAMs have similar structures and densities. For

comparison with the SAMs formed on the particles, I measured the critical surface tensions of the SAMs on SiO_2/Si substrates. Figure 3-7 shows the Zisman plots of advancing and receding contact angles of various liquids on SAM-coated Si/SiO_2 substrates. The trend in Figure 3-7 is similar to that in Figure 3-6 in which the trend of the curve shifts to the right with the increasing content of EG_3OMe on the substrates. The critical surface tensions on each SAM-coated surface were obtained at $cos\ \theta = 1$ --the condition where the surface is completely wetted by the liquid-- from Figure 3-7 and the data are listed in Table 3-5. The hysteresis (i.e. θ_A-θ_R) in the contact angle measurements gave a range of critical surface tensions for each SAM-coated surface. The results in Table 3-4 and 3-5 show that the critical surface tension of a SAM estimated from the floatability measurement falls within the range of those measured using the contact angle methods. This agreeable result demonstrates that floatability measurement provides a reliable means to estimate critical surface tensions of the surface of particles. Similar conclusion has been reported by Yarar and Kaoma whom obtained similar values of critical surface tension for solids from flotation method and Zisman plot[8] .

3.3.6. Floatability of Particles of Different Sizes

Figure 3-8 shows the floatability data of C18 SAM-coated Viva Silica particles and C18 SAM-coated Porasil particles. The average size of Viva silica particles is 5 μm, while that of Porasil particles is 17.5 μm. Thermogravimetric analysis showed that the surface coverages of C18 SAM on the Viva Silica and Porasil particles were similar (i.e. 6.7 μmol/m^2 and 5.8 μmol/m^2, respectively). The results in Figure 3-8 indicate that the floatability behavior of the coated silica particles was affected by the size of the particles.

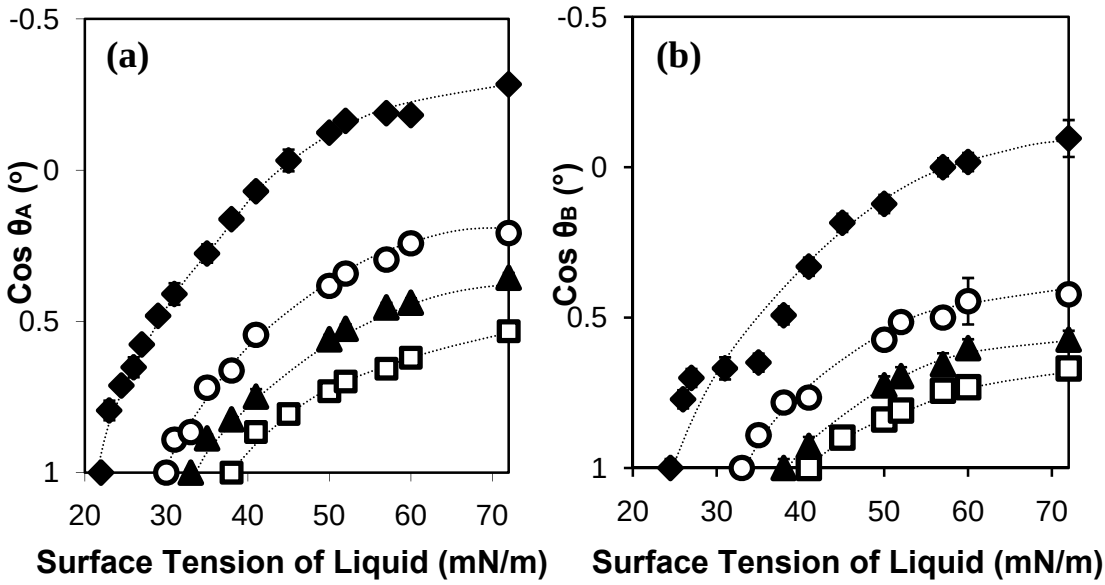

Figure 3-7: Zisman plots of (a) advancing liquid contact angle (θ_A) and (b) receding liquid contact angle (θ_R) measured on the SiO_2/Si substrates functionalized with (♦) 100% C8, (○) 5%/95% EG_3OMe/C8, (▲) 20%/80% EG_3OMe/C8, and (□) 100% EG_3OMe in solutions. Liquids of varying surface tensions comprised mixtures of deionized water and absolute ethanol. The lines are added as guides to the eye.

Table 3-5: Critical Surface Tensions (γ_c) from Advancing Contact Angle (θ_A) and Receding Contact Angle (θ_R) Measurements

Solution Composition	γ_c, θ_A (mN/m)	γ_c, θ_R (mN/m)
100 mol% C8	23 ± 1	26 ± 1
5/95 mol% EG_3OMe/C8	30 ± 1	33 ± 1
20/80 mol% EG_3OMe/C8	33 ± 1	38 ± 1
100 mol% EG_3OMe	38 ± 1	42 ± 1

Further, the particles with a larger average diameter have a higher critical surface tension, as estimated using the method by Yarar and Kaoma. Similar result has been reported by Marmur et al.[16] on the floatability of coated glass beads of different sizes. Hornsby and Leja[7, 40] argued that the smaller-size particle would be floated whereas the larger-size

particle would be non-floatable, due to insufficient particle-bubble aggregate stability of the larger-size particle in a solution of a specific surface tension. This phenomenon suggests that one could use flotation method to separate different sizes of particles from a collection of particles of the same surface characteristics.

It is worth noting that the flotation curves of Viva Silica coated with C8 and C18 SAMs (compare the curves in Figure 3-6 and Figure 3-8) can be superimposed which indicates that both samples had similar values of critical surface tension. This conclusion agrees well with contact angle measurements on the two SAMs on SiO_2/Si substrates. The critical surface tension of C18 SAM obtained from the advancing contact angle measurement was 22 mN/m, while that of C8 SAM was 23 mN/m.

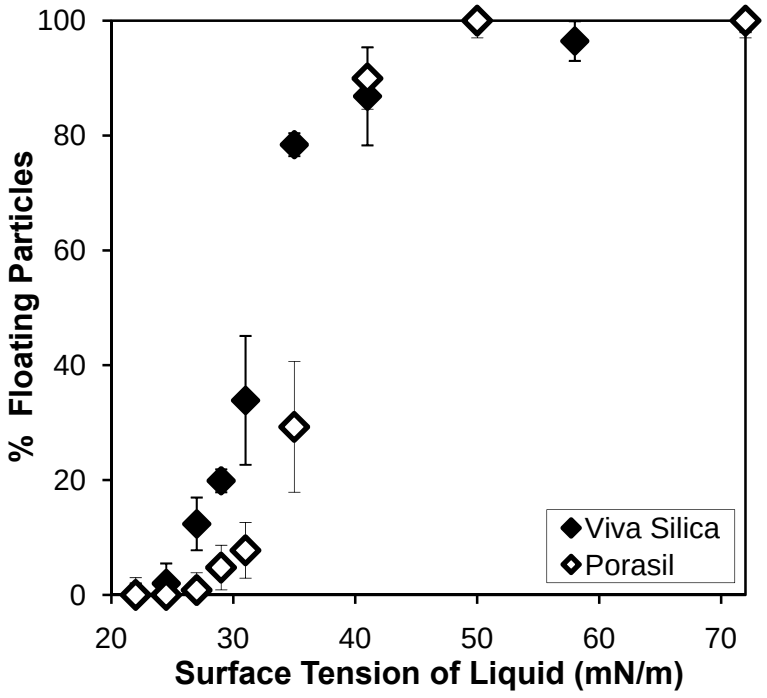

Figure 3-8: Floatability data of Viva Silica (5 μm of average diameter) and Porasil particles (17.5 μm of average diameter) that had been coated with C18 SAM.

3.4. Conclusions

In this chapter, I describe the functionalization of the surface of porous silica particles with mixed SAMs of EG_3OMe and C8. The surface compositions of the mixed SAM-coated particles were analyzed using XPS and the results show similarity to those of mixed SAMs formed on flat substrates, using the same self-assembly conditions. The surface energies on mixed SAM-coated particles were analyzed using the developed microscale flotation method. This method allows the measurements using a small quantity of sample through the application of a spectroscopic method rather than a gravimetric method for determining the amount of floating/sinking particles in the flotation experiments. The results from flotation experiments show differences in surface energies for the mixed SAMs-coated silica particles with respect to varying mole ratios of EG_3OMe and C8 in the silanization solutions. Further analysis of the flotation curves provides estimates on the critical surface tension of mixed SAM-coated silica particles.

3.5. References

1. Gooding, K. M.; Regnier, F. E., *HPLC of Biological Macromolecules*. 2002; Vol. 87, p 162-168.

2. Buchmeiser, M. R., New synthetic ways for the preparation of high-performance liquid chromatography supports. *Journal of Chromatography A* **2001,** *918* (2), 233-266.

3. Fatumbi, H. O.; Bruch, M. D.; Wirth, M. J., Silicon-29 and carbon-13 NMR characterization of mixed horizontally polymerized monolayers on silica gel. *Anal. Chem.* **1993,** *65* (15), 2048-2054.

4. Wirth, M. J.; Fatunmbi, H. O., Horizontal polymerization of mixed trifunctional silanes on silica. 2. Application to chromatographic silica gel. *Analytical Chemistry* **1993,** *65* (6), 822-826.

5. Zisman, W. A., Contact Angle, Wettability and Adhesion. *Advanced Chemical Series* **1964,** *43*, 1-51.

6. Salvato, J. A.; Nemerow, N. L.; Agardy, F. J., *Environmental Engineering*. 5th ed.; John Wiley & Sons, Inc.: Hoboken, N. J., 2003.

7. Hornsby, D. T.; Leja, J., Critical surface tension and the selective separation of inherently hydrophobic solids. *Colloids and Surfaces* **1980,** *1* (3-4), 425-429.

8. Yarar, B.; Kaoma, J., Estimation of the critical surface tension of wetting of hydrophobic solids by flotation. *Colloids and Surfaces* **1984,** *11*, 429-436.

9. Ozkan, A.; Yekeler, M., A new microcolumn flotation cell for determining the wettability and floatability of minerals. *Journal of Colloid and Interface Science* **2003,** *261* (2), 476-480.

10. Peng, F. F., Surface energy and induction time of fine coals treated with various levels of dispersed collector and their correlation to flotation responses. *Energy and Fuels* **1996,** *10*, 1202-1207.

11. Kulkarni, S. A.; Ogale, S. B.; Vijayamohanan, K. P., Tuning the hydrophobic properties of silica particles by surface silanization using mixed self-assembled monolayers. *Journal of Colloid and Interface Science* **2008,** *318* (2), 372-379.

12. Chau, T. T., A review of techniques for measurement of contact angles and their applicability on mineral surfaces. *Minerals Engineering* **2009,** *22* (3), 213-219.

13. Ulusoy, U.; Yekeler, M.; Hicyilmaz, C., Determination of the shape, morphological and wettability properties of quartz and their correlations. *Minerals Engineering* **2003,** *16*, 951-964.

14. Williams, M. C.; Fuerstenau, D. W., A simple flotation method for rapidly assessing the hydrophobicity of coal particles. *International Journal of Mineral Processing* **1987,** *20*, 153-157.

15. Mutchler, J. P.; Menkart, J.; Schwartz, M., Rapid estimation of critical surface tension of fibers. *Advanced Chemical Series* **1967,** *86*, 7-14.

16. Marmur, A.; Chen, W.; Zograff, G., Characterization of particle Wettability by the Measurement of Floatability. *Journal of Colloid and Interface Science* **1985,** *113* (1), 114-120.

17. Bandriss, S.; Margel, S., Synthesis and characterization of self-assembled hydrophobic monolayer coatings on silica colloids. *Langmuir* **1993,** *9*, 1232-1240.

18. Brandriss, S.; Borchardt, G.; Kreuter, J.; Margel, S., Radiolabeled 75Se-silica nanoparticles: synthesis, characterization and coating with [omega]-functionalized alkylsilane compounds. *Reactive Polymers* **1995,** *25* (2-3), 111-125.

19. Tedjo, C.; Laibinis, P. E., Modulating protein-surface interactions using mixed self-assembled monolayers of methoxy-terminated-tri(ethylene glycol)-terminated and alkyl terminated trichlorosilanes. *In preparation*.

20. Sander, L. C.; Wise, S. A., Synthesis and characterization of polymeric C18 stationary phases for liquid chromatography. *Analytical Chemistry* **1984,** *56* (3), 504-510.

21. Cestari, A. R.; Airoldi, C., A new elemental analysis method based on thermogravimetric data and applied to alkoxysilane immobilized on silicas. *Journal of Thermal Analysis* **1995,** *44*, 79-87.

22. Vansant, E. F.; Van Der Voort, P.; Vranken, K. C., *Characterization and Chemical Modification of the Silica Surface*. Elsevier: Amsterdam, 1995.

23. Wang, R.; Baran, G.; Wunder, S. L., Packing and Thermal Stability of Polyoctadecylsiloxane Compared with Octadecylsilane Monolayers. *Langmuir* **2000,** *16* (15), 6298-6305.

24. Jaroniec, C. P.; Gilpin, R. K.; Jaroniec, M., Adsorption and Thermogravimetric Studies of Silica-Based Amide Bonded Phases. *The Journal of Physical Chemistry B* **1997,** *101* (35), 6861-6866.

25. Iler, R. K., The Chemistry of Silica. *John Wiley & Sons* **1979,** *Chapter 6*.

26. Scholten, A. B.; de Haan, J. W.; Claessens, H. A.; van de Ven, L. J. M.; Cramers, C. A., Fundamental Study of Residual Silanol Populations on Alkylsilane-Derivatized Silica Surfaces. *Langmuir* **1996,** *12* (20), 4741-4747.

27. Mirji, S. A., Adsorption of octadecyltrichlorosilane on Si(1 0 0)/SiO2 and SBA-15. *Colloids and Surfaces A: Physicochemical and Engineering Aspects* **2006,** *289* (1-3), 133-140.

28. Mirji, S. A.; Halligudi, S. B.; Sawant, D. P.; Jacob, N. E.; Patil, K. R.; Gaikwad, A. B.; Pradhan, S. D., Adsorption of octadecyltrichlorosilane on mesoporous SBA-15. *Applied Surface Science* **2006,** *252* (12), 4097-4103.

29. Claessens, H. A.; De Haan, J. W.; Van De Ven, L. J. M.; De Bruyn, P. C.; Cramers, C. A., Chromatographic and solid state nuclear magnetic resonance study of the changes in reversed-phase packings for high-performance liquid chromatography at different eluent compositions. *Journal of Chromatography A* **1988,** *436*, 345-365.

30. Srinivasan, G.; Sander, L.; Müller, K., Effect of surface coverage on the conformation and mobility of C18-modified silica gels. *Analytical and Bioanalytical Chemistry* **2006,** *384* (2), 514-524.

31. Srinivasan, G.; Meyer, C.; Welsch, N.; Albert, K.; Muller, K., Influence of synthetic routes on the conformational order and mobility of C18 and C30 stationary phases *Journal of Chromatography A* **2006,** *1113* (1-2), 45-54.

32. Sander, L. C.; Wise, S. A., Influence of stationary phase chemistry on shape recognition in liquid chromatography. *Analytical Chemistry* **1995,** *67*, 3284-3292.

33. Kessel, C. R.; Granick, S., Formation and characterization of a highly ordered and well-anchored alkylsilane monolayer on mica by self-assembly. *Langmuir* **1991,** *7* (3), 532-538.

34. Wasserman, S. R.; Whitesides, G. M.; Tidswell, I. M.; Ocko, B. M.; Pershan, P. S.; Axe, J. D., The structure of self-assembled monolayers of alkylsiloxanes on silicon: a comparison of results from ellipsometry and low-angle x-ray reflectivity. *Journal of the American Chemical Society* **1989,** *111* (15), 5852-5861.

35. Tedjo, C.; Laibinis, P. E., Modulating protein-surface interactions using mixed self-assembled monolayers of methoxy-terminated-tri(ethylene glycol)-terminated and alkyl-terminated trichlorosilanes
In preparation **2009**.

36. Miller, N. T.; Feibush, B.; Karger, B. L., Wide-pore silica-based ether-bonded phases for separation of proteins by high-performance hydrophobic-interaction and size exclusion chromatography. *Journal of Chromatography A* **1985,** *316*, 519-536.

37. Carraro, C.; Yauw, O. W.; Sung, M. M.; Maboudian, R., Observation of Three Growth Mechanisms in Self-Assembled Monolayers. *The Journal of Physical Chemistry B* **1998,** *102* (23), 4441-4445.

38. Parikh, A. N.; Allara, D. L.; Azouz, I. B.; Rondelez, F., An Intrinsic Relationship between Molecular Structure in Self-Assembled n-Alkylsiloxane Monolayers and Deposition Temperature. *The Journal of Physical Chemistry* **1994,** *98* (31), 7577-7590.

39. Silberzan, P.; Leger, L.; Ausserre, D.; Benattar, J. J., Silanation of silica surfaces. A new method of constructing pure or mixed monolayers. *Langmuir* **1991,** *7* (8), 1647-1651.

40. Hornsby, D. T.; Leja, J., Critical surface tension of floatability. *Colloids and Surfaces* **1983,** *7* (4), 339-349.

CHAPTER IV

PREPARATION AND CHARACTERIZATION OF CHROMATOGRAPHIC COLUMNS

4.1. Introduction

High performance liquid chromatography (HPLC) has become the dominant separation tool in many industries. HPLC is primarily used as an analytical technique to detect and quantify analytes of interest from a sample mixture. HPLC is also used as a preparative technique to isolate and purify compounds. As listed in Table 1-1 in Chapter 1, there are different types of liquid chromatographic methods that one can select to achieve a certain separation objective. Ultimately, one would want to achieve the highest quality of a separation, regardless of any method used.

The performance of a chromatographic column is typically measurable through several parameters such as resolution (R_s), plate count (N), and peak asymmetry (A_s)[1]. Resolution characterizes the amount of separation between two analytes' peaks. Resolution can be calculated from a chromatogram using the following equation,

$$R_{s_{1,2}} = \frac{2\Delta t_R}{1.7(w_{0.5_1} + w_{0.5_2})} \qquad (4\text{-}1)$$

where Δt_R is the retention time difference between the peaks and $w_{0.5}$ is the peak width at 50% of a peak height. Plate count, also known as column efficiency, is a measure of the quality of a separation based on the dispersion of a single peak in a column. Plate count equals to column length L divided by the length of a theoretical plate, H. Plate count can be conveniently determined from a chromatogram through the following equation:

$$N = 5.54 \frac{{t_R}^2}{{w_{0.5}}^2} \equiv \frac{L}{H} \qquad (4\text{-}2)$$

A useful dimensionless parameter commonly used to describe column efficiency in literatures is the reduced plate height h,

$$h = \frac{H}{d_p} \qquad (4\text{-}3)$$

where d_p is particle diameter. The reduced plate height facilitates the comparison of column efficiency irrespective of column length and particle diameter. Peak asymmetry is a common practical measure of the quality of a column. As columns age, the peak symmetry usually deteriorates and one observes peak tailing. There are several ways to measure peak tailing. A common one is the ratio of the width of the tail of the peak to the width of the front of the peak at either 5 or 10% of the height of the peak[1].

Plate count is typically determined from the chromatogram of an unretained analyte[1]. The time taken by an unretained analyte to flow through a column is defined as void time (t_0). Void times are used in liquid chromatography for calculations of various parameters such as void volume, average linear mobile phase velocity, retention factor, distribution constant or partition coefficient, plate count, separation factor, relative retention of peaks, resolution of two peaks[2]. Void time or void volume in liquid chromatography can be determined using several methods. The most common method is to use tracer substances such as inorganic salts (e.g. sodium nitrate or sodium nitrite) or organic compounds (e.g. uracil)[2, 3]. The tracer substance should be selected such that its size (molecular weight) allows full penetration of the porous structure of the chromatographic medium. Surface interactions of the tracer substance with the chromatographic medium must be avoided. The tracer needs to be chemically inert,

stable, and easily detected. Other methods of void time determination include the column weight method, methods using homologous series of analytes, isotopically labeled compounds, and minor disturbance method[2, 3].

This chapter describes the preparation of chromatographic columns containing SAMs-coated silica particles. Porasil silica particles were used as the base support for chromatographic packing materials instead of Viva Silica particles (the base support used in the previous chapter) due to the particle size requirements for use in the glass columns purchased from Waters Corp. The surface coverages of C18 SAM and EG_3OMe SAM on the Porasil and Viva Silica particles were determined using thermogravimetric analysis (TGA). The void time of a typical chromatographic column used in this research was determined and column efficiency was calculated based on the chromatogram of an unretained analyte.

4.2. Materials and Methods

4.2.1. Particles Functionalization and Characterization

Bulk silica particles (Porasil^{TM}, 125 Å of pore size, 15-20 μm of particle size) were obtained from Waters Corp. (Milford, MA, USA). These particles were functionalized either with octadecyltrichlorosilane (C18) or $Cl_3Si(CH_2)_{11}(OCH_2CH_2)_3OCH_3$ (EG_3OMe). Porasil particles were functionalized by suspending ~0.55 g of particles in a 25 mL of toluene solution containing 3.0 μmoles of alkyltrichlorosilane in a round bottom glass flask. The suspension was magnetically stirred for up to 24 h at room temperature for C18 deposition or at 60 ^oC for EG_3OMe deposition on the surface of the silica particles. After cooling to room temperature, the

mixture was centrifuged to remove unreacted silane. The collected particles underwent a series of washing cycles involving alternating steps of resuspension in a fresh solvent and centrifugation (3x with toluene, 3x with ethanol). At the end of washing cycle, ethanol was decanted from the centrifuge tube and the particles were dried in an oven at 80 ^{o}C for 1 h before storage or packing into a column.

The coatings on the particles were thermogravimetrically analyzed using an Instrument Specialist Inc. Model TGA-1000. Typically, ~5 mg of silica particles were used for an analysis, and samples were heated in air at a rate of 20 ^{o}C/min from 25 to 800 ^{o}C. Mass losses due to the coatings and to dehydration were determined by comparison to data obtained in the complementary TGA experiments on unfunctionalized silica particles.

4.2.2. Column Packing and Characterization

The coated particles were flow-packed with HPLC grade methanol into AP minicolumns (Waters Corp.) according to the column manufacturer's recommendation. The AP minicolumn has a diameter of 0.5 cm and can accommodate a packed bed height of 4.0 to 6.0 cm [4]. The column packing procedure is as follows. Circa 0.5 g of particles were suspended in 8 mL of methanol. This slurry was then poured into an open column. The slurry was allowed to settle and after a few hours the excess methanol from the top of the bed was removed and the column was capped and connected to a HPLC pump. The bed in the column was pressure packed by flowing methanol from 0 to 1 mL/min in flow rate increments of 0.1 mL/min. The packed column was then equilibrated with the mobile phase before chromatographic experiments. Chromatographic retention experiments were

performed using a Waters HPLC system. This system consists of a Waters 1525 binary HPLC pump, a Waters 2489 UV/Vis detector, and a PC station containing Breeze 2 software. Uracil, $NaNO_3$ and various proteins (e.g. lysozyme, ribonuclease A, α-chymotrypsin, bovine serum albumin (BSA)) were used as tracer substances to determine the void time of a chromatographic column containing EG_3OMe-coated silica particles.

4.3. Results and Discussion

4.3.1. Thermogravimetric Analysis of Coated Silica Particles

Fig. 4-1 shows typical TGA curves for native porasil and functionalized porasil particles. The significant weight losses observed from the curves of the EG_3OMe porasil and C18 porasil in comparison to that of the native particles provide confirmation of the presence of coatings after functionalization procedure. There are two identifiable weight loss regions for C18 porasil. The region below 200 ^oC shows weight loss of adsorbed water. C18 coating on the particles started to decompose at a temperature around 240 ^oC. Similar decomposition temperatures have been reported by several research groups for C18 deposited on silica beads[5] and mesoporous silica (SBA-15)[6, 7]. In addition to the C18 SAM decomposition, the weight loss in the region above 240 ^oC is also attributed to dehydroxylation of silanols that had not reacted with the silane[5]. Similarly, the curve for EG_3OMe porasil in Figure 4-1 also indicates two weight loss regions. This curve shows that the EG_3OMe coating on the porasil particles decomposed at a temperature ~40 ^oC lower than that of C18 coating. Similar decomposition temperature of EG_3OMe coating was also observed on EG_3OMe coated-Viva Silica particles (data not shown).

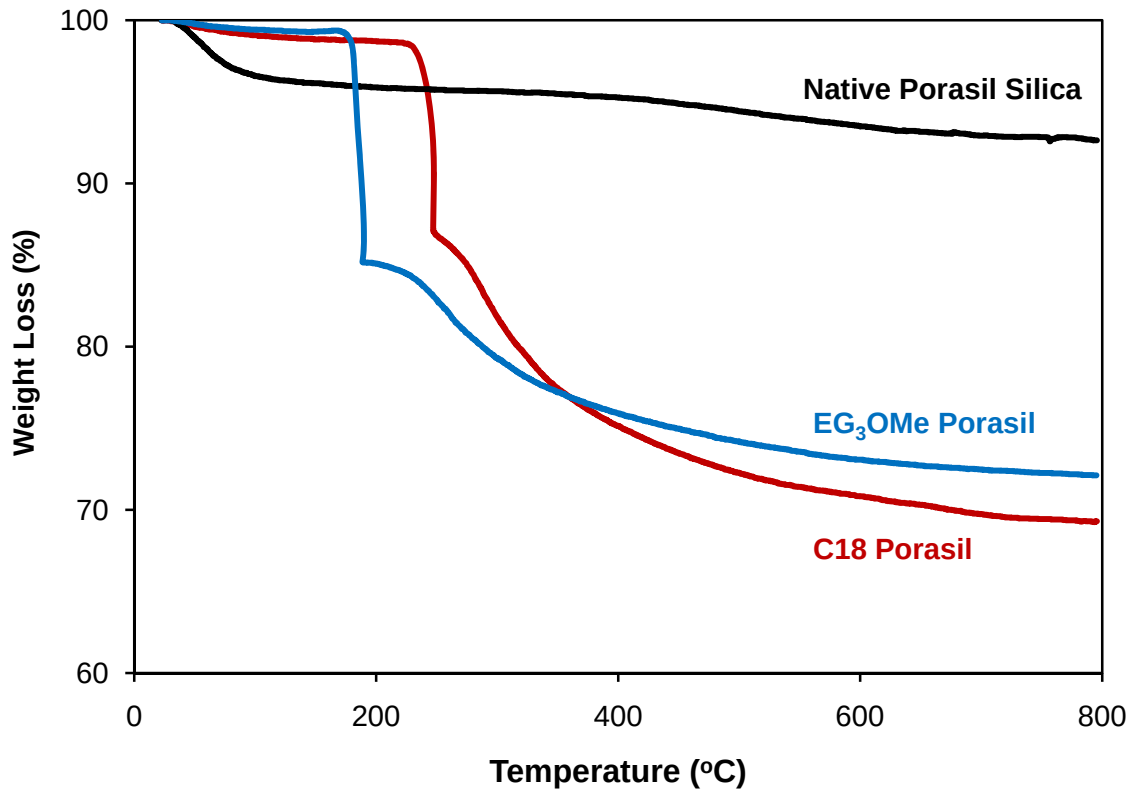

Figure 4-1: TGA curves of native porasil silica, EG_3OMe-coated porasil and C18-coated porasil.

The difference in the weight loss between the coated silica and pristine silica at the temperatures above 200 °C was used for estimating the surface coverages of the SAMs on silica particles. Table 4-1 lists the values of surface coverage of C18 and EG_3OMe coatings on porasil particles that were estimated using a method described in the previous chapter. The surface coverage of EG_3OMe on particle surface was lower than that of C18 due to the 3-dimensional structure of tri(ethylene glycol) chain that takes more molecular space than an alkyl chain (e.g. C18) that can assume an all trans configuration upon assembly onto a surface[8, 9]. Table 4-1 also shows that the surface coverages of C18 and EG_3OMe on Porasil particles are similar to those on Viva Silica.

Table 4-1: Surface Coverage (Γ) of Silanes on Porasil and Viva Silica Particles

Type of Silane	$\Gamma_{porasil}$ (μmol/m^2)	$\Gamma_{viva\ silica}$ (μmol/m^2)[a]
C18	6.0 ± 0.2	6.7 ± 0.4
EG_3OMe	3.9 ± 0.4	3.9 ± 0.3

[a]Data from Chapter 3

4.3.2. Column Characterization

Figure 4-2 shows a Waters glass AP minicolumn that had been packed with functionalized Porasil silica particles. A packed column typically contained ~ 0.5 g of particles and had a bed height of ~ 5.3-5.6 cm. The column can withstand a pressure drop up to 1500 psi.

Figure 4-2: AP Minicolumn packed with functionalized porasil particles.

Column Void Time

The determination of column void time requires a tracer substance that is inert, stable, easily detected, and able to penetrate the porous structure of a stationary phase. I selected several molecules as potential tracers to determine the void time of a column containing EG_3OMe-coated silica particles. The values of void time determined using these tracers are listed in Table 4-2. Uracil and $NaNO_3$ are small molecule tracers that are

commonly used to determine the void time of a chromatographic column[3, 10]. Table 4-2 shows that uracil was retained the longest in the column when eluted isocratically with phosphate buffer at pH 7. $NaNO_3$ was also retained longer in the column as compared to other tracers. BSA shows the least retention as compared to other tracers in Table 4-2. This result suggests that BSA might be partially excluded from the column as its largest molecular surface area (i.e. 140 x 40 $Å^2$) is roughly half the average area of a pore opening (i.e. pore size of 125 Å). Ribonuclease A and α-chymotrypsin exhibited a column void time of 0.65 min despite the differences in their molecular weights. Lysozyme showed a higher retention as compared to ribonuclease A, despite their similar molecular weights. This behavior could be due to some interactions between the positively charged lysozyme (pI = 11) and the residual silanols on the support in the buffer at pH 7. Thus, I conclude that ribonuclease A and α-chymotrypsin provide the best estimate of column void time. In addition, the molecular sizes of these proteins are much less than the pore diameter of the particles. Thus, the estimated void time is not due to molecular exclusion from the porous structure of the column.

One of the uses of void time is to provide information about column porosity (i.e. porosity = void volume/column volume). Using the void time estimated here, the typical porosity of the columns used in this research was ~0.6.

Table 4-2: Void Time Determination using Tracer Substances[a]

Tracer Substance	Molecular Weight (g/mol)	Molecular Dimension ($Å^3$)[b]	*t* (min)
Uracil	112	-	0.89
$NaNO_3$	85	-	0.77
Ribonuclease A	13,800	37 x 45 x 34	0.64
Lysozyme	14,000	30 x 30 x 45	0.77
α-Chymotrypsin	25,000	40 x 40 x 51	0.65
BSA	66,000	140 x 40 x 40	0.46

[a] Stationary phase is EG_3OMe-coated silica particles. Mobile phase is phosphate buffer at pH 7. Flow rate = 1.0 mL/min. Column volume = 1.1 mL.

[b]Molecular dimensions of ribonuclease A, lysozyme, α-chymotrypsin, and BSA were obtained from references[11-14], respectively.

Plate Count

The plate count of the EG_3OMe column was estimated from the chromatogram of 'unretained' ribonuclease A. Figure 4-3 shows the chromatogram of ribonuclease A eluted with phosphate buffer at pH 7 at a retention time of 0.64 min. At this 'unretaining' condition, one can safely assume that the peak width of the sample's chromatogram is mainly due to molecular dispersion in the column rather than due to molecular interaction with the support in the column. Using eq. 4-2 and 4-3, the plate count and reduced plate height of the column were 115 and 27, respectively. The plate count is about an order of magnitude lower than those of typical commercial columns. The acceptable reduced plate height for commercial columns is typically less than 3[1]. Thus, these calculations suggest that the columns used in this research need to be optimized.

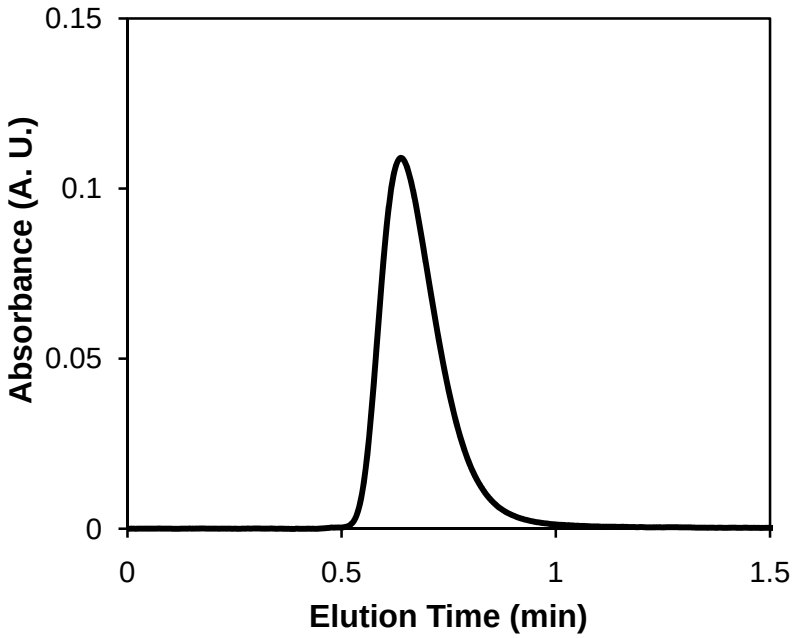

Figure 4-3: Chromatogram of ribonuclease A as eluted with phosphate buffer at pH 7 from a column containing 100%EG support. Eluted ribonuclease A was detected using UV/Vis spectrophotometer at a wavelength of 280 nm.

Column Care and Stability

After each protein chromatographic experiment, a column was flushed with phosphate buffer, followed by pure water, then stored in methanol. When needed, a column can be washed with a solution containing 20% of isopropanol in phosphate buffer to remove irreversibly bound proteins. In our lab, a good column could last for about 2 months and undergo several hundreds of sample injections. Highly asymmetric peak and increased retention time of an unretained analyte provide indications of column deterioration.

4.4. Conclusions

The work described in this chapter serves as an introduction to the next chapter. The value of void time determined in this chapter is useful to determine and compare retention factors of proteins from chromatographic experiments. Unfortunately, the result here also shows that the columns used in this research (especially those in the next chapters) are not optimized as indicated by the low value of the calculated reduced plate height. Optimization of these columns may need to be performed in the future.

4.5. References

1. Neue, U. D., *HPLC Columns Theory, Technology, and Practice*. Wiley-VCH, Inc.: New York, 1997.

2. Dominguez, J. A. G.; Diez-Masa, J. C., Retention parameters in chromatography. *Pure Applied Chemistry* **2001,** *73* (6), 969-992.

3. Rimmer, C. A.; Simmons, C. R.; Dorsey, J. G., The measurement and meaning of void volumes in reversed-phase liquid chromatography. *Journal of Chromatography A* **2002,** *965* (1-2), 219-232.

4. *Waters AP-Minicolumn Care and Use Manuals 038832TP, Revision 2*. Waters Corp.

5. Wang, R.; Baran, G.; Wunder, S. L., Packing and Thermal Stability of Polyoctadecylsiloxane Compared with Octadecylsilane Monolayers. *Langmuir* **2000,** *16* (15), 6298-6305.

6. Mirji, S. A., Adsorption of octadecyltrichlorosilane on Si(1 0 0)/SiO2 and SBA-15. *Colloids and Surfaces A: Physicochemical and Engineering Aspects* **2006,** *289* (1-3), 133-140.

7. Mirji, S. A.; Halligudi, S. B.; Sawant, D. P.; Jacob, N. E.; Patil, K. R.; Gaikwad, A. B.; Pradhan, S. D., Adsorption of octadecyltrichlorosilane on mesoporous SBA-15. *Applied Surface Science* **2006,** *252* (12), 4097-4103.

8. Tedjo, C.; Laibinis, P. E., Modulating protein-surface interactions using mixed self-assembled monolayers of methoxy-terminated-tri(ethylene glycol)-terminated and alkyl terminated trichlorosilanes. *In preparation*.

9. Wasserman, S. R.; Whitesides, G. M.; Tidswell, I. M.; Ocko, B. M.; Pershan, P. S.; Axe, J. D., The structure of self-assembled monolayers of alkylsiloxanes on silicon: a comparison of results from ellipsometry and low-angle x-ray reflectivity. *Journal of the American Chemical Society* **1989,** *111* (15), 5852-5861.

10. Stanley, B. J.; Foster, C. R.; Guiochon, G., On the reproducibility of column performance in liquid chromatography and the role of the packing density. *Journal of Chromatography A* **1997,** *761* (1-2), 41-51.

11. Tilton, R. F. J.; Dewan, J. C.; Petsko, G. A., Effects of temperature on protein structure and dynamics: X-ray crystallographic studies of the protein ribonuclease-A at nine different temperatures from 98 to 320 K. *Biochemistry* **1992,** *31* (9), 2469-2481.

12. Kim, J.; Somorjai, G. A., Molecular Packing of Lysozyme, Fibrinogen, and Bovine Serum Albumin on Hydrophilic and Hydrophobic Surfaces Studied by Infrared−Visible Sum Frequency Generation and Fluorescence Microscopy. *Journal of the American Chemical Society* **2003,** *125* (10), 3150-3158.

13. Barbaric, S.; Luisi, P. L., Micellar solubilization of biopolymers in organic solvents. 5. Activity and conformation of .alpha.-chymotrypsin in isooctane-AOT reverse micelles. *Journal of the American Chemical Society* **1981,** *103* (14), 4239-4244.

14. Wright, A. K.; Thompson, M. R., Hydrodynamic structure of bovine serum albumin determined by transient electric birefringence. *Biophysical Journal* **1975,** *15* (2 Pt 1), 137-141.

CHAPTER V

INFLUENCE OF SURFACE HYDROPHOBICITY OF MIXED SELF-ASSEMBLED MONOLAYERS (SAMS)-COATED SUPPORTS ON PROTEIN RETENTION IN CHROMATOGRAPHY

5.1. Introduction

High performance liquid chromatography (HPLC) is widely used for protein purification both in research and manufacturing scales. When maintaining protein bioactivity is critical, hydrophobic interaction chromatography (HIC) is often the preferred HPLC method. In HIC, proteins are separated based on their surface hydrophobicities using a gradient of salt in the mobile phase[1]. Protein retention is achieved at a high salt concentration in the mobile phase and elution is achieved by decreasing the salt concentration during the chromatographic process[2-4]. HIC utilizes hydrophilic based stationary supports that are functionalized with alkyl or aryl groups to create weakly hydrophobic surface[3, 5]. HIC mobile phase is typically a buffered aqueous solution containing salts[3, 5]. The weakly hydrophobic support and the aqueous eluent provide 'mild' conditions for protein separation which results in the high recovery of protein bioactivity after the separation process[3, 6-8].

A variety of HIC stationary supports with different based materials and surface functional groups with varying surface densities are available commercially[3, 5]. It becomes challenging for one to select an appropriate support to separate a protein of interest. Often times, one purchases several HIC columns and perform 'trial and error' runs to determine the most suitable column. Shaltiel[9] introduced a commercial kit that

contains a homologous series of small columns of sepharose based supports modified with alkyl groups of various chain lengths (e.g. C1 to C10). The usage of the kit was to determine the lowest member of the homologous series capable of retaining the desired protein at low salt concentration (i.e. 10-100 mM). Hjerten et al. [10] also employed a similar approach to Shaltiel's using a homologous alkyl agarose series with charged and uncharged surfaces. Jennissen[11] introduced the concept of critical hydrophobicity for selecting a chromatographic support. In order to achieve separation, a protein has to adsorb on the support and the coating of the support has to be chosen such that adsorption is achieved without protein denaturation. The procedure of selecting the appropriate support includes the selection of suitable alkyl chain length and the chain surface density. Finally the salt concentration in the mobile phase has to be optimized for a complete adsorption of a specified amount of protein on the critical hydrophobicity support (at the previously chosen alkyl chain length and chain surface density)[11]. All these works clearly indicate that the level of hydrophobicity of the chromatographic supports plays an important role in protein separation and specifically on protein retention. The ability to systematically relate the level of hydrophobicity of a column to protein retention in the column would be very useful in column selection and in predicting the retention time of a target protein.

Depositing self-assembled monolayers (SAMs) of organosilanes on the surface of hydroxylated silica is a widely used technique in the development of silica based supports for HPLC[12-14]. Examples of such supports are C18-silica and C8-silica which are widely used for analytical chromatography of proteins in the reversed-phase mode[5, 14-17]. SAMs provide a reliable means for tailoring surfaces at the molecular scale[18-20]. Wirth et al.[16, 17]

used mixtures of short- and long-chain n-alkyltrichlorosilanes to form SAMs on silica supports with controlled surface densities and molecular selectivities for small molecules separation. For HIC, some workers have developed silica particles derivatized with Carbowax PEG 400[7] and alkyl silanes terminated with short oligo(ethylene glycol) species[8, 21, 22]. To my knowledge, most of the silica based HIC supports are coated with pure ethylene glycol-terminated silanes which are highly hydrophilic. In contrast, a variety of alkyl derivatized agarose or other polymeric supports have been developed to provide varying level of hydrophobicity for protein chromatography[3, 5]. In comparison to silane-on-silica system, the surface properties of these polymeric systems are poorly defined.

In this chapter, the effects of the surface hydrophobicity of a support on protein-support interactions during a chromatographic process are examined. For this purpose I prepared chromatographic columns containing silica supports that have been functionalized with varying composition of mixed self-assembled monolayers (SAMs) of $Cl_3Si(CH_2)_{11}(OCH_2CH_2)_3OCH_3$ (referred as EG_3OMe) and n-octyltrichlorosilane (referred as C8). Pure SAMs of EG_3OMe have been shown to produce a hydrophilic coating on flat substrate that resists protein adsorption[23]. Whitesides and coworkers reported that films formed from SAMs terminating in short ethylene glycol chains (only 3 to 6 repeat units in length) is enough to exhibit 'inertness' toward protein adsorption on gold surfaces[24-27]. Pure SAM of C8 produces hydrophobic surface that absorbs proteins[23, 28]. The two-component mixed SAMs used in this research enabled the creation of thin films on silica particles and SiO_2/Si substrates that vary in their surface hydrophobicities in a controlled manner. The results in Chapter 3 showed that the mixed SAMs deposited

on silica particles and on SiO_2/Si substrates had similar surface chemical compositions. Using columns that had been packed with mixed SAMs-coated silica particles, isocratic retention data of several model proteins were obtained from chromatographic experiments. The hydrophobicities of the mixed SAMs-coated silica supports were determined by liquid contact angle measurements of the corresponding mixed SAMs deposited on SiO_2/Si substrates. The wettabilities of the silica supports were not directly measured since the wettability measurement on particulate materials is highly susceptible to experimental errors[29]. Chapter 3 demonstrated that surface energies of mixed SAMs-coated silica particles determined by the developed flotation method were consistent with the values obtained from contact angle measurements on the SiO_2/Si substrates coated with the SAMs. The energies involve in protein adsorption both on SiO_2/Si substrates and silica particles were described by considering a reversible process of protein adsorption with minimal change in the protein conformation during the adsorption process. The results demonstrated that protein retention and separation in a chromatographic column is controllable by selecting the appropriate level of column hydrophobicity in addition to the effect of salt in the mobile phase. The approach described in this chapter would allow one to systematically select the appropriate column for protein separation and reduce the 'trial and error' process during a column selection.

5.2. Theory

In this section, I derive a series of relevant equations that describe the energies involved in protein-surface interactions on flat substrate and silica particles. I adopt a protein-surface interaction model as depicted in Figure 5-1. The main assumptions here

are: (1) protein adsorption onto a surface is treated as a reversible process, and (2) the protein retains its conformation when it adsorbs onto and desorbs from the surface.

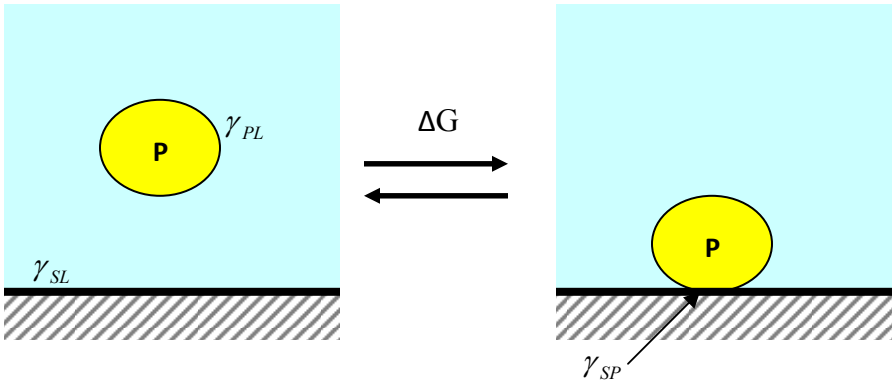

Figure 5-1: A mechanistic representation of the adsorption of a protein (P) from a liquid (L) onto a solid substrate (S). γ_{SL}, γ_{PL}, and γ_{SP} are the energies for the solid-liquid, protein-liquid, and solid-protein interfaces, respectively.

Equations for describing protein adsorption onto a flat substrate

The adsorption of a protein from a liquid onto a solid substrate is often driven by the interfacial energy between the liquid and the solid surface. When the solid-liquid interfacial energy is high (for example as for hydrophobic surface in contact with water), the protein can behave as a surfactant and adsorb at the solid-liquid interface to reduce the interfacial energy. A surface that has a high interfacial energy with water (i.e. not wettable by water) generally will exhibit a high water contact angle.

The wettability of a solid is often determined by measurements of a liquid contact angle on the solid surface. Such measurements can be related to the interfacial energies of the three interacting surfaces, namely the solid, vapor, and liquid surfaces, through Young's equation[30],

$$\gamma_{LV}\cos\theta = \gamma_{SV} - \gamma_{SL} \tag{5-1}$$

where θ is the contact angle, and γ_{LV}, γ_{SV}, and γ_{SL} are the energies of liquid-vapor, solid-vapor, and solid-liquid interfaces, respectively. For a system where solid and liquid phases are in contact over a well-defined area, the work of adhesion (W_{SL}) between these two phases is given by

$$W_{SL} = \gamma_{SV} + \gamma_{LV} - \gamma_{SL} \tag{5-2}$$

and represents the work necessary to separate a unit area of the solid-liquid interface into solid-vapor and liquid-vapor interfaces[31]. This work of adhesion is equal to the change in the free energy of the system. The work of adhesion between the solid and liquid phases can be connected to the wettability of the solid phase by the liquid phase through the Young-Dupré equation[31],

$$W_{SL} = \gamma_{LV}(1+\cos\theta) \quad \text{(energy/surface area)} \tag{5-3}$$

For the case depicted in Figure 5-1, the total change in the free energy of the system is equal to the reversible work of adhesion for the protein molecule adsorbing onto the solid surface times the surface contact area between the protein and the surface (A_{sp}), or

$$\Delta G = (\gamma_{SP} - \gamma_{SL} - \gamma_{PL})A_{sp} \quad \text{(energy)} \tag{5-4}$$

Assuming that two phases are immiscible and interact only through additive dispersion forces, the interfacial energy between a solid phase (S) and a protein phase (P), γ_{SP}, can be defined by the Girifalco-Good equation[32] as

$$\gamma_{SP} = \gamma_{SV} + \gamma_{PV} - 2(\gamma_{SV}\gamma_{PV})^{1/2} \tag{5-5}$$

where γ_{SV} and γ_{PV} are the energies of solid-vapor and protein-vapor interfaces, respectively. Similarly, γ_{SL} and γ_{PL} can be described in the same way as in eq. 5-5. Substituting the respective interfacial energies into eq. 5-4, we obtain

$$\Delta G = [-2\gamma_{LV} + 2(\gamma_{PV}\gamma_{LV})^{1/2} + 2\gamma_{SV}{}^{1/2}(\gamma_{LV}{}^{1/2} - \gamma_{PV}{}^{1/2})]A_{sp} \qquad (5\text{-}6)$$

The combination of the Young's and Girifalco equations to express γ_{SV} yields

$$\gamma_{SV}{}^{1/2} = \frac{\gamma_{LV}{}^{1/2}(\cos\theta + 1)}{2} \qquad (5\text{-}7)$$

Substituting eq. 5-7 into eq. 5-6, we can obtain

$$\Delta G = (1 - \cos\theta)(\gamma_{PV}{}^{1/2}\gamma_{LV}{}^{1/2} - \gamma_{LV})A_{sp} \qquad (5\text{-}8)$$

Eq. 5-8 predicts a linear change in the total free energy upon protein adsorption with changes in the cosine of contact angle for the surface, provided the contact area between the protein and the surface, A_{sp} is constant.

For the case of a solid surface that forms a hydrogel-like structure upon hydration e.g. oligo or poly(ethylene glycol)-coated surfaces, there is an energy term (ΔG_0) that has to be added to eq. 5-8. In this research, ΔG_0 refers to the energy of dehydration of the tri(ethylene glycol) moieties upon protein adsorption onto the mixed SAM-coated solid substrate. Thus, the free energies for protein adsorption onto a mixed SAM-coated substrate can be described as

$$\Delta G = [\Delta G_0 + (1 - \cos\theta)(\gamma_{PV}{}^{1/2}\gamma_{LV}{}^{1/2} - \gamma_{LV})]A_{sp} \qquad (5\text{-}9)$$

Equations for protein interacting with the surface of a chromatographic support

In chromatography, the change in free energy upon protein adsorption onto the surface of a chromatography support can be related to the retention time that a protein requires to exit the column[33]. In the column, a protein can be considered to be either

moving in the mobile phase at the flow velocity of this phase or to be adsorbed onto the surface and be immobile. It is assumed that there is no change in the conformation of the protein when it adsorbs onto the surface. Depending on the interaction energy between a protein and a surface, the protein is expected to partition between the mobile and stationary phases. The change in the free energy between the adsorbed and free states (ΔG) can be related to the partitioning between the two states:

$$\Delta G = G_{adsorbed} - G_{free} \tag{5-10}$$

$$\frac{C_s}{C_m} = \exp\left(-\frac{\Delta G}{RT}\right) \tag{5-11}$$

or

$$\frac{N_s.V_m}{N_m.V_s} = \exp\left(-\frac{\Delta G}{RT}\right) \tag{5-12}$$

where C and N denote the concentration of protein and the number of moles of protein, respectively. The subscript s and m denote the stationary and mobile phases. V_s and V_m are volume of the stationary phase and mobile phase, respectively, with $\phi = V_s/V_m$. R is ideal gas constant and T is temperature. From eq. 5-12, the percentage of free protein in the mobile phase can be expressed as

$$\%free = \frac{1}{1+\phi\exp\left(-\frac{\Delta G}{RT}\right)} \tag{5-13}$$

For a column volume V_{column}, the time (t_o) for an unretained protein to exit the column is

$$t_o = \frac{V_{column}}{v_{mobile}} \tag{5-14}$$

where v_{mobile} is the velocity of the mobile phase through the column. The time required for a retained protein to flow through and exit the column is t_R and is given by

$$t_R = t_0\left(1+\phi\exp\left(-\frac{\Delta G}{RT}\right)\right) \tag{5-15}$$

Further rearrangement of eq. 5-15 gives the retention factor *k* as

$$k = \frac{t_R - t_0}{t_0} = \phi\exp\left(-\frac{\Delta G}{RT}\right) \tag{5-16}$$

Horvath and coworkers adapted the solvophobic interaction theory to describe the effect of salt on protein retention in chromatography[2]. According to the theory, in the absence of special binding effects between the protein and salt, the change in the free energy of a system upon protein retention is associated with the free energy changes due to electrostatic effect and hydrophobic effect. At sufficiently high salt concentrations when the mechanism of retention is affected predominantly by hydrophobic interactions, the retention increases with both the molal salt concentration in the mobile phase and the size of the protein or its hydrophobic moiety. This behavior is often mathematically described as follows,

$$\ln k = S[salt] + \ln k_0 \tag{5-17}$$

The slope *S* is related to the hydrophobic contact area between the protein and the surface[2, 4, 34]. k_0 is the value of retention factor in a mobile phase containing no salt. I modified eq. 5-17 into eq. 5-18 by choosing a reference state (i.e. salt concentration of 0.5 M in mobile phase). The value of slope *S* in eq. 5-18 is the same as in eq. 5-17, while the intercept $k_{0.5}$ is the retention factor of a protein when it is isocratically eluted from a column with 0.5 M of salt in the mobile phase.

$$\ln k = S([salt] - [0.5M]) + \ln k_{0.5} \qquad (5\text{-}18)$$

Substituting the retention factor k in eq. 5-16 with that in eq. 5-18, we obtain an equation that describes the change in the free energy upon protein retention in chromatographic column as a function of the salt concentration in the mobile phase,

$$-\frac{\Delta G}{RT} = \ln k = S([salt] - [0.5M]) + \ln k_{0.5} - \ln \phi \qquad (5\text{-}19)$$

5.3. Materials and Methods

5.3.1. Proteins and Chemicals

Lysozyme (chicken egg white), albumin (bovine serum) and α-chymotrypsin (bovine pancreas), ribonuclease A (bovine pancreas), trypsin inhibitor (soybean) were from Sigma. 50 mM of phosphate buffer (pH 7) for mobile phase was made by dissolving KH_2PO_4 (Fisher Scientific) in pure water. The pH was adjusted with the addition of KOH. Salts such as Na_2SO_4, $(NH_4)_2SO_4$, and NaCl were obtained from Fisher Scientific. All aqueous solutions were filtered through 0.45 μm filter. HPLC grade methanol (Fisher Scientific) was used as received. For forming self-assembled monolayers on substrates, n-octyltrichlorosilane (C8) was purchased from Gelest (Morrisville, PA, USA), while $Cl_3Si(CH_2)_{11}(OCH_2CH_2)_3OCH_3$ (EG_3OMe) was synthesized in our laboratory[28].

5.3.2. Chromatographic Stationary Phase

Bulk silica particles (Porasil™, 125 Å of pore size, 15-20 μm of particle size) were obtained from Waters Corp. (Milford, MA, USA). These particles were functionalized with EG_3OMe and C8 silanes (at various mixed compositions) by a

method that is described in the previous chapter. The functionalized particles were flow-packed with methanol into AP minicolumns (Waters Corp.) according to the column manufacturer's recommendation. The column diameter was 0.5 cm with final bed heights of 5.3-5.6 cm. Before protein retention experiments, columns were equilibrated with at least 20 column volumes of phosphate buffer. For clarity purposes, a column packed with particles functionalized with silanes from a solution with a composition of x%/y% EG_3OMe/C8 is labeled as x%EG. For example, a column containing particles functionalized in a solution containing silanes with a composition of 80%/20% EG_3OMe/C8 is labeled as 80%EG.

5.3.3. Protein Retention Measurements

The experiments were performed with a HPLC system equipped with Waters 1525 Binary HPLC pump and a manual injector (Rheodyne, model 7725i) with 5 µl injection loop. Protein elution was detected with a Waters 2489 UV/Vis Detector using a wavelength of 280 nm. Individual protein was dissolved in pure water to a concentration of 5.5 mg/ml. Protein solutions were filtered through 0.45 µm filter before injection into the HPLC system. The sample injection volume was 5 µL. Isocratic elution was performed with 50 mM of phosphate buffer containing various amount of Na_2SO4 at a flow rate of 1 mL/min. The desired Na_2SO4 concentrations that entered the column were obtained by blending mobile phase A (50 mM phosphate buffer at pH 7) and mobile phase B (1 M of Na_2SO_4 in 50 mM phosphate buffer at pH 7). After each isocratic run, the column was flushed with 10-15 column volumes of 0.2 M of Na_2SO_4 in phosphate

buffer and then equilibrated with 10 column volumes of buffer containing the appropriate salt concentration prior to the next sample injection.

5.4. Results and Discussion

5.4.1. Effect of Salt Concentration on Protein Retention

The effect of adding salt such as Na_2SO_4 at various concentrations in the mobile phase to elute lysozyme from a column containing 100%EG is shown in Figure 5-2. Na_2SO_4 in this case acts as a 'salting-out' reagent. At higher concentration of Na_2SO_4 in the mobile phase, the protein was retained longer in the column. Further, Figure 5-2 shows that as lysozyme spends more time in the column, its peak width gets wider and peak height gets shorter as compared to the sample with a lower retention time. This behavior is as expected due to the increased opportunity of dispersion with longer time spent in the column.

Figure 5-3 shows the influence of Na_2SO_4 concentration in the mobile phase on the retention of lysozyme in columns containing mixed SAMs-coated supports. The data shown in Figure 5-3 were obtained at sufficiently high concentrations of salt in the mobile phase, where the changes in *ln k* were linear to the changes in salt concentration. This behavior indicates that the system was operating in the 'salting out' regime[2, 35]. As the surface density of EG_3OMe SAM on the supports increased from 70%EG to 100%EG, the hydrophobicity level of the columns decreased, and the protein was less retained for a concentration of salt. Thus, more amount of salt is required to retain a protein in a less hydrophobic column for the same level of retention factor. The data in Figure 5-3 were fitted using eq. 5-18 and the values of the slopes are listed in Table 5-1.

The value of the slope is related to the hydrophobic contact area between the protein and the surface[34-36]. Table 5-1 shows that for lysozyme, the values of the slope are essentially the same within experimental error for all columns except for that containing the 70%EG support. This result suggests that the hydrophobic contact area between lysozyme and the surfaces of the first three supports in Table 5-1 was unchanged regardless of the differences in the hydrophobicity of the supports. Affected by the increased level of hydrophobicity of the 70%EG support, lysozyme may undergo a change in its conformation upon interaction with the surface. This would lead to a change in its hydrophobic contact area as shown by the different value of the slope.

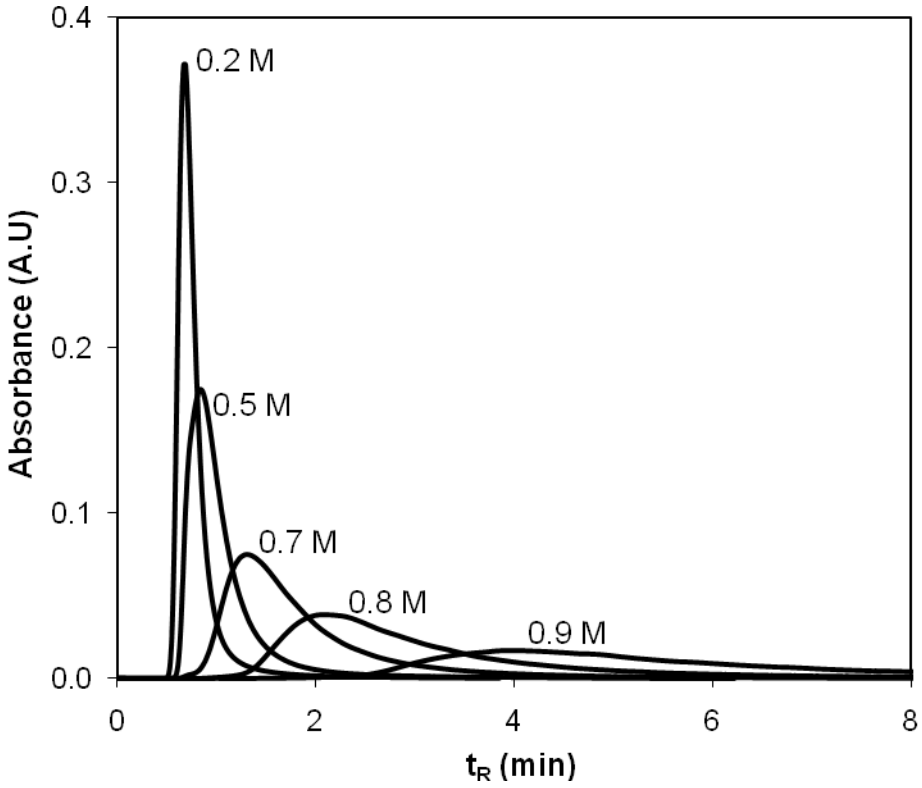

Figure 5-2: Isocratic retention data of lysozyme eluted from a column containing 100%EG support at various Na_2SO_4 concentrations in the mobile phase (50 mM phosphate buffer of pH 7) with flow rate of 1 ml/min. t_R denotes protein retention time.

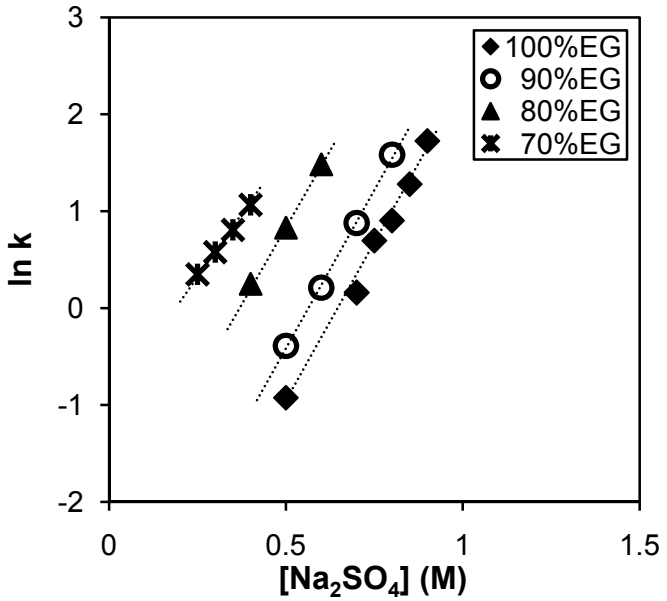

Figure 5-3: Retention factors of lysozyme as isocratically eluted at various Na_2SO_4 concentrations in the mobile phase from columns containing 100%EG, 90%EG, 80%EG, and 70%EG supports. The error for the values of slopes (S) and intercepts ($ln\ k_{0.5}$) of the plots is ± 0.3. Lines are added as guides to the eye.

I performed isocratic retention experiments with three other proteins using mixed SAMs-coated supports and the results are shown in Figure 5-4. The data in Figure 5-4 also obey the linear relationship that is predicted by eq. 5-18. The values of the slope for each set of retention data are listed in Table 5-1. For a particular protein, the slopes obtained from different types of support were similar. This result suggests the proteins did not change, or could undergo minimal change on, its hydrophobic surface contact area as they interacted with different level of column hydrophobicity. However, there was an exception for ribonuclease A eluted from the column containing 80%EG support. It is possible that the increase in the value of slope (i.e. hydrophobic contact area) was due to protein unfolding upon interaction with the surface of 80%EG support.

Table 5-1: Values of Slope (*S*) and $ln\ k_{0.5}$ from the Retention Data of Several Model Proteins

Support	Ribonuclease A		Lysozyme		Trypsin inhibitor		α-Chymotrypsin	
	S	$ln\ k_{0.5}$	*S*	$ln\ k_{0.5}$	*S*	$ln\ k_{0.5}$	*S*	$ln\ k_{0.5}$
100%EG	6.6	-4.4	6.6	-1.0	10.6	2.1	9.6	-1.3
90%EG	6.5	-3.6	6.6	-0.4	11.6	4.3	10.7	0.3
80%EG	7.9	-2.1	6.2	0.8			10.5	3.6
70%EG			4.8	1.5				

Values of $ln\ k_{0.5}$ were calculated using eq. 5-18.

Table 5-2: Physical Properties of Model Proteins Used in the Protein Retention Experiments

Protein	Molecular weight (kDa)	pI	Charged area ($Å^2$)[a]	Polar area ($Å^2$)[a]	Non-polar area ($Å^2$)[a]	Chain configuration
Ribonuclease A	13.8	9.4	927	2401	3462	single
Lysozyme	14	11.0	907	2548	3230	single
Trypsin inhibitor	20.5	4.5				single
α-Chymotrypsin	25	8.7	1238	3991	5426	tri-polypeptide

[a]Data from Chalikian et al.[37]

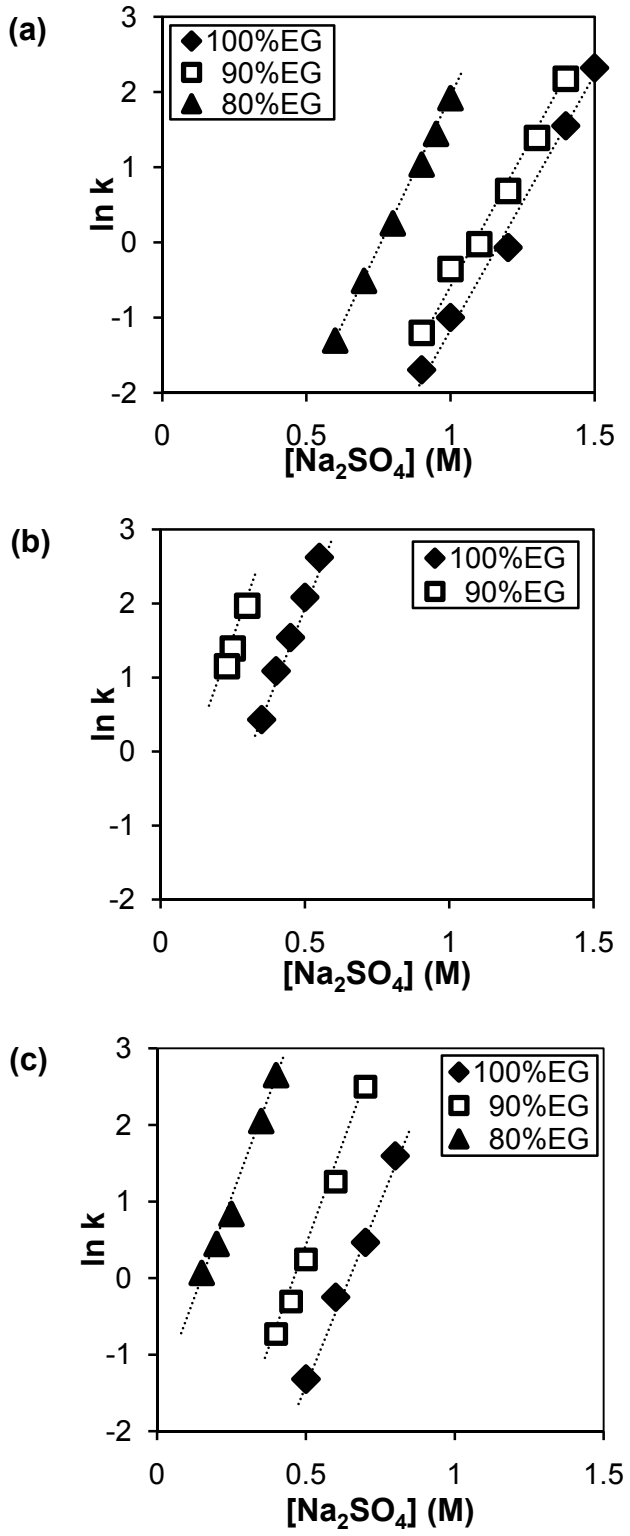

Figure 5-4: Retention factors of (a) ribonuclease A, (b) trypsin inhibitor, (c) α-chymotrypsin as isocratically eluted at various Na_2SO_4 concentrations from columns containing 100%EG, 90%EG, and 80%EG supports. Lines are added as guides to the eye.

Ignoring the values of the slope for ribonuclease A and lysozyme obtained from the columns containing 80%EG and 70%EG supports, respectively, the average values of the slopes for ribonuclease A, lysozyme, trypsin inhibitor, and α-chymotrypsin were 6.6, 6.5, 11.1, and 10.3, respectively. Ribonuclease A and lysozyme, having similar molecular sizes and non-polar surface areas (Table 5-2), exhibited similar average values of slope. The slope for α-chymotrypsin was greater than those for ribonuclease A and lysozyme. This is comparative to α-chymotrypsin having a larger molecular size and non-polar area than the other two proteins, as shown in Table 5-2. Interestingly, the slope for trypsin inhibitor was slightly larger than that for α-chymotrypsin although it had slightly smaller molecular size. Unfortunately, I could not find the surface areas for trypsin inhibitor from literatures for the purpose of comparison with the other proteins in this research. From experimental observation, trypsin inhibitor exhibited a behavior of a 'sticky' protein as it was highly retained in all tested columns in comparison to other proteins. It is possible that trypsin inhibitor has a larger non-polar surface area than α-chymotrypsin despite the fact that it has a smaller molecular weight than α-chymotrypsin.

It can be concluded from the result that there is a general relationship between the value of a slope (hydrophobic contact area) and the non-polar surface area of a protein. Katti et al. [36] have reported similar result. In general, larger size of protein is expected to have larger hydrophobic contact area[8, 22, 34]. However, the level of this hydrophobic contact area is dependent on the configuration of the protein under the prevailing experimental condition[34]. The distribution of the non-polar area on the surface a protein can also influence the size of hydrophobic contact area between a protein and the surface[38].

The value of an intercept from a plot of *ln k* vs. salt concentration indicates a relative strength of hydrophobic interaction between a protein and a support[4]. In reference to eq. 5-18, $ln\ k_{0.5}$ is the relevant intercept. Table 5-1 shows that for all proteins, the values of $ln\ k_{0.5}$ increased as the proteins interacted with supports of increasing level of hydrophobicity (i.e. decreasing %EG). This trend is as expected since the strength of hydrophobic interactions is influenced by the level of hydrophobicity of a surface. Comparing the values of $ln\ k_{0.5}$ between the proteins in a particular column, these values increased in the same order as the values of the slope, with trypsin inhibitor exhibiting the strongest hydrophobic interaction. This trend seems reasonable since the strength of hydrophobic interaction would be proportional to the hydrophobic contact area between a protein and a surface. However, we can see an exception in Table 5-1. The values of $ln\ k_{0.5}$ obtained from a column containing 100%EG for α-chymotrypsin was close to that of lysozyme, although α-chymotrypsin had a value of slope that is almost twice that of lysozyme. One possible explanation to this behavior is that EG_3OMe SAM coating on the 100%EG support exhibits minimal interaction with hydrophilic proteins such as α-chymotrypsin and lysozyme in the mobile phase containing low concentration of salt (e.g. 0.5 M of Na_2SO_4). It has been reported in literatures that EG_3OMe SAMs exhibit 'inertness' toward several proteins in the phosphate buffer saline solution (this buffer contains the total of 0.15 M of salt)[23, 28, 39].

5.4.2. Effect of Salt Type on Protein Retention

Figure 5-5(a) shows the influence of salt concentration on the isocratic elution of lysozyme through the 100%EG column using mobile phases that contained three different types of salt. For a salt concentration, the level of lysozyme retention was different with respect to different salts, with retention increasing with salt type in the following order: $NaCl<(NH_4)_2SO_4<Na_2SO_4$, especially at high salt concentration. This order follows the Hofmeister series for the precipitation of proteins from aqueous solutions[3, 40].

In the practice of protein precipitation from a solution, the solubility or 'salting out' of protein in a solution is influenced by the ionic strength of the solution. Figure 5-5b shows the effect of ionic strength of the mobile phase on the lysozyme retention. The data in this figure seems to indicate that all types of salt provide similar change in retention factor with respect to the change in the ionic strength. For a value of ionic strength, the level of lysozyme retention increased with salt type in the following order: $(NH_4)_2SO_4<Na_2SO_4<NaCl$. For $(NH_4)_2SO_4$ and Na_2SO_4, both yield the same value of ionic strength for a value of salt concentration since they have the same numbers of cations and anions. However, the data for both salts in Figure 5-5(b) do not coincide together, suggesting that factors other than the level of ionic strength in the mobile phase affect protein retention.

According to the hydrophobic interaction model that was proposed by Melander and Horvath, protein retention is linear with molal salt concentration and depends upon the surface tension of the mobile phase[2]. The surface tension of a salt solution can be approximately described by

$$\gamma = \gamma^{o} + \sigma m \qquad (5\text{-}20)$$

where γ^{o} is the surface tension of pure water, m is the molality of the salt, and σ is the molal surface tension increment[2, 41]. Using the values of σ reported by Melander and Horvath[2] and eq. 5-20, I plotted the lysozyme retention data as a function of the surface tension of the mobile phase in Figure 5-5(c). This figure shows that mobile phases containing Na_2SO_4 and $(NH_4)_2SO_4$ produced similar effect of surface tension on protein retention. Elution data using NaCl in mobile phase, however, does not coincide with the rest of the data. This means that factors other than the surface tension of a mobile phase also influence protein retention. Fausnaugh and Regnier have observed similar phenomenon and suggested that specific interactions between salt ions and proteins may play a role, which may alter the protein chromatographic behavior[4].

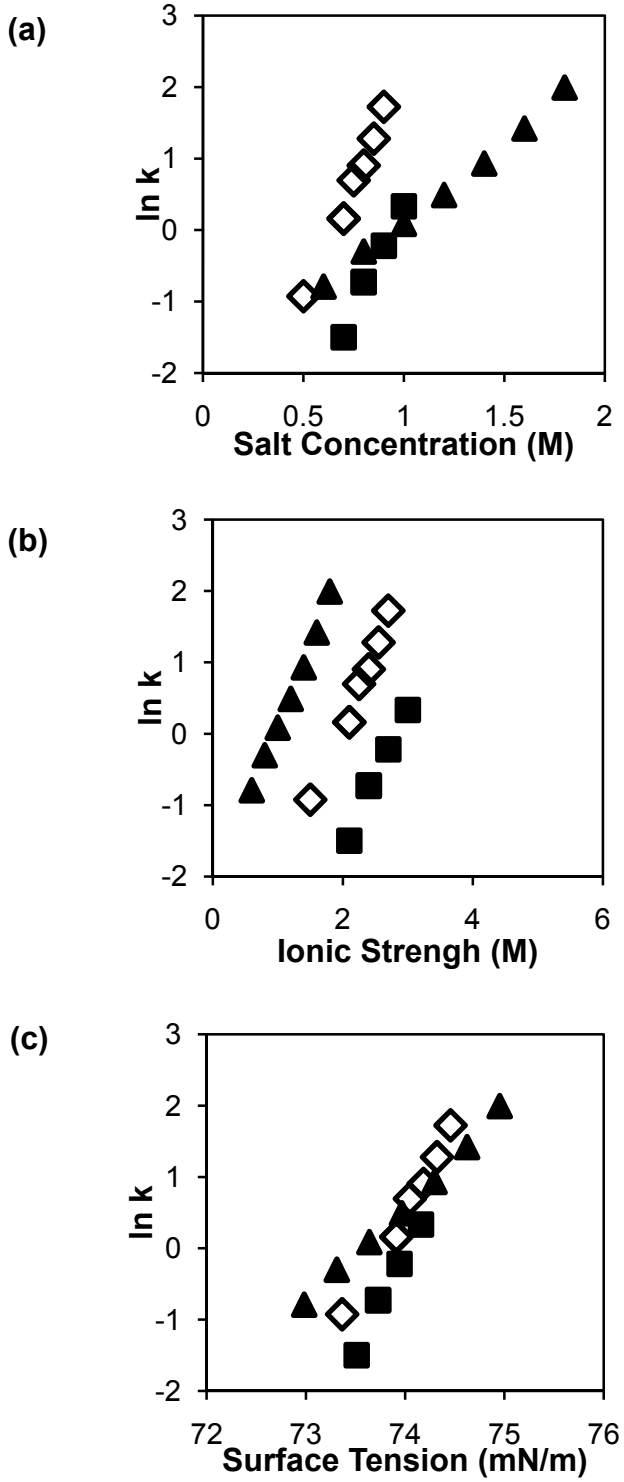

Figure 5-5: Retention data for lysozyme eluted isocratically through a column containing 100%EG support using mobile phases that contained (◇)Na_2SO_4, (■) $(NH_4)_2SO_4$, and (▲)NaCl. (a) Effect of salt concentration in the mobile phase, (b) effect of the ionic strength of the mobile phase, (c) effect of the surface tension of the mobile phase.

5.4.3. Influence of Surface Hydrophobicity of Chromatographic Supports on Protein Retention

In section 5.4.2, I concluded that the strength of protein-surface interaction (i.e. *ln* $k_{0.5}$) is related to the level of surface hydrophobicity of the support. Here I analyze such relationship using energetic equations that were described at the beginning of this chapter. For the case of protein adsorption onto a flat substrate, eq. 5- 9 predicts the change in total free energy upon protein adsorption with respect to the change in the contact angle of a reference liquid on the surface. For the case of protein adsorption onto a chromatographic support, eq. 5-19 describes the change in total free energy upon protein adsorption as a function of salt concentration in the mobile phase.

Having the same type of mixed SAM coating both on flat substrate and silica support, one can relate the free energy changes upon protein adsorption measured on the flat substrate and silica support. A linear relationship between the protein retention time and the hydrophobicity of a support (represented by the cosine of a liquid contact angle, *cos* θ) is obtained by equating eq. 5-9 and eq. 5-19,

$$\ln k = \frac{(1-\cos\theta)(\gamma_{LV} - \gamma_{LV}^{1/2}\gamma_{PV}^{1/2})A_{sp}}{RT} - \frac{\Delta G_0 A_{sp}}{RT} + \ln\phi \qquad (5\text{-}21)$$

Analyzing eq. 5-21 at 0.5 M of Na_2SO_4 in phosphate buffer at pH 7, I obtain

$$\ln k_{0.5} = \frac{(1-\cos\theta_{0.5})(\gamma_{LV} - \gamma_{LV}^{1/2}\gamma_{PV}^{1/2})A_{sp}}{RT} - \frac{\Delta G_0 A_{sp}}{RT} + \ln\phi \qquad (5\text{-}22)$$

where *cos* $\theta_{0.5}$ is the cosine of the contact angle of a drop of liquid containing 0.5 M of Na_2SO_4 in phosphate buffer at pH 7 on a mixed SAM-coated substrate. It is preferable to measure the contact angle of a reference liquid on the mixed SAM-coated flat support

rather than on the mixed SAM-coated particulate support since contact angle measurements on flat substrate are straightforward and the result is more reliable than that on particulate materials[29].

The $k_{0.5}$ values of the experimental and calculated retention data (using eq. 5-18) are plotted against the wettability (or hydrophobicity) of the respective mixed SAM-coated SiO_2/Si substrates in Figure 5-6. This figure shows that eq. 5-18 provides a good prediction on the retention factors ($ln\ k_{0.5}$) of lysozyme and α-chymotrypsin. The experimental $ln\ k_{0.5}$ values of ribonuclease A suggest that its retentions were unaffected when eluted with a mobile phase containing 0.5 M of Na_2SO_4 in phosphate buffer from columns containing 100%EG, 90EG%, and 80%EG supports. Since eq. 5-18 for ribonuclease A was derived from the data at high salt concentration region, the prediction of $ln\ k_{0.5}$ values for ribonuclease A is underestimated by eq. 5-18. Retention data for trypsin inhibitor could not be obtained experimentally since this protein was highly retained at salt concentrations just below 0.5 M.

The experimental data in Figure 5-6 were obtained from single protein elution. For a hypothetical case of running a sample containing the four proteins used in this research, one could expect the following separation behavior. Using 100%EG support (the least hydrophobic support), it is expected that lysozyme, ribonuclease A, and α-chymotrypsin would be eluted together at a retention time close to the void column time and these proteins would be well separated from trypsin inhibitor. With 90%EG support, one would expect a better separation between ribonuclease A and the other two proteins (lysozyme and α-chymotrypsin) at the beginning of the elution period. Further, using 80%EG support, the four proteins could be well-separated, although there is a possibility of permanent retention of the trypsin inhibitor in the column. The result in Figure 5-6

demonstrates that protein retention can be potentially controlled by selecting the appropriate level of hydrophobicity of the support. It is worth noting that the hydrophobicities of the supports used in this work were close to each other. However, such slight differences result in significant differences in the level of protein retention.

The calculated data in Figure 5-6 can be fitted using eq. 5-22 which has straight lines having positive slopes (α) and negative intercepts (β), where

$$\alpha = \frac{(\gamma_{LV} - \gamma_{LV}^{1/2}\gamma_{PV}^{1/2})A_{sp}}{RT} \qquad \text{and} \qquad \beta = -\frac{\Delta G_0 A_{sp}}{RT} + \ln\phi$$

The values of α, β, and $\Delta G_0.A_{sp}$ for the four proteins are listed in Table 5-4. The value of $\Delta G_0.A_{sp}$ for each protein indicates the free energy of a mol of protein at the condition of $\cos\theta = 1$ and can be estimated from the value of β. The values of α, β, and $\Delta G_0.A_{sp}$ for each individual protein show correlations with the values of S that were determined earlier in this chapter.

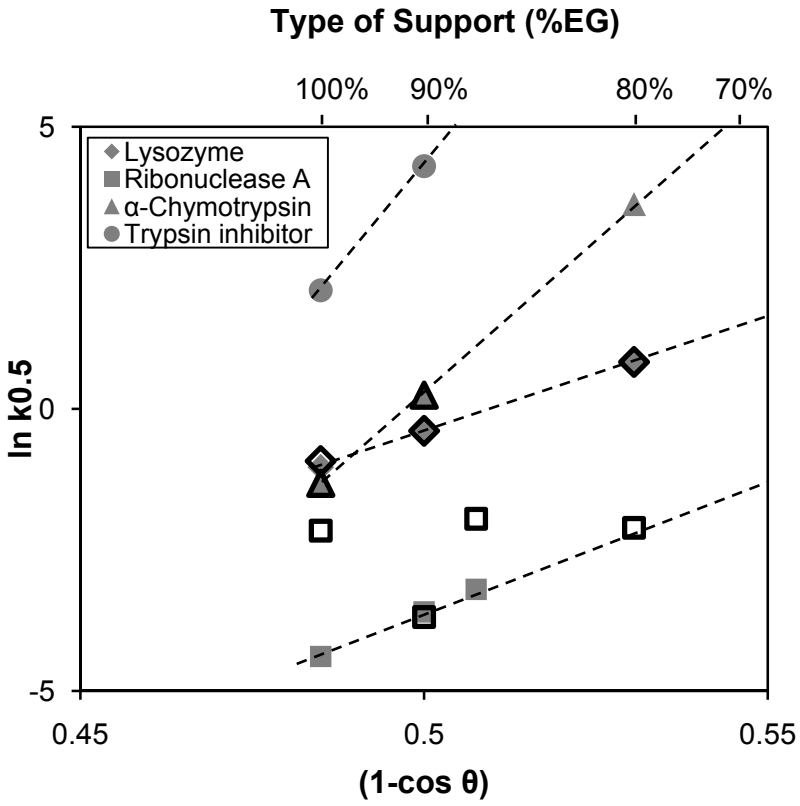

Figure 5-6: The effect of support hydrophobicity (as measured by wetting measurement) on the retention factors of proteins when eluted with a mobile phase containing 0.5 M of Na_2SO_4 in phosphate buffer ($ln\ k_{0.5}$). *Cos θ* is the cosine of a drop of liquid containing 0.5 M of Na_2SO_4 in phosphate buffer at pH 7 on a mixed SAM-coated SiO_2/Si substrate. Filled symbols denote calculated data and open symbols denote experimental data. The error in contact angle measurement is 0.5°. Lines were added as guides to the eye.

Table 5-4: Values of Slope (α), Intercepts (β) and $\Delta G_0.A_{sp}$ for Data in Figure 5-6

Protein	α	β	$\Delta G_0.A_{sp}$(kJ/mol)
Ribonuclease A	50	-30	70
Lysozyme	40	-20	50
Trypsin inhibitor	150	-70	170
α-chymotrypsin	110	-50	130

Predicting isocratic protein retention time based on salt concentration and surface hydrophobicity of a support

Eq. 5-22 provides a relationship between *ln* $k_{0.5}$ and the wettability (or hydrophobicity) of a surface. Substituting *ln* $k_{0.5}$ in eq. 5-18 with that in eq. 5-22, one can obtain a general equation for predicting isocratic protein retention factor or retention time based on the information of the salt concentration in the mobile phase and the wettability (or hydrophobicity) of the support, i.e.

$$\ln k = S([salt] - 0.5M) + \alpha(1 - \cos\theta) + \beta \tag{5-23}$$

$$t_R = t_0(1 + \exp\{S([salt] - 0.5M) + \alpha(1 - \cos\theta) + \beta\}) \tag{5-24}$$

Figure 5-7 shows 3-D plots of logarithmic retention factors and normalized retention times of ribonuclease A, lysozyme, and α-chymotrypsin, that were predicted using the above equations for any possible combinations of salt concentration and support hydrophobicity. For the conditions that result in the predicted values of *ln k* below -2.0, the resulting predicted retention times (t_R) essentially have values that are very close to the column void time (t_0), or in other words, the protein is predicted to be eluted at ~t_0. This prediction is reasonable since a protein is typically unretained at the condition of low salt concentration and/or with highly hydrophilic support. Comparing the predicted *ln k* values of the proteins, a set of condition(s) (i.e. salt concentration and column hydrophobicity) can be chosen to achieve the best separation condition for a mixture containing the three proteins. Figure 5-8 shows the combined 3-D plots of the three proteins. This figure suggests that one should choose conditions outside the lines of intersection between the planes since at these conditions one would obtain poor separation (i.e. low resolution) of the three proteins.

Figure 5-9 shows chromatograms of a sample containing a mixture of ribonuclease A and lysozyme that was eluted isocratically from columns containing supports of different surface hydrophobicity. In both chromatograms, ribonuclease A was eluted earlier than lysozyme. The chromatograms also show that the retention of ribonuclease A was similar in both columns. On the other hand, lysozyme was retained longer (hence eluted later) in the column containing 90%EG support, as compared to the column containing 100%EG support. The first chromatogram shows that the two proteins were poorly resolved when eluted from a column containing 100%EG support. However, the second chromatogram shows that the resolution between the two proteins was improved using a column containing 90%EG support. Using eq. 4-1 (from Chapter 4) to calculate resolution between the two proteins in both columns, the resolution in columns containing 100%EG and 90%EG supports are ~0.5 and ~1, respectively. This result demonstrates that resolution of proteins can be tuned by choosing a column of the appropriate surface hydrophobicity.

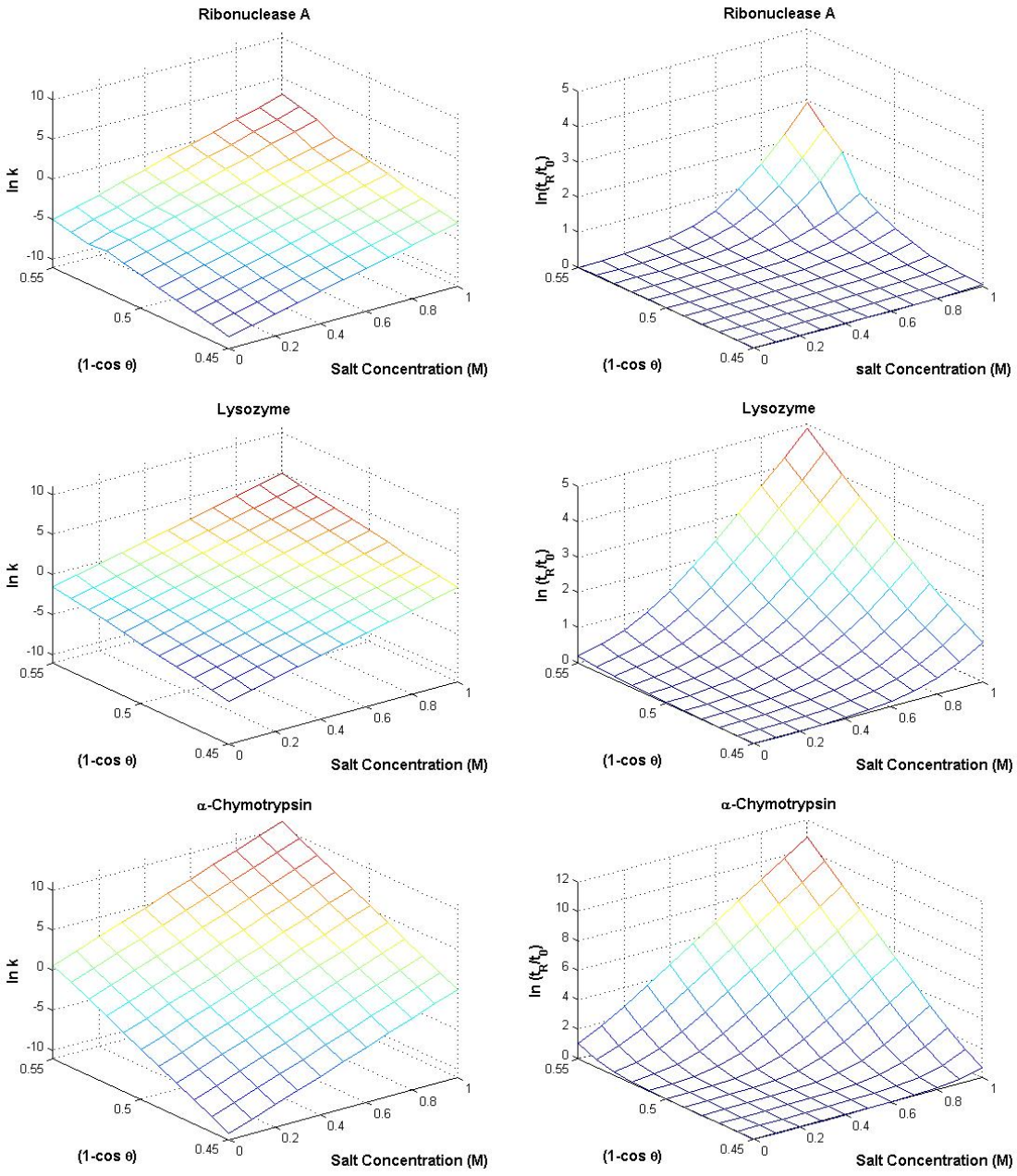

Figure 5-7: 3-D plots of the natural logarithm of retention factors *k* (first column) and the natural logarithm of normalized retention times *ln* (t_R/t_0) (second column) of ribonuclease A, lysozyme, and α-chymotrypsin as functions of the surface hydrophobicity of the support $(1 - \cos\theta)$ and salt concentration (Na_2SO_4) in the mobile phase. t_0 is column void time.

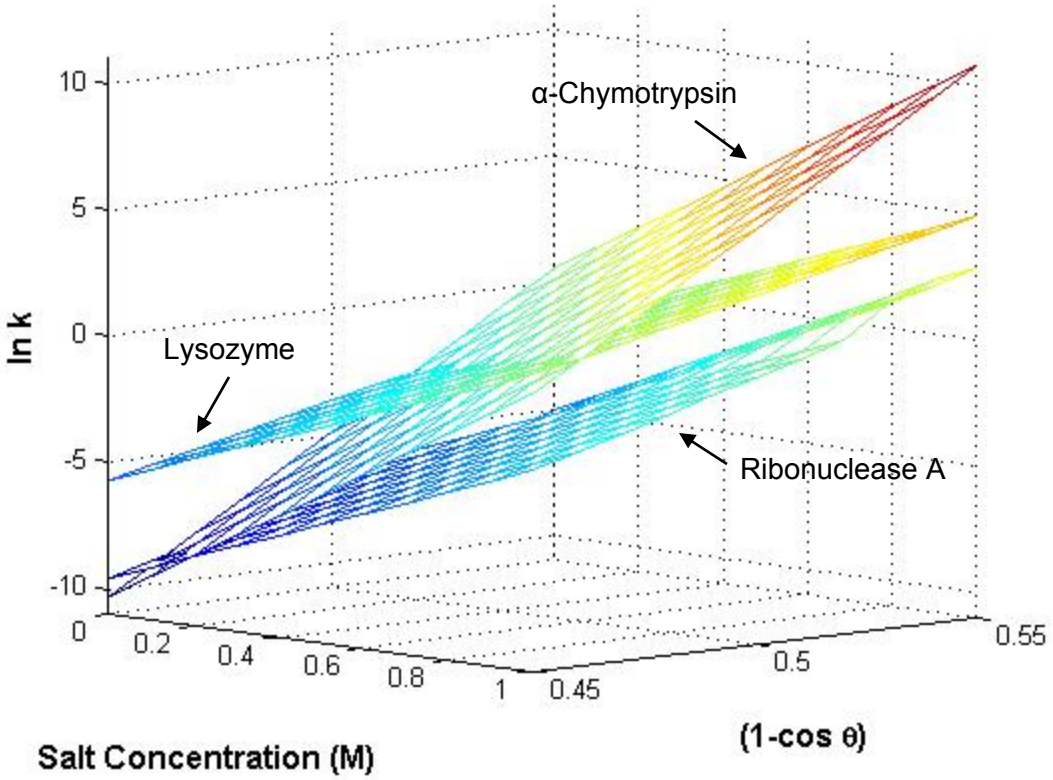

Figure 5-8: Combined 3-D plots of the natural logarithms of the retention factors *k* for ribonuclease A, lysozyme, and α-chymotrypsin as a function of the surface hydrophobicity of the support *(1 – cos θ)* and salt concentration (Na_2SO_4).

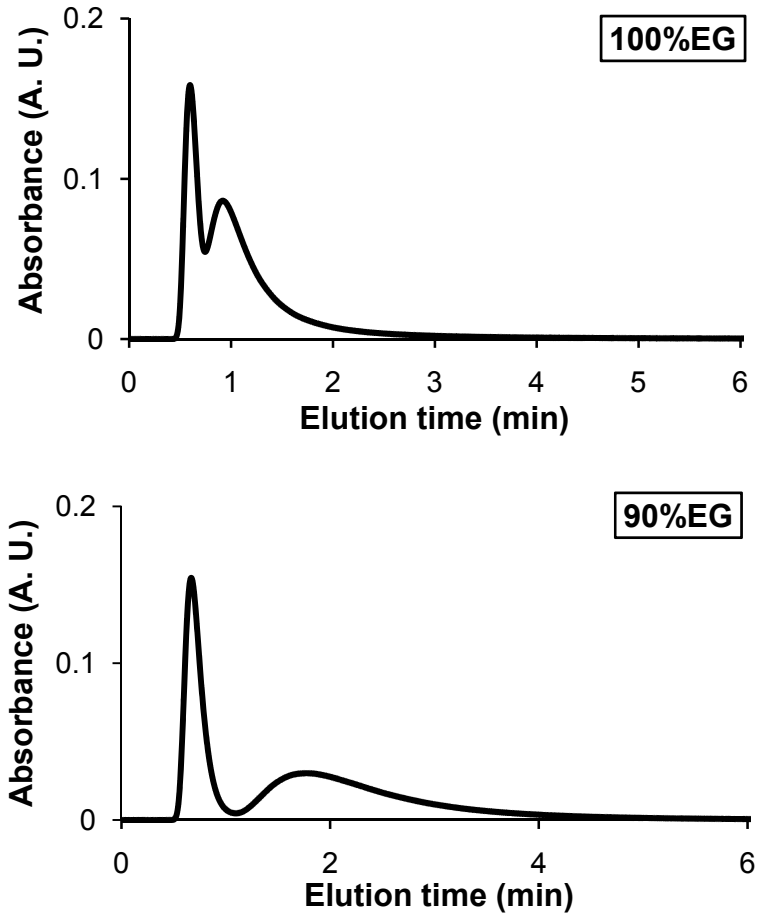

Figure 5-9: Chromatograms of samples containing 5 mg/mL of ribonuclease A and 3.5 mg/mL of lysozyme in pure water that were eluted from columns containing 100%EG and 90%EG supports with mobile phase containing 0.5 M of Na_2SO_4 in phosphate buffer at pH 7. The first and second peaks in the above chromatograms indicate ribonuclease A and lysozyme, respectively.

5.5. Conclusions

The influence of the surface hydrophobicity of chromatographic supports on the retention of a protein in a chromatographic process is investigated. For the purpose of such study, mixed-SAMs of silanes are deposited on the surface of silica particles as well as on flat support exposing silica surface, to create coatings with controlled chemical compositions (or surface hydrophobicities). It is worth noting that contact angle measurement provides a convenient and reliable method for determining the wettability

(or level of hydrophobicity) of a flat substrate. Such advantage is not available for particulate materials such as chromatographic supports. Using equations that describes energies involve upon protein interactions with the supports, protein retention in a chromatographic column can be systematically related with the hydrophobicity of the support. The results show that protein retention and separation in a chromatographic column is controllable by selecting the appropriate level of column hydrophobicity in addition to the effect of salt on protein retention.

In general, the information about the hydrophobicity of a chromatographic column is rarely available from column manufacturers. What is typically known are the types of functional group on a support, the chain length and surface density of the particular functional group. All these support characteristics contribute to the hydrophobicity of the surface of a support which affects protein retention. The result in this chapter shows that systematic relationship between the hydrophobicity of supports and protein retention factors is useful for predicting protein retention times and/or resolutions between proteins in a column. In a broader aspect, the generic approach that is proposed here would be applicable for hydrophobic interaction of chromatography of proteins.

5.6. References

1. Xiao, Y.; Rathore, A.; O'Connell, J. P.; Fernandez, E. J., Generalizing a two-conformation model for describing salt and temperature effects on protein retention and stability in hydrophobic interaction chromatography. *Journal of Chromatography A* **2007,** *1157* (1-2), 197.

2. Melander, W.; Horváth, C., Salt effects on hydrophobic interactions in precipitation and chromatography of proteins: An interpretation of the lyotropic series. *Archives of Biochemistry and Biophysics* **1977,** *183* (1), 200.

3. Queiroz, J. A.; Tomaz, C. T.; Cabral, J. M. S., Hydrophobic interaction chromatography of proteins. *Journal of Biotechnology* **2001,** *87* (2), 143-159.

4. Fausnaugh, J. L.; Regnier, F. E., Solute and mobile phase contributions to retention in hydrophobic interaction chromatography of proteins. *Journal of Chromatography A* **1986,** *359*, 131.

5. Gooding, K. M.; Regnier, F. E., *HPLC of Biological Macromolecules*. 2002; Vol. 87, p 162-168.

6. Miller, N. T.; Karger, B. L., High-performance hydrophobic-interaction chromatography on ether-bonded phases : Chromatographic characteristics and gradient optimization. *Journal of Chromatography A* **1985,** *326*, 45.

7. Chang, J.-p.; El Rassi, Z.; Horva´th, C., Silica-bound polyethyleneglycol as stationary phase for separation of proteins by high-performance liquid chromatography. *Journal of Chromatography A* **1985,** *319*, 396.

8. Miller, N. T.; Feibush, B.; Karger, B. L., Wide-pore silica-based ether-bonded phases for separation of proteins by high-performance hydrophobic-interaction and size exclusion chromatography. *Journal of Chromatography A* **1985,** *316*, 519-536.

9. Shaltiel, S., Hydrophobic chromatography. *Methods in Enzymology* **1974,** *34*, 126-140.

10. Hjertén, S.; Rosengren, J.; Pahlman, S., Hydrophobic interaction chromatography : The synthesis and the use of some alkyl and aryl derivatives of agarose. *Journal of Chromatography A* **1974,** *101* (2), 281-288.

11. Jennissen, H. P., Hydrophobic interaction chromatography: the critical hydrophobicity approach. *International Journal of Biochromatography* **2000,** *5* (2), 131-163.

12. Claessens, H. A.; van Straten, M. A., Review on the chemical and thermal stability of stationary phases for reversed-phase liquid chromatography. *Journal of Chromatography A* **2004,** *1060* (1-2), 23-41.

13. Buchmeiser, M. R., New synthetic ways for the preparation of high-performance liquid chromatography supports. *Journal of Chromatography A* **2001,** *918* (2), 233-266.

14. Buszewski, B.; Jezierska, M.; Wełniak, M.; Berek, D., Survey and Trends in the Preparation of Chemically Bonded Silica Phases for Liquid Chromatographic Analysis. *Journal of High Resolution Chromatography* **1998,** *21* (5), 267-281.

15. Claessens, H. A.; van Straten, M. A., Review on the chemical and thermal stability of stationary phases for reversed-phase liquid chromatography. *Journal of Chromatography A* **2004,** *1060* (1-2), 23.

16. Wirth, M. J.; Fatunmbi, H. O., Horizontal polymerization of mixed trifunctional silanes on silica. 2. Application to chromatographic silica gel. *Analytical Chemistry* **1993,** *65* (6), 822-826.

17. Wirth, M. J.; Fairbank, R. W. P.; Fatunmbi, H. O., Mixed self-assembled monolayers in chemical separations. *Science* **1997,** *275*, 44-47.

18. Love, J. C.; Estroff, L. A.; Kriebel, J. K.; Nuzzo, R. G.; Whitesides, G. M., Self-assembled monolayers of thiolates on metals as a form of nanotechnology. *Chemical Reviews* **2005,** *105*, 1103-1169.

19. Ulman, A., *An introduction to Ultrathin organic films*. Academic Press: Boston, 1991.

20. Ulman, A., Formation and structure of self-assembleld monolayers. *Chemical Reviews* **1996,** *96*, 1533-1554.

21. Hatch, R. G., Chromatography of Proteins on a Silica-Based Support with Polyethylene Glycol Ligands. *Journal of Chromatographic Science* **1990,** *28* (4), 210-214.

22. Janzen, R.; Unger, K. K.; Giesche, H.; Kinkel, J. N.; Hearn, M. T. W., Evaluation of advanced silica packings for the separation of biopolymers by high-perforamnce liquid chromatography : V. Performance of non-porous monodisperse 1.5-µm bonded silicas in the separation of proteins by hydrophobic-interaction chromatography. *Journal of Chromatography A* **1987,** *397*, 91.

23. Lee, S.-W.; Laibinis, P. E., Protein resistant coatings for glass and metal oxide surfaces derived from oligo(ethylene glycol)-terminated alkyltrichlorosilanes. *Biomaterials* **1998,** *19* (18), 1669-1675.

24. Ostuni, E.; Grzybowski, B. A.; Mrksich, M.; Roberts, C. S.; Whitesides, G. M., Adsorption of proteins to hydrophobic sites on mixed self-assembled monolayers *Langmuir* **2003,** *19* (5), 1861-1872.

25. Pale-Grosdemange, C.; Simon, E. S.; Prime, K. L.; Whitesides, G. M., Formation of self-assembled monolayers by chemisorption of derivatives of oligo(ethylene glycol) of structure $HS(CH_2)_{11}(OCH_2CH_2)_mOH$ on gold. *Journal of the American Chemical Society* **1991,** *113* (1), 12-20.

26. Prime, K. L.; Whitesides, G. M., Self-assembled organic monolayers: model systems for studying adsorption of proteins at surfaces. *Science* **1991,** *252*, 1164-1167.

27. Prime, K. L.; Whitesides, G. M., Adsorption of proteins onto surfaces containing end-attached oligo(ethylene oxide): a model system using self-assembled monolayers. *Journal of the American Chemical Society* **1993,** *115* (23), 10714-10721.

28. Tedjo, C.; Laibinis, P. E., Modulating protein-surface interactions using mixed self-assembled monolayers of methoxy-terminated-tri(ethylene glycol)-terminated and alkyl terminated trichlorosilanes. *In preparation*.

29. Chau, T. T., A review of techniques for measurement of contact angles and their applicability on mineral surfaces. *Minerals Engineering* **2009,** *22* (3), 213-219.

30. Young, T., An Essay on the Cohesion of Fluids. *Philosophical Transactions: Royal Society of London* **1805,** *95*, 65-87.

31. Adamson, A. W.; Gast, A. P., *Physical Chemistry of Surfaces*. 6th ed.; John Wiley & Sons, Inc.: New York, 1997.

32. Girifalco, L. A.; Good, R. J., A Theory for the Estimation of Surface and Interfacial Energies. I. Derivation and Application to Interfacial Tension. *The Journal of Physical Chemistry* **1957,** *61* (7), 904.

33. Vailaya, A.; Horvath, C., Retention Thermodynamics in Hydrophobic Interaction Chromatography. *Industrial & Engineering Chemistry Research* **1996,** *35* (9), 2964-2981.

34. Melander, W. R.; El Rassi, Z.; Horváth, C., Interplay of hydrophobic and electrostatic interactions in biopolymer chromatography : Effect of salts on the retention of proteins. *Journal of Chromatography A* **1989,** *469*, 3-27.

35. Machold, C.; Deinhofer, K.; Hahn, R.; Jungbauer, A., Hydrophobic interaction chromatography of proteins: I. Comparison of selectivity. *Journal of Chromatography A* **2002,** *972* (1), 3-19.

36. Katti, A.; Maa, Y.; Horváth, C., Protein surface area and retention in hydrophobic interaction chromatography. *Chromatographia* **1987,** *24* (1), 646-650.

37. Chalikian, T. V.; Totrov, M.; Abagyan, R.; Breslauer, K. J., The Hydration of Globular Proteins as Derived from Volume and Compressibility Measurements: Cross Correlating Thermodynamic and Structural Data. *Journal of Molecular Biology* **1996,** *260* (4), 588-603.

38. Mahn, A.; Lienqueo, M. E.; Asenjo, J. A., Effect of surface hydrophobicity distribution on retention of ribonucleases in hydrophobic interaction chromatography. *Journal of Chromatography A* **2004,** *1043* (1), 47-55.

39. Herrwerth, S.; Eck, W.; Reinhardt, S.; Grunze, M., Factors that Determine the Protein Resistance of Oligoether Self-Assembled Monolayers: Internal Hydrophilicity, Terminal Hydrophilicity, and Lateral Packing Density. *Journal of the American Chemical Society* **2003,** *125* (31), 9359-9366.

40. Pahlman, S.; Rosengren, J.; Hjertén, S., Hydrophobic interaction chromatography on uncharged sepharose® derivatives : Effects of neutral salts on the adsorption of proteins. *Journal of Chromatography A* **1977,** *131*, 99-108.

41. Heydweiller, G., *Annals of Physics* **1910,** *33*, 145-185.

Appendix A

Equations describing free energy change upon protein retention in a chromatographic column

The change in the free energy between the adsorbed and free states (ΔG) can be related to the partitioning between the two states:

$$\Delta G = G_{adsorbed} - G_{free} \tag{A-1}$$

$$\frac{C_s}{C_m} = \exp\left(-\frac{\Delta G}{RT}\right) \tag{A-2}$$

or

$$\frac{N_s V_m}{N_m V_s} = \exp\left(-\frac{\Delta G}{RT}\right) \tag{A-3}$$

C and N denote concentration of protein and number of moles of protein, respectively. The subscript s and m denotes stationary phase and mobile phase. V_s and V_m are volume of the stationary phase and mobile phase, with $\phi = V_s / V_m$. R is ideal gas constant and T is temperature. A simple modification will result in

$$\frac{N_s}{N_m} + \frac{N_m}{N_m} = 1 + \phi \exp\left(-\frac{\Delta G}{k_B T}\right) \tag{A-4}$$

From eq. A-4, the percentage of free protein in the mobile phase can be expressed as

$$\%\, free = \frac{1}{1 + \phi \exp\left(-\frac{\Delta G}{RT}\right)} \tag{A-5}$$

As the fraction of free protein in the system will flow through the column with a velocity of the mobile phase (v_{mobile}) and the fraction of the protein adsorbed to the support will be immobile ($v_{stationary}$), the average velocity for the proteins through the column will be

$$v_{average} = (v_{mobile})(\%\, free) + (v_{stationary})(\%adsorbed) \tag{A-6}$$

$$v_{average} = \frac{v_{mobile}}{1 + \phi \exp\left(-\frac{\Delta G}{k_B T}\right)} \tag{A-7}$$

For a column volume of V_{column}, the time (t_o) for the mobile phase to exit the column is

$$t_o = \frac{V_{column}}{v_{mobile}} \tag{A-8}$$

The time required for a protein to flow through and exit the column is defined as the protein retention time (t_R) and is given by

$$t_{protein} = \frac{V_{column}}{v_{average}} = t_o\left(1 + \phi \exp\left(-\frac{\Delta G}{k_B T}\right)\right) \tag{A-9}$$

Further, the additional time for the protein to exit the column after the solvent front is

$$t_{protein} - t_o = t_o \phi \exp\left(-\frac{\Delta G}{k_B T}\right) \tag{A-10}$$

Further rearrangement of eq. A-10 gives retention factor, *k*,

$$k = \frac{t_R - t_0}{t_0} = \phi \exp\left(-\frac{\Delta G}{k_B T}\right) \tag{A-11}$$

CHAPTER VI

ANALYSIS OF PROTEIN MASS RECOVERY FROM CHROMATOGRAPHY

6.1. Introduction

High performance liquid chromatography (HPLC) has become an essential tool in biotechnology. Numerous proteins have been separated by HPLC for analytical and preparative separation purposes[1-5]. For analytical purposes, reversed-phase (RP) chromatography is the preferred method as RP-HPLC can provide a high resolution separation of proteins in a short time[1, 4]. However, the aggressive conditions used in RP-HPLC (i.e. a hydrophobic stationary phase and an organic solvent based-mobile phase) often denature the proteins during the separation process. Another HPLC mode that is often used to separate proteins is hydrophobic interaction chromatography (HIC). HIC utilizes milder conditions as compared to those of RP-HPLC (i.e. a less hydrophobic stationary phase and a water based-mobile phase) that greater preserve the protein bioactivity through the separation process. Thus, HIC is the preferred method for preparative separation purposes, particularly for the isolation and purification of bioactive proteins. HIC typically provides high mass and activity recoveries. However, less than complete protein mass recovery is often observed for separations by HIC[6-10].

In this chapter, the mass recoveries of several proteins studied in the isocratic retention experiments are analyzed from the chromatograms. Effects of salt concentration, protein type and molecular weight, and the surface hydrophobicity of the support on the mass recovery of proteins are investigated.

6.2. Materials and Methods

Isocratic retention experiments were performed using a Waters HPLC system with a procedure as described in the previous chapter. The sample injection volume was 5 μL. Mobile phases containing 50 mM of phosphate buffer at pH 7 with various amount of Na_2SO_4 were delivered into the chromatographic columns at a flow rate of 1 mL/min. After each isocratic run, a column was flushed with 10 to 15 column volumes of 0.2 M of Na_2SO_4 in phosphate buffer to remove bound proteins from the column. This procedure was then followed by a column equilibration using 10 column volumes of phosphate buffer containing the appropriate salt concentration prior to the next sample injection.

The recovery of a protein mass (M) after an isocratic elution from a chromatographic column was determined from the protein chromatogram by integrating the area under the protein peak using the Breeze 2 Software (Waters Corp.). The percentage of mass recovery was calculated using the following equation,

$$\%\,\mathrm{Recovery} = \frac{M}{M_0} x100\% \qquad (6\text{-}1)$$

M_0 was obtained from the chromatogram of a protein when it was eluted from the HPLC system without column being connected to it.

6.3. Results and Discussion

Chapter 5 showed that changes in the mixed SAM composition on the surface of the support and in the concentration of salt in the mobile phase affected the retention times for the eluted proteins. In these experiments, the yield of collected protein was found to be affected by changes in these two parameters. Figure 6-1 shows the recoveries of several proteins after isocratic elution from chromatographic columns containing

supports varying surface composition. As shown in Chapter 2, changes in the surface chemical composition of the support affect its surface hydrophobicity, increasing in the order: 100%EG < 90%EG < 80%EG < 70%EG. A common trend for each of the examined proteins in Figure 6-1 is that the percent mass recovery of each protein decreases as the concentration of salt in the mobile phase is increased. In comparing the results across the different supports, Figure 6-1 also suggests that column hydrophobicity affects the mass recovery of a protein. The mass recoveries from columns that contained supports of higher hydrophobicities exhibited a higher sensitivity to changes in salt concentrations. To and Lenhoff[11] observed a similar behavior in their studies of the isocratic retention of various proteins in several commercial HIC columns containing supports of different base materials and surface functionalities. Comparing the percent recoveries of several proteins in a particular column, the result in Figure 6-1(a-c) indicates that the percent of recovery is weakly related to the protein molecular weight.

It is worth noting that most proteins reversibly adsorbed to the support during the elution experiments as they could be recovered in high yield when eluted with a mobile phase that contained low concentrations of salt. This behavior was observed for ribonuclease A, lysozyme (except when eluted from the column containing the 70%EG support) and α-chymotrypsin. For the case of trypsin inhibitor eluted from 100%EG and 90%EG columns, there were permanent mass losses of about 40% and 60% of the initial injected mass, respectively (Figure 6-1(a-b)). Figure 6-1(d) shows that ~50% of initially loaded lysozyme mass was permanently lost in the column that contained a 70%EG support. This result indicates that there is a maximum surface hydrophobicity threshold (θ_{max}) above which the conformation of a protein may be disrupted due to strong protein-

support interactions and that caused the protein to adsorb irreversible onto the support. From the result in Figure 6-1, the θ_{max} for lysozyme appears to be between the hydrophobicity levels of the columns containing 70%EG support and 80%EG support. For trypsin inhibitor, a column containing a support with a hydrophobicity level less than that of the 100%EG column is required to avoid a permanent mass loss during a chromatographic elution. Jennissen et al.[12] have suggested that conducting a protein separation close to the hydrophobicity threshold would be ideal since at this threshold, the proteins should not adsorb onto the support when using low salt concentrations in the mobile phase, but will be made to adsorb by shifting to higher salt concentrations.

Rate of Protein Mass Loss in Chromatography

Qualitatively, the data in Figure 6-1 indicate that the protein mass loss in a column is influenced by the salt concentration in the mobile phase and the hydrophobicity of the support. Chapter 5 showed that the salt concentration in a mobile phase affects the time spent by a protein on the surface of a support in a column (i.e. protein retention time). It is unclear in Figure 6-1 whether the changes in protein mass loss are affected directly by changes in the salt concentration in the mobile phase or from a secondary effect caused to the effective protein residence time in the column by the increased salt concentration. To determine the primary factor responsible for the changes in mass recovery, I analyzed the protein recovery data with respect to the protein retention time that was measured at various salt concentrations. By this analysis, a simple first-order rate equation (eq. 6-2) could be applied to describe the protein recovery data with respect to time.

$$\frac{M}{M_0} = \exp(-k_L t) \qquad (6\text{-}2)$$

In eq. 6-2, M_0 is the initial protein mass injected into a column, M is the mass of recovered protein, and k_L is a rate loss constant. A plot of *ln* (M/M_0) or *ln (% recovery)* vs. retention time should yield a straight line with a slope of $-k_L$ if the recovery data obey this simple first-order rate equation, despite the differences in salt concentrations.

Figure 6-2 shows the plots of *ln (% recovery)* for the proteins with respect to their retention times across the various examined chromatographic supports at different salt concentrations. The data in Figure 6-2 could be readily fitted by straight lines suggesting that the rate of mass recovery could be described by a simple first-order rate expression. Further, the obtained rate loss constant for each set of recovery data suggests that mass loss in a column after elution with various salt concentrations is not dependent on the salt concentration, but is dependent on the time spent by the protein on the surface of the support. If the mass loss is dependent on salt concentration, one would obtain different value of k_L at different retention times because each point in Figure 6-2 was obtained at a specific salt concentration. From these data, the primary role of salt concentration on mass recovery is mainly to lengthen the time spent by a protein within the column. Specifically, increases in the salt concentration results in the protein adsorbing for a longer period of time on the surface of the support in the column. From Figure 6-2, the rate loss constant for the examined proteins are not the same, suggesting them to be specific for each protein.

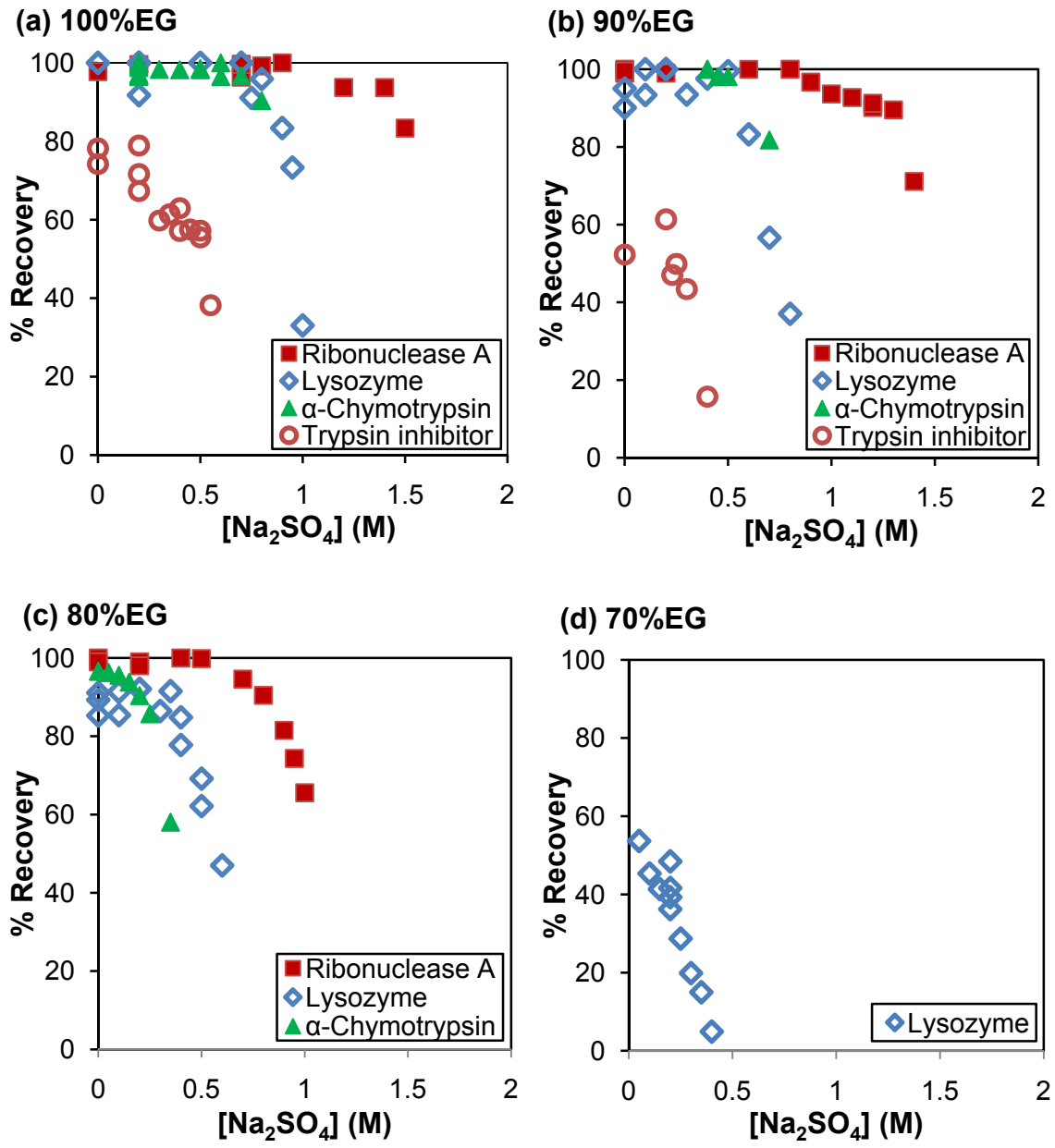

Figure 6-1: Mass recoveries of lysozyme, ribonuclease A, α-chymotrypsin, and trypsin inhibitor after isocratic elution from columns containing 100%EG, 90%EG, 80%EG, and 70%EG supports using various salt concentrations in the mobile phase.

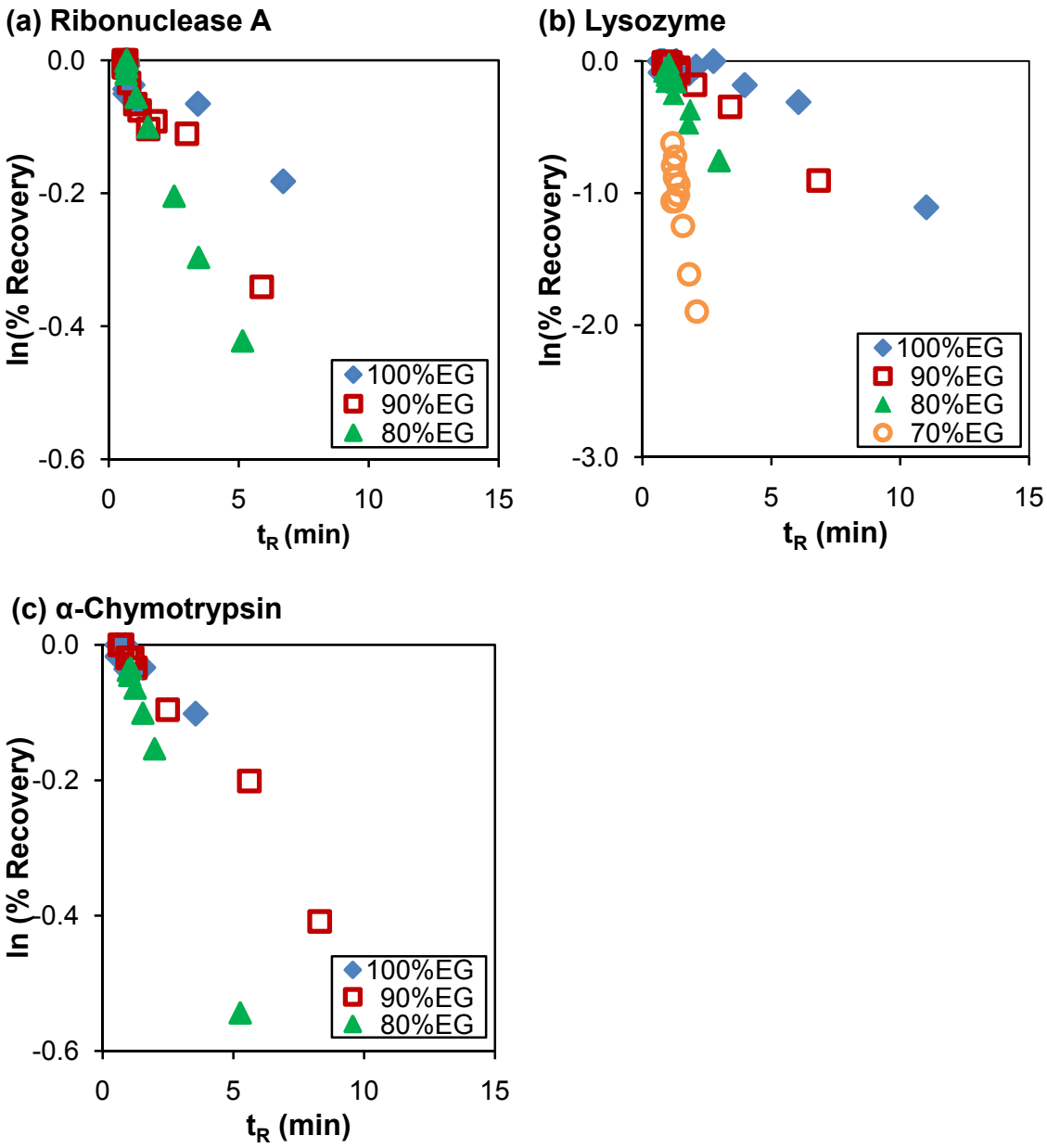

Figure 6-2: Semi-log plots of the mass recoveries of ribonuclease A, lysozyme, and α-chymotrypsin from chromatographic columns containing 100%EG, 90%EG, 80%EG, and 70%EG supports.

Influence of Surface Hydrophobicity of a Support on the Protein Rate Loss Constant k_L

In Figure 6-2, protein recoveries were lower using supports containing higher content of C8 SAM. These supports exhibited surfaces that were hydrophobic. Figure 6-3 compares the relationships between the values of k_L, obtained from slopes of the data in Figure 6-2, with the hydrophobicities of the supports, as represented by the cosine of the water contact angle measured on the support. As in Chapter 5, here the surface hydrophobicity of the mixed SAM coated-support was indirectly determined by measuring the water contact angle on a mixed SAM of the same composition that had been deposited onto a flat substrate. In Figure 6-3, the increase in the value of slope k_L with respect to an increase in the hydrophobicity of the support suggests that the support hydrophobicity affects the level of protein loss in a column. This is in a way similar to the result from the static protein adsorption experiments in Chapter 2 wherein surfaces of higher hydrophobicity levels adsorbed more proteins.

In order to better understand the relationships in Figure 6-3, the parameters (i.e. k_L and $\cos\theta$) were analyzed in a way where the energies associated with each factor could be compared. For k_L, it can be related to an activation energy associated with the rate of protein mass loss in the column using Arrhenius' law, i.e.

$$k_L = Ae^{-\frac{E_a}{RT}} \tag{6-3}$$

where A is a pre-exponential factor, E_a is an activation energy, R is the molar gas constant and T is temperature. For surface hydrophobicity, $\cos\theta$ is related to the surface tension of the support (γ_{SV}) which is described by the Young's equation (see eq. 5-1 in Chapter 5):

$$\cos\theta = \frac{\gamma_{SV} - \gamma_{SL}}{\gamma_{LV}} \tag{6-4}$$

where, γ_{LV} is the surface tension of pure water as pure water was used to measure the wettability of the surface of the support. γ_{SL} is the interfacial tension between the solid and liquid phases.

Figure 6-4 shows the energy relationships between the rate loss constants k_L and the hydrophobicities of the supports for each examined protein. The energies on the y-axis is represented by $ln\ k_L$ as the values of $ln\ k_L$ is proportional to the negative of activation energy of the particular rate loss constant. The plots in this figure suggest that the change in the energies related to the protein rate loss constant is approximately linear with respect to the change in the surface energy of the support. The values of the activation energy are higher on the surface of higher energy (i.e. high $cos\ \theta$ values) which indicate a less tendency of mass loss when a protein interacts with surfaces of low hydrophobicity.

Mechanistic Model for Protein-Surface Interactions in Chromatography

Figure 6-5 shows a mechanistic model of the interactions between a protein molecule with the surface of a support based on the results from this research. In Chapter 5, the retention of a protein in a chromatographic column was described as an equilibrium partitioning between the mobile phase and the support as the protein moves through the column. The measured retention time t_R yields a retention factor k, which can be related to an equilibrium constant K_{eq} of the system (i.e. $K_{eq} = k / \phi$, where ϕ is a phase ratio). At high salt concentrations in the mobile phase, the protein spends more time on the surface of the support. The longer the protein spends on the surface of the support, the greater is the propensity for mass loss in the column. This process may occur under the

conditions of high salt concentration with a specific rate loss constant k_L. The conformation and the activity of the adsorbed proteins on the support were not examined.

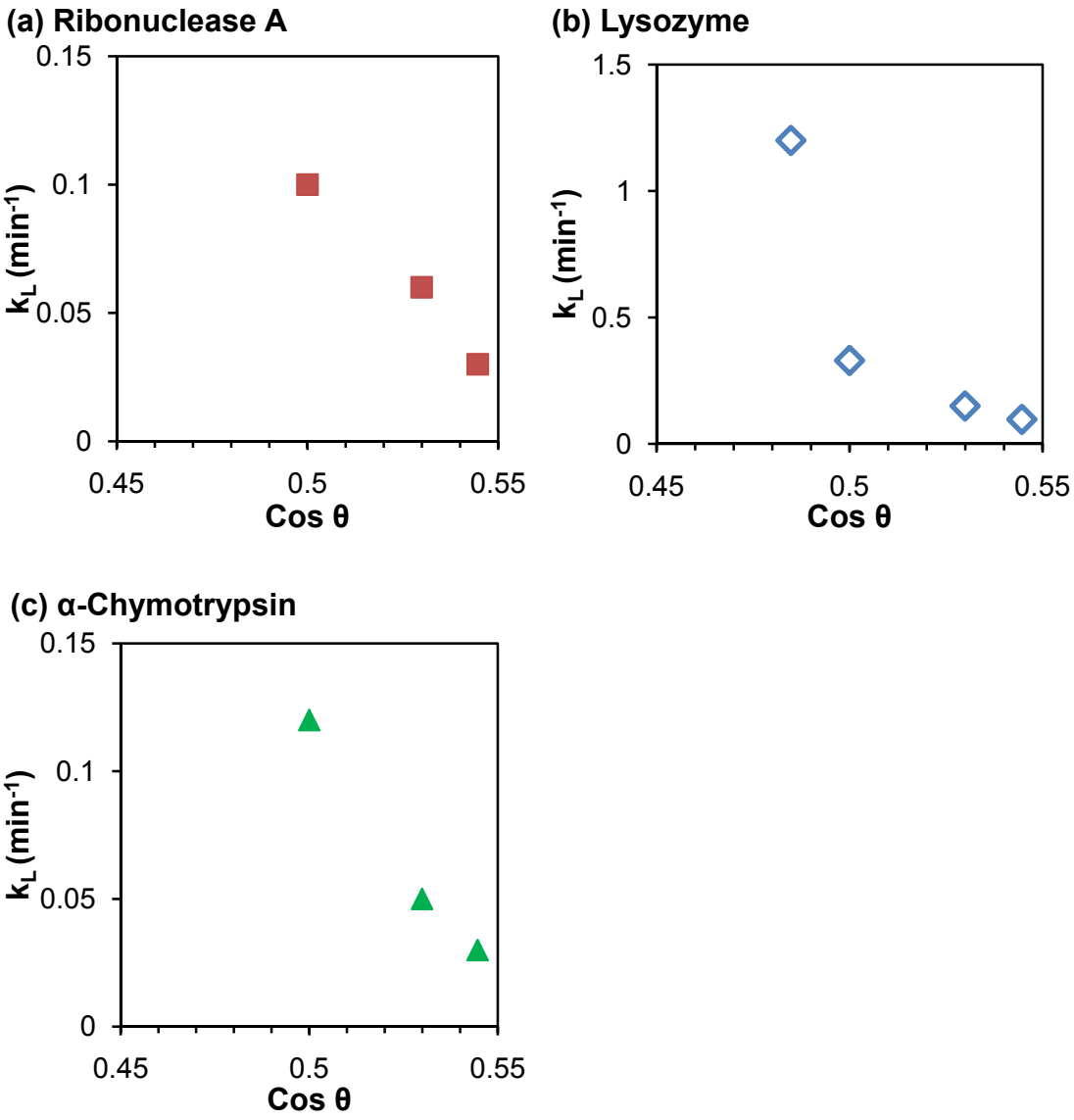

Figure 6-3: Effect of the hydrophobicity of a support (*cos θ*) on the rate loss constants (k_L) of ribonuclease A, lysozyme, and α-chymotrypsin. Hydrophobicity of a support was determined from water contact angle measurements, as described in Chapter 5.

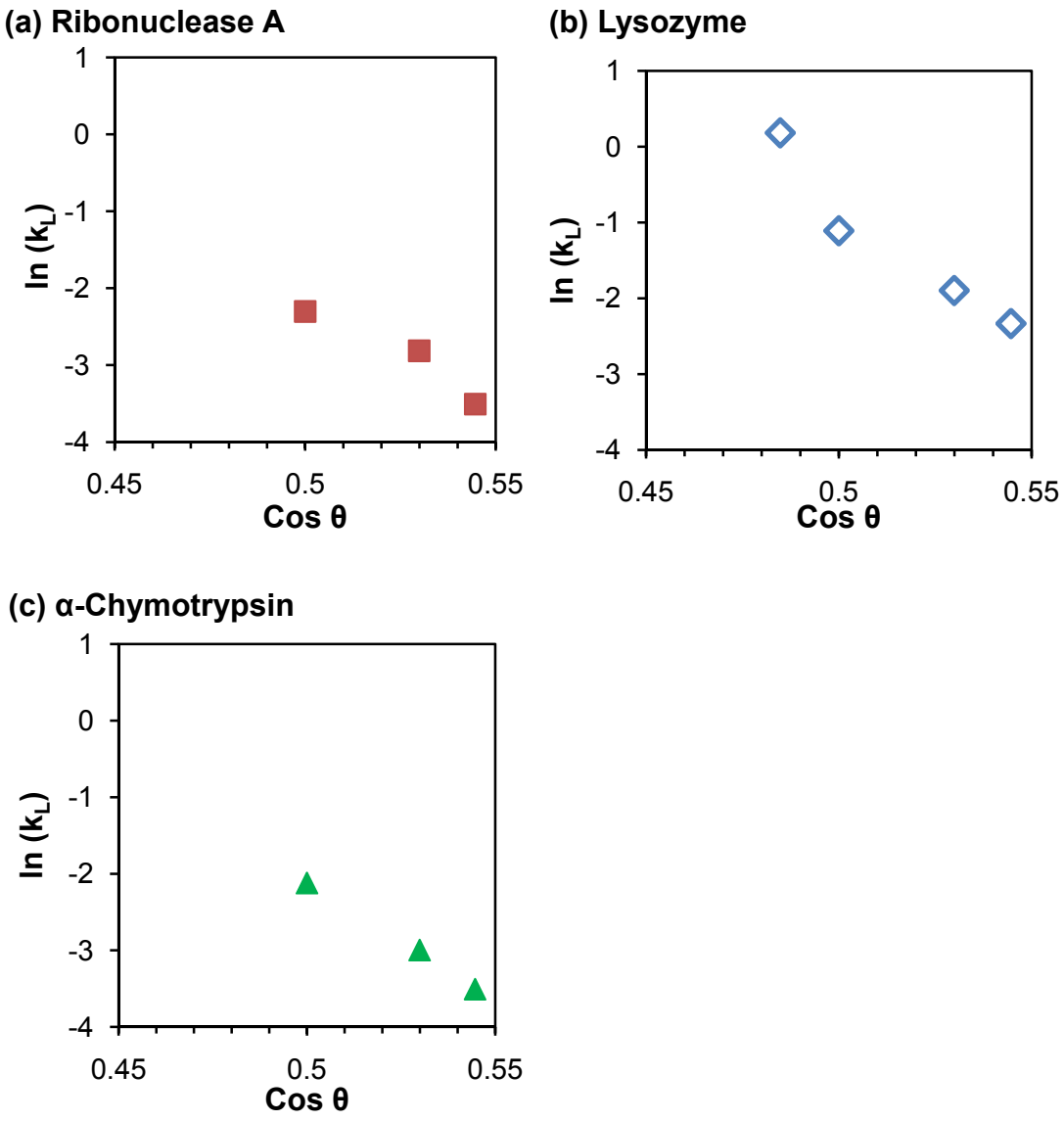

Figure 6-4: Energy relationships between protein rate loss constants (k_L) and surface hydrophobicity of the support ($cos\ \theta$)

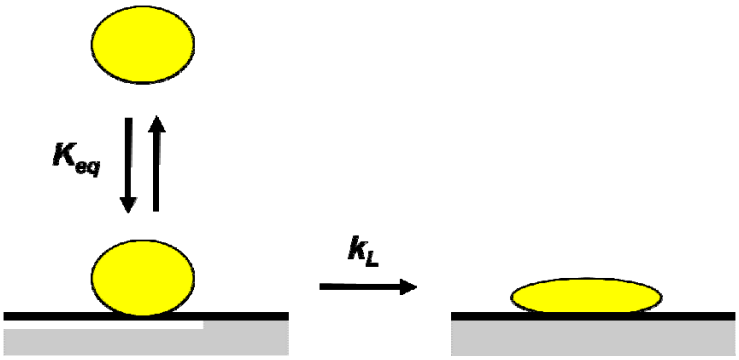

Figure 6-5: A mechanistic model of protein-support interaction in a chromatographic column. K_{eq} is an equilibrium constant of protein retention in the column and k_L is a rate loss constant.

6.4. Conclusions

The mass recovery data of several proteins after isocratic elution at various salt concentrations show that there is a tendency of increased mass loss at the conditions of high salt concentrations in the mobile phase and high hydrophobicity level of the support in the column. The recovery behavior is specific with respect to a protein and is weakly dependent on the molecular weight of the protein. It is worth noting that most proteins reversibly bound on the support in a column in that they can be recovered when eluted at a lower salt concentration in the mobile phase. There is a maximum surface hydrophobicity threshold (θ_{max}) above which there is a permanent protein loss in the column. Thus, one needs to choose a column that has a hydrophobicity level of less than θ_{max} to ensure reversible protein adsorption.

First order fitting of the recovery data suggests that the rate of protein loss in a chromatographic column is a function primarily of the time spent by the protein adsorbed onto surface of the support. The activation energy that affects the rate of protein loss on a support shows a linear free energy relationship with the hydrophobicity of the support.

Specifically, the activation energy for the rate of protein loss decreases with an increase in the hydrophobicity of the support.

6.5. References

1. Hanson, M.; Unger, K. K.; Mant, C. T.; Hodges, R. S., Optimization strategies in ultrafast reversed phase chromatography of proteins. *Trends in Analytical Chemistry* **1996,** *15* (2), 102-110.

2. Josic, D.; Lim, Y.-P., Analytical and preparative methods for purification of antibodies. *Food Technology and Biotechnology* **2001,** *39* (3), 215-226.

3. Aguilar, M.-I.; Hearn, M. T. W., High-resolution reversed-phase high-performance liquid chromatography of peptides and proteins. *Methods in Enzymology* **1996,** *270*, 3-26.

4. Chen, H.; Horvath, C., High-speed high-performance liquid chromatography of peptides and proteins. *Journal of Chromatography A* **1995,** *705*, 3-20.

5. Gooding, K. M.; Regnier, F. E., *HPLC of Biological Macromolecules*. 2002; Vol. 87, p 162-168.

6. Wu, S.-L.; Benedek, K.; Karger, B. L., Thermal behavior of proteins in high-performance hydrophobic-interaction chromatography On-line spectroscopic and chromatographic characterization. *Journal of Chromatography A* **1986,** *359*, 3-17.

7. Goheen, S. C.; Gibbins, B. M., Protein losses in ion-exchange and hydrophobic interaction high-performance liquid chromatography. *Journal of Chromatography A* **2000,** *890* (1), 73-80.

8. Fausnaugh, J. L.; Kennedy, L. A.; Regnier, F. E., Comparison of hydrophobic-interaction and reversed-phase chromatography of proteins. *Journal of Chromatography A* **1984,** *317*, 141.

9. Benedek, K., Thermodynamics of [alpha]-lactalbumin denaturation in hydrophobic-interaction chromatography and stationary phases comparison. *Journal of Chromatography A* **1988,** *458*, 93-104.

10. Ingraham, R. H.; Lau, S. Y. M.; Taneja, A. K.; Hodges, R. S., Denaturation and the effects of temperature on hydrophobic-interaction and reversed-phase high-performance liquid chromatography of proteins : Bio-gel tsk-phenyl-5-pw column. *Journal of Chromatography A* **1985,** *327*, 77-92.

11. To, B. C. S.; Lenhoff, A. M., Hydrophobic interaction chromatography of proteins: I. The effects of protein and adsorbent properties on retention and recovery. *Journal of Chromatography A* **2007,** *1141* (2), 191.

12. Jennissen, H. P., Hydrophobic interaction chromatography: the critical hydrophobicity approach. *International Journal of Biochromatography* **2000,** *5* (2), 131-163.

CHAPTER VII

CONCLUSIONS AND FUTURE STUDIES

7.1. Conclusions

This research provides a generic and systematic approach for efficient protein chromatography by using mixed self-assembled monolayers of $Cl_3Si(CH_2)_{11}(OCH_2CH_2)_3OCH_3$ (EG_3OMe) and $Cl_3Si(CH_2)_7CH_3$ (C8) to create surfaces of varying surface energies (or hydrophobicities). The research reported in this thesis started from the establishment of self-assembly conditions of pure EG_3OMe SAM and the deposition of mixed SAMs on SiO_2/Si substrates in Chapter 2, to the development of mixed SAMs-coated SiO_2 particles in Chapter 3, followed by the preparation of chromatographic columns in Chapter 4. Finally, the performance of chromatographic columns and the effects of column hydrophobicities on protein retention and mass recovery were investigated in Chapter 5 and 6.

The self-assembly conditions for forming good quality of EG_3OMe films on SiO_2/Si substrates were established in Chapter 2. The conditions are: (1) use RCA cleaned substrates, (2) a self-assembly temperature of 60 ^oC, (3) and toluene-based solutions containing a trace amount of water. The resulting EG_3OMe films exhibit protein repellent properties as tested against several proteins. Under these conditions, surfaces of different energies were successfully created by depositing mixed SAMs of EG_3OMe and C8 silanes onto SiO_2/Si substrates. Ellipsometric and XPS results were used to estimate the chain densities within these mixed SAMs. The results show that the densities within

mixed SAMs are higher than those of the pure SAMs due to the ability of the C8 silanes to incorporate in between EG_3OMe silanes, thus forming dense underlying alkyl regions within the mixed SAMs. Static protein adsorption experiments conducted on these surfaces show that the level of protein adsorption on a substrate can be modulated by varying the surface energy of the substrate using mixed SAMs of EG_3OMe and C8. An interesting finding in this work is that for highly hydrophilic surfaces (e.g. those containing a high proportion of EG_3OMe in the mixed SAMs), slight changes in the wettability properties resulted in significant changes to their protein repellent properties.

Chapter 3 described the surface functionalization of porous silica particles with mixed SAMs of EG_3OMe and C8, and the characterization of the resulting coated particles. XPS results showed that mixed SAMs-coated silica particles have similar surface chemical compositions to those of mixed SAMs formed on SiO_2/Si substrates under the same self-assembly condition. The surface energies of the mixed SAM-coated particles were analyzed by a flotation method. The developed flotation method allows measurements of a small quantity of sample through the application of spectroscopic method rather than gravimetric method for determining the amount of floating/sinking particles in the flotation experiments. The results from flotation experiments showed differences in surface energies on mixed SAMs-coated particles with respect to varying mol ratios of EG_3OMe and C8 in the silanization solutions. The critical surface tensions of the mixed SAM-coated silica particles that were estimated using the developed flotation method were similar to those of the same mixed SAMs deposited on SiO_2/Si substrates. Critical surface tensions of the mixed SAMs-coated SiO_2/Si substrates were measured using Zisman's method.

Characterization of the properties of chromatographic columns packed with mixed SAM-coated silica particles were described in Chapter 4. The columns used in this research had a typical packed bed size of 0.5 cm x 5.5 cm. The void time for these columns was ~0.65 min as determined from the isocratic elution of ribonuclease A. The void time determined here was useful to determine and compare retention factors of proteins from chromatographic experiments. The calculation of column efficiency of a typical packed column used in this research indicated that the column was not optimized yet as indicated by the low value of its reduced plate height. Optimization of the chromatographic columns can potentially be carried out as a future work.

The influence of surface hydrophobicity of a chromatographic support on the retention of a protein in a chromatographic process was investigated in Chapter 5. Here, protein retentions in chromatographic columns were systematically related with the hydrophobicities of supports using equations that describe the energies involved upon protein interactions with the supports. Isocratic protein retention experiments were carried out in columns packed with mixed SAMs-coated silica particles. The same mixed SAMs were deposited on SiO_2/Si substrates and the hydrophobicities of the surfaces were determined from liquid contact angle measurements. The results in this chapter showed that protein retention and separation in a chromatographic column is controllable by selecting the appropriate level of column hydrophobicity in addition to the effect of salt on protein retention. The generic approach that was proposed would be applicable for hydrophobic interaction of chromatography of proteins.

Chapter 6 analyzed the mass recoveries of several proteins from isocratic experiments that were described in Chapter 5. Isocratic retention data at various salt

concentrations showed that there was a tendency of increased mass loss at high salt concentrations in the mobile phase and high level of hydrophobicity of the column. The recovery behavior was specific with respect to protein and was weakly dependent on the protein molecular weight. First order analysis of the recovery data showed that the rate of protein mass loss in the column was a function of time, not salt concentration. The rate of mass loss in the column was influenced by the surface hydrophobicity of the support.

In overall, this research provides a systematic way of controlling protein retention in a chromatographic column by tuning the hydrophobicity of the support in the column. With proper selection, a surface hydrophobicity can be produced so that a protein can be effectively retained by a support without resulting in its permanent loss during chromatography.

7.2. Future Studies

Extension of this research can be started by improving the efficiency of the columns since it will improve the resolution of a separation process. The bioactivities of the proteins eluted from chromatographic columns should be investigated. Finally, the supports developed in this research should be tested under gradient mode for application in hydrophobic interaction chromatography. A non-chromatographic work that can stem from this research is to investigate protein adsorption on flat substrates of various surface energies under dynamic conditions. The result of this work could provide relationships between flat surface protein adsorption and chromatographic protein retention.

7.2.1. Improvement of Column Efficiency

The result in Chapter 4 indicates that the efficiency of the chromatographic columns used in this research needs to be improved. There are several variables that can affect the efficiency of a column: column packing procedure, flow rate of mobile phase, particle size, and pore size of the particles.

The width of a peak in a chromatogram indicates the dispersion of a sample in a column. The level of dispersion is dependent on the way the column is packed. In this research, all columns were packed by slurry method with methanol as recommended by the column's manufacturer. This packing procedure may not result in the most optimized packed bed. An optimal packing procedure is a combination of optimized slurry concentration, slurry viscosity, slurry solvent and flow rate of the solvent used during the packing procedure[1, 2]. Thus the improvement of the column packing procedure should be considered in the future.

A good measure for peak broadening in a column is the height equivalent to a theoretical plate (H). The relationship between H and liquid velocity in the column u, is described by the following van Deemter equation[1]:

$$H = A + \frac{B}{u} + Cu \qquad (7\text{-}1)$$

where A is related to eddy dispersion and is a function of the size and distribution of the interparticle channels and other nonuniformities in the packed bed. B is related to molecular diffusion in the axial direction. C is related to mass transfer resistance in the packed bed. Eq. 7-1 suggests that there is an optimal velocity (or flow rate) where one would obtain the minimum H. At lower velocities, the efficiency is reduced by means of molecular diffusion corresponding to term B in eq. 7-1. At high velocities, and thus

shorter residence time over the column, peak broadening is increasing as result of limiting intraparticle diffusion as represented by term *C* in equation. Particle size is an important variable for determining optimal liquid velocity as particle size provides the characteristic length for diffusion. The effect of flow rate on the efficiency of the column was not investigated in the current research. Constructing a van Deemter plot would be useful to pin down the flow rate for optimum efficiency in addition to the improvement of column packing procedure.

The average pore size of the particles used in this research was 125 Å. This size may be at the borderline of usefulness for protein separation. The diffusion of a molecule in the pores of a support slows down measurably as the pore size becomes smaller than about 10 times the size of the molecule[1]. This restricted diffusion affects separation efficiency greatly. Thus, utilizing particles of larger pore size such as 300 Å should be considered in the future. There have been studies that reported better separation efficiencies and resolutions using large pore size of particles for protein chromatography[3-5].

7.2.2. Analysis of Protein Activity and Conformational Change

A good separation provides high resolution, high mass recovery and high activity recovery of an analyte. Mass recoveries of proteins upon isocratic elution experiments were investigated in this research. The activities of the recovered proteins may need to be investigated in the future. Upon interaction with a surface, a protein can change its conformation. This conformation change can be reversible or irreversible and may or may not affect protein activity. Reversible conformational change suggests that the

protein refolds to its original conformation after adsorption-desorption process from a surface. A protein would still retain its activity after a conformational change when this change does not affect the conformation of the amino acids around its active site. These factors need to be taken into account when studying protein activity after a chromatographic separation. In addition, using a protein that is sensitive towards unfolding or denaturation may be useful for the investigation of protein activity. For example, α-lactalbumin is unstable in a solution without Ca^{2+}. α-lactalbumin has been used to analyze the effects of chromatographic conditions on protein stability after chromatographic elution[6].

7.2.3. Hydrophobic Interaction Chromatography of Proteins

Ultimately, the packing materials developed in this research would find their usage as supports for hydrophobic interaction chromatography (HIC) of proteins. The research reported in this thesis only explored chromatographic separation under isocratic elution conditions while HIC requires gradient mode. In order to assess the packing materials developed in this research as novel supports for protein separation, there will be a need to characterize the performance of the columns containing these supports under a gradient mode after the efficiency of these columns is improved.

7.2.4. Protein Adsorption on Flat Surfaces under Dynamic Condition

Typically, protein adsorption studies on flat surfaces have been performed under static conditions and the levels of adsorption have been measured using ellipsometry[7-9], XPS[10], radio-labeling[11], or dye quantification[12]. In these approaches, a surface is

contacted with a protein solution for a period of time (3-24 h), subsequently removed from solution, rinsed with clean buffer, dried and characterized. For surfaces that appear to strongly adsorb proteins, the adsorbed layers must be able survive the shear forces applied during the rinsing procedure. For surfaces that weakly adsorb proteins, the measured protein levels may be influenced by the conditions used in the rinsing step. As a result of differences in these steps, there can be variations across different laboratories in terms of the transition from the non-adsorbing to the adsorbing surfaces.

Protein adsorption experiments have also been conducted under dynamic conditions. These experiments are especially useful in the biomedical area for studying the fouling behavior on a biomedical implant. Such experiments are typically done in a flow cell. The level of protein adsorption on these surfaces has been characterized by techniques such as Fourier Transform Infrared Spectroscopy coupled with attenuated total reflectance optics (FTIR-ATR)[13, 14], total internal reflection fluorescence (TIRF) system[10], surface plasmon resonance (SPR)[15-17] or 'end point' techniques that do not provide on-line measurements (e.g. ELISA method[18]).

In the area of biomaterials research, there have been conflicting results on the role that shear rate had on protein adsorption. Across various studies, the amount of adsorption onto a surface has been reported to increase[19, 20], be unaffected[14, 20], or to decrease[18] with increasing shear rate during adsorption. These conflicting results could possibly be explained from work in the polymer research area on the response of block copolymer brushes subjected to shear flow. In a study done by Anastassopolos et al.[21], they observed that there was a critical shear rate above which physically adsorbed polymeric chains desorbed from a surface. The values of desorption threshold (or critical

shear rate) decreased as the molecular weights of the tethered polymeric chains increased. The findings here suggest that the level of protein adsorption can also be affected by shear rate when the protein-surface interactions are below certain levels. As such, the expectation is that the critical shear rates will depend on the characteristics of the protein, its size, the chemistry of the surface, and interactions between the protein and the surface.

The effect of shear flow on the adsorption of various types of proteins on mixed SAM surfaces can be investigated *in-situ* using a flow cell that has been integrated with a TIRF system. Fluorescently labeled proteins will be used as they are required for their detection in TIRF. It is expected that the conditions of intermediate wettabilities will show the largest effect of shear rate on protein adsorption. The results from this study will likely to address the threshold conditions for establishing non-fouling behavior on flat surfaces.

7.3. References

1. Neue, U. D., *HPLC Columns Theory, Technology, and Practice*. Wiley-VCH, Inc.: New York, 1997.

2. Stanley, B. J.; Foster, C. R.; Guiochon, G., On the reproducibility of column performance in liquid chromatography and the role of the packing density. *Journal of Chromatography A* **1997,** *761* (1-2), 41-51.

3. Wu, D.-R.; Greenblatt, H. C., Effect of stationary phase on preparative protein separation in reversed-phase chromatography. *Journal of Chromatography A* **1995,** *702*, 157-162.

4. Pearson, J. D.; Mahoney, W. C.; Hermodson, M. A.; Regnier, F. E., Reversed-phase supports for the resolution of large denatured protein fragments. *Journal of Chromatography* **1981,** *207*, 325-332.

5. Wilson, K. J.; Wieringen, E. V.; Klauser, S.; Berchtold, M. W., Comparison of the high-performance liquid chromatography of peptides and proteins on 100- and 300-Å reversed-phase supports. *Journal of Chromatography* **1982,** *237*, 407-416.

6. Xiao, Y.; Freed, A. S.; Jones, T. T.; Makrodimitris, K.; O'Connell, J. P.; Fernandez, E. J., Protein instability during HIC: describing the effects of mobile phase conditions on instability and chromatographic retention. *Biotechnology and Bioengineering* **2006,** *93* (6), 1177-1189.

7. Hoffmann, C.; Tovar, G. E. M., Mixed self-assembled monolayers (SAMs) consisting of methoxy-tri(ethylene glycol)-terminated and alkyl-terminated dimethylchlorosilanes control the non-specific adsorption of proteins at oxidic surfaces. *Journal of Colloid and Interface Science* **2006,** *295* (2), 427-435.

8. Lee, S.-W.; Laibinis, P. E., Protein Resistant Coatings for Glass and Metal Oxide Surfaces Derived from Oligo(ethylene glycol)-terminated Alkyltrichlorosilanes. *Biomaterials* **1998,** *19*, 1669.

9. Prime, K. L.; Whitesides, G. M., Adsorption of proteins onto surfaces containing end-attached oligo(ethylene oxide): a model system using self-assembled monolayers. *Journal of the American Chemical Society* **1993,** *115* (23), 10714-10721.

10. Michel, R.; Pasche, S.; Textor, M.; Castner, D. G., Influence of PEG Architecture on Protein Adsorption and Conformation. *Langmuir* **2005,** *21* (26), 12327-12332.

11. Gonçalves, I. C.; Martins, M. C. L.; Barbosa, M. A.; Ratner, B. D., Protein adsorption on 18-alkyl chains immobilized on hydroxyl-terminated self-assembled monolayers. *Biomaterials* **2005,** *26* (18), 3891-3899.

12. Clare, T. L.; Clare, B. H.; Nichols, B. M.; Abbott, N. L.; Hamers, R. J., Functional Monolayers for Improved Resistance to Protein Adsorption:â€‰ Oligo(ethylene glycol)-Modified Silicon and Diamond Surfaces. *Langmuir* **2005,** *21* (14), 6344-6355.

13. Cha, W.; Beissinger, R. L., Macromolecular mass transport to a surface: effects of shear rate, pH, and ionic strength. *Journal of Colloid and Interface Science* **1996,** *177*, 666-674.

14. Pitt, W. G.; Cooper, S. L., FTIR-ATR studies of the effect of shear rate upon albumin adsorption onto polyurethaneurea. *Biomaterials* **1986,** *7*, 340-347.

15. Barrett, D. A.; Power, G. M.; Hussain, M. A.; Pitfield, I. D.; Shaw, P. N.; Davies, M. C., Protein interactions with model chromatographic stationary phases constructed using self-assembled monolayers. *Journal of Separation Science* **2005,** *28* (5), 483-491.

16. Li, L.; Chen, S.; Jiang, S., Protein interactions with oligo(ethylene glycol) (OEG) self-assembled monolayers: OEG stability, surface packing density and protein adsorption. *Journal of Biomaterials Science, Polymer Edition* **2007,** *18*, 1415-1427.

17. Mrksich, M.; Sigal, G. B.; Whitesides, G. M., Surface Plasmon Resonance Permits in Situ Measurement of Protein Adsorption on Self-Assembled Monolayers of Alkanethiolates on Gold. *Langmuir* **1995,** *11* (11), 4383-4385.

18. Kim, J.; Ryu, G.; Shin, I.; Lee, K.; Han, D.; Kim, Y.; Min, B., Effects of shear rates on protein adsorption in the total artificial heart. *ASAIO Journal* **1992,** *38* (3), M532-M535.

19. Chuang, H. Y. K.; King, W. F.; Mason, R. G., Interaction of plasma proteins with artificial surfaces *Journal of Laboratory and Clinical Medicine* **1978,** *92*, 483-496.

20. Lee, R. G.; Kim, S. W., Adsorption of proteins onto hydrophobic polymer surfaces: Adsorption isotherms and kinetics. *Journal of Biomedical Materials Research* **1974,** *8* (5), 251-259.

21. Anastassopolous, D. L.; Spiliopoulos, N.; Vradis, A. A.; Toprakcioglu, C.; Baker, S. M.; Menelle, A., Shear-induced desorption in polymer brushses. *Macromolecules* **2006,** *39*, 8901-8904.